Technical University of Denmark

DTU

Exploring the properties and possibilities of self-assembling

Andersen, Karsten Brandt; Svendsen, Winnie Edith; Castillo, Jaime

Publication date:
2013

Link back to DTU Orbit

DTU Library
Technical Information Center of Denmark

Ph.D. Thesis

Exploring the properties and possibilities of self-assembling nanotubes and nanoparticles for nano-bio sensors

Karsten Brandt Andersen

Lyngby, 2013

DTU Nanotech
Technical University of Denmark

DTU Nanotech
Department of Micro- and Nanotechnology

Supervisor: Asc. Prof. Winnie Edith Svendsen
Co Supervisor: Ass. Prof. Jaime Castillo-León

Abstract

The study (and potential application) of diphenylalanine peptide nanotubes is a popular topic that in recent years has experienced a boost in activity. This activity has been propelled forward by new articles continuously being published presenting even more spectacular properties of the nanotube structures ranging from piezo electricity over semi conductance to fluorescence. If such peptide nanotubes could be controlled and incorporated in sensors such as a biological field effect transistor it would greatly reduce the fabrication costs while at the same time providing researchers with new and exciting possibilities. The major driving forces supporting the interest in the peptide nanotubes is the fast and simple assembly process combined with their remarkable stability towards alcohols, organic solvents, and biological analytes that was presented shortly after the self-assembling properties of the diphenylalanine peptide was reported.

The self-assembly process of the peptide nanotubes is entropy driven relying solely on hydrophobic packing of the aminoacid side groups and π-π interactions of the phenyl rings as stabilizing entities. As such it seems surprising that the peptide nanotubes should be as stable as reported. In this work, a more detailed study has demonstrated that the peptide nanotubes dissolve in most liquids including water.

Despite the solubility of the peptide nanotubes in most liquids they remain remarkable stable under bombardment with heavy ions in dry conditions. This makes the peptide nanotubes excellent candidates as a water soluble alternative to traditional photolithography masks. In the present work we have demonstrated a rapid and low cost fabrication of silicon nanowires, in which process the silicon nanowire was defined in a dry etching procedure masked by the peptide nanotubes. To utilize this fabrication approach a manipulation method capable of orienting the peptide nanotubes at wafer scale has been developed. Furthermore, we have demonstrated that the peptide nanotubes can be used as a lift off material for the fabrication of nanoslits in metal surfaces.

The water solubility of the peptide nanotubes allow the patterning of polymer materials not compatible with the organic solvents (used to remove the photoresists in traditional microfabrication techniques). In the final part of the project we have demonstrated a rapid and mild fabrication of conducting polymer nanowire devices and illustrated their potential use as sensitive temperature sensor.

Resumé

Studiet (og den potentielle brug) af diphenylalanin peptid nanorør er et populært forskningsområde, der i de senere år har oplevet en stror fremgang i aktivitet. Denne aktivitet har været drevet frem af en kontinuerlig publicering af nye artikler, som præsenterer endnu mere opsigtsvækkende egenskaber ved nanorørene, Der blandt andet inkluderer piezoelektricitet, halvlederegenskaber og fluorescens. Hvis disse peptid nanorør kunne kontroleres og inkorporeres i sensorer som for eksempel biologiske felteffekttransistorer, ville det drastisk reducere fabrikationsomkostningerne og samtidig give forskerne nye og spændende muligheder. den hurtige og milde samleproces kombineret med deres spektakulærer stabilitet mod alkoholer, organiske opløsningsmidler og biologiske analyter, der blev præsenteret kort efter, at de selvorganiserende egenskaber af diphenylalanin peptiderne var rapporteret, har været nogle af de primære drivkræfter bag denne opblomstring.

Peptid nanorørenes selvorganiserende proces er entropisk drevet og de eneste stabiliserende faktorer er den hydrofobiske pakning af sidegrupperne og π-π interaktionerne mellem phenylringene. Derfor virker det overraskende, at peptid nanorørene skulle være så stabile som rapporteret. I denne afhandling har et mere detaljeret studie vist, at peptid nanorørene opløses i de fleste væsker inklusiv vand.

På trods af peptid nanorørenes opløselighed i de fleste væsker er de dog stadig meget stabile ved tørre betingelser under bombardement med tunge ioner. Dette gør peptid nanorørene til glimrende kandidater som et vandopløseligt alternativ til traditionelle fotolitografi resister. I dette projekt er en hurtig og billig fabrikation af silicon nanowires blevet demonstreret. I denne process er silicium nanowireren defineret i en tør ætsningsprocedure, hvor masken består af peptid nanorørene. For at denne fabrikationsproces kan udnyttes fuldt ud, er en manipuleringsmetode, som er i stand til at orientere peptid nanorørene på wafer skala, blevet udviklet. Derudover har vi demonstreret at peptid nanorørene kan benyttes som en lift off maske i fabrikationen af nanorevner i metaloverflader.

Peptid nanorørenes vandopløselighed tillader en mønstring af polymer materialer, som ikke er kompatibel med organiske opløsningsmidler (bruges til at fjerne fotoresist i traditionel mikrofabrikationsteknikker). I den sidste del af projektet har vi demonstreret en hurtig og mild fabrikation af ledende polymer nanowire devices og illustreret potentialet af disse som temperatur sensorer.

Preface

This thesis describes the most important results achieved during my Ph.D. work at DTU Nanotech Department of micro and nanotechnology at the Technical University of Denmark, The work was carried out in the period from August 2008 to January 2013. The thesis was submitted on January 11$^{\text{th}}$, 2013, in partial fulfillment of the requirements for the academic degree, Doctor of Philosophy (Ph.D.).

The work has been carried out under the supervision of associate professor Winnie Edith Svendsen and Senior Researcher Jaime Castillo-León in the Nano Bio Integrated Systems group (NaBIS) at DTU Nanotech.

Kongens Lyngby, January 11th 2013

Karsten Brandt Andersen

DTU Nanotech
Department of Micro- and Nanotechnology
Technical University of Denmark
DTU - Building 345 East
DK-2800 Kongens Lyngby
Denmark

Acknowledgements

Throughout this project many people have been involved and contributed to the results presented in this thesis in their own way.

First I would like to acknowledge and express my gratitude to my two supervisors, for their insight (both professionally and personally) and support over the last three and a half years. To Winnie Edith Svendsen for allowing me to do this work and giving me the freedom to operate this complex field. For your enthusiasm and the many discussion we have had about new, innovative and in some cases crazy ideas. We have worked closely together for the last six years in many different topics and no matter the topic I have always felt that you were able to ask the right questions to move the research forward. To Jaime Castillo-León for teaching me the ways of self-assembly, for always having time to look over experimental data and discuss the meaning of these, for believing me when the rest of the research field still believed that the peptide nanotubes were stable and for having the courage to contradict an entire field. Thank you for taking your time to teach me the ways of writing scientific articles.

I have been lucky to make this project in a fantastic research group where it is a policy that the doors to the offices always are open and all discussions of new ideas are encouraged. I would like to thank all current and previous members of the NaBIS group. To Luigi Sasso for sharing my frustrations with the diphenylalanine material in times when it did not behave as we initially expected and for many long discussions both about scientific and less scientific subjects. I have enjoyed working together with you both on the supervision of shared students and in the ideation and development of our patent. To Dorota Kwasny for sharing an office with me during the last couple of years and for always having the snack position updated. I have enjoyed working together with you as supervisors for several students. To Maria Dimaki and Casper Hyttel Clausen for help with the design and realization of the first experimental setups for the DEP manipulation. To the imdepance crew Romén Rodriguez Trujìllo and Mohammad Ajine for many discussions and for co-inventing matlab trouble shooting guy: Bob. To Søren Skov and Lars Andresen for being part of the initial silicon nanowire development and for our trips around the country for meetings with collaborators. To Indumathi Vedarethinam for getting me started on the development of a tissue culture platform that has sparked many new ideas. Also thank you to Jan Bert Gramsbergen from SDU for a fruitful collaboration in the development of this tissue culture system. With his enthusiasm and never ending optimism Aghiad Ghazal in the final part of my project made me again believe in the potential of the peptide nanotubes, for this I am thankful.

I would like to express a special thanks to the students that I have been involved in supervising: Julie Kirkegaard and Michael Jørgensen for the development of the functionalization procedure and

Contents

List of Figures

Motivation and basic concepts

1.1 Thesis Objectives and Outline

1.1.1 Motivation

The bottom up fabrication of nanomechanical and electrical devices has intrigued scientists for many years with the potential for low cost, fast and easy fabrication of sensor and sensor networks. Through self-assembling processes, nature is able to build the most remarkable structures ranging from the tiniest proteins to much more complex structures. If we were able to control only a fraction of these self-assembling processes the possibilities are unlimited. The major challenge in the exploitation of the self-assembly process lies in the establishment of a connection from the self-assembled structure(s) to the macroscopic world.

Self-assembled structures such as the diphenylalanine peptide nanotubes, which is the subject of the present work, offer a fast and inexpensive approach to the realization of nanosized structures. Considering the huge and expensive machines used in the traditional fabrication approach for the realization of such structures this is remarkable. Despite all the benefits of such self-assembled structures it is, as mentioned above, difficult to realize devices that relies solely on the bottom up self-assembled structures. If the goal of the fabrication procedure is the production of sensor system the self-assembled structures face an additional challenge, besides the challenge with establishing contact to the macroscopic world, namely: The material properties of the self-assembled structures. Compared to standard semiconducting sensor materials they posses insufferior electrical and mechanical properties. Despite the shortcomings discussed above the self-assembled structures is still an interesting material doe to their ability to produce lots of objects in nanometer scale in an inexpensive procedure. The later being more pronounced when working with biological self-assembled structures, since the self-assembly process of these often inexpensive structures traditionally takes place at room temperature under mild conditions and therefore does not rely on expensive equipment during fabrication. In this project effort has been invested in the realization of a reliable, rapid and inexpensive fabrication approach, where the self-assembled diphenylalanine peptide nanotubes are used as a nanolithography fabrication tool. In this way the geometry of the self-assembled peptide nanotubes are transferred to more traditional sensor materials to realize low cost nanostructures while maintaining the material properties of more traditional sensor

maetrial such as silicon or other semiconducting materials. The self-assembled structures will in this fabrication approach replace the e-beam lithography or other nanolithography tools during the fabrication of nanosensors. In order to combine the top down and the bottom up fabrication approaches one needs to develop a manipulation approach that enable the positioning of the self-assembling structures at the proper location on the top down fabricated structures.

The goal of this project is to establish a fabrication platform for the controlled, rapid and low cost fabrication of nanowire devices utilizing a self-assembled PNT to mask the nanowire itself. In this approach other self-assembled structures of course can replace the PNT to provide the user with a wide range of different geometries to be used in the fabrication of the nanostructured part of the sensors or electronics.

1.1.2 Outline

The first two chapters of the thesis will be focussed on a short discussion of the driving forces in self-assembly processes in general and the self-assembly mechanism for diphenylalanine peptide nanostructures in particular. A short review on previous application of the diphenylalanine peptide nanotubes will be given in the final part of chapter 1. In chapter 2 a more in depth characterization of the peptide nanotubes formed by the diphenylalanine monomers, which is the focus of the remaining thesis, will be provided. This characterization will be based partly on previously published results and partly on experiments conducted during the current project.

   The remainder of the thesis will be based on the published and submitted articles from this project. These chapters will be arranged so that prior to each article a short introduction to the article will be given. At the end of the chapters a small paragraph with concluding remarks positioning the published article with respect to the overall project will be provided. In these concluding remarks also potential challenges that still must be faced will be discussed.

   In chapter 3 the stability of the peptide nanotubes under liquid conditions will be addressed. In the initial phase of the project the peptide nanotube structures were, based on previously published data, believed to be stable in most solutions. However the issue of stability is not as straight forward as one might think. This part of the characterization is included in a separate chapter since this investigation affected the aim of the project greatly.

   Under dry conditions the peptide nanotubes however, remains stable and are able to withstand prolonged ion bombardment. This topic will be addressed in chapter 4, where also the potential use of the peptide nanotubes as a clean room fabrication tool is discussed and demonstrated. In chapter 5 the properties of the peptide nanotubes as a masking material is further explored for both dry etching for the formation of silicon nanowires and in lift off procedures for the formation of gold nanoslits. In this chapter the central focus is the development of a manipulation approach capable of positioning the peptide nanotubes at wafer scale in a parallel approach.

   The water solubility of the peptide nanotube allow the patterning of organic materials incompatible with acetone, which is used in traditional photolithography. In chapter 6 conducting polymer nanowires has been realized from the conductive polymer PEDOT based on the PNT lithography approach.

   Finally, Chapter 7 and 8 provides a conclusion and an outlook of the project respectively.

1.2 Self-Assembly Driving Forces

In nature many different self-assembling structures exist. Our life depends on a very well functioning self-assembly process. In the body numerous new entities from simple proteins to entire
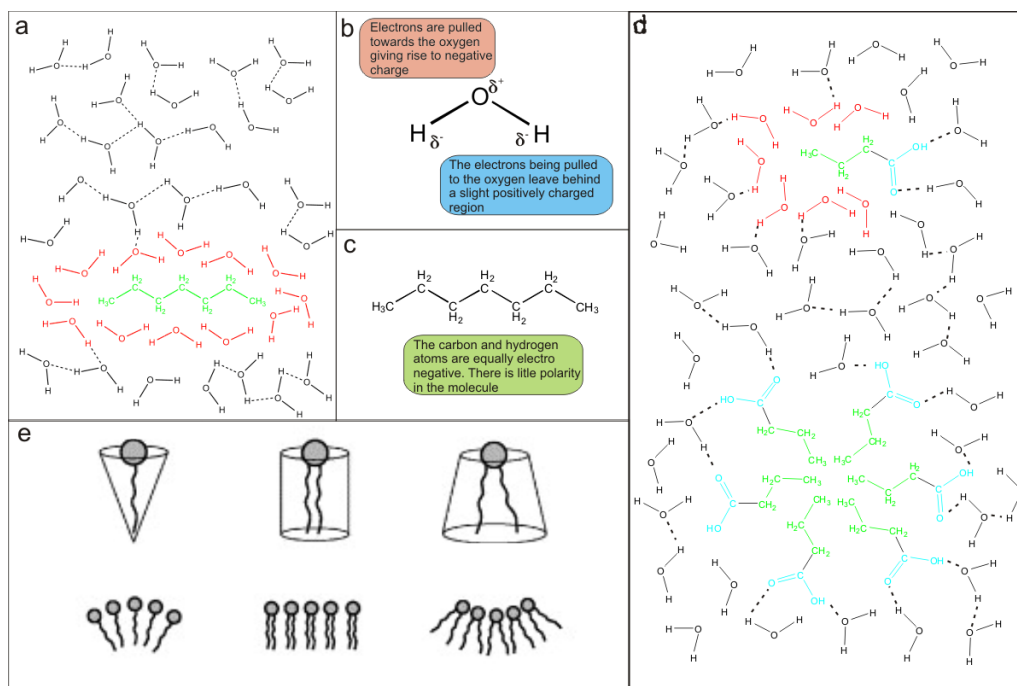
Figure 1.1: *Self-assembly is an entropy driven process where the interaction between polar water molecules, illustrated in **b**, and nonpolar molecules, illustrated in **c**, is minimized to ensure maximal entropy of the system. In liquid water the molecules form and break up hydrogen bonds spontaneously to neighboring water or other polar molecules in a continuous process as illustrated in the top part of **a**. When a nonpolar molecule as a heptane is submerged in the water it induces order in the water surrounding it (illustrated by the red water molecules in the lower part of **a**). If a molecule with a polar end and a non polar end is submerged in water the polar groups can interact with the water molecules and participate in the dynamic hydrogen bonding process and hence does not induce order to the surrounding molecules whereas the nonpolar part induces order in the same way as the heptane molecule (again illustrated by the red water molecules in the top part of **d**). To increase the entropy of the system such molecule will self-assemble to minimize the contact between the nonpolar parts and the water molecules as illustrated in the lower part of **d**. Depending on the relative size of the polar and nonpolar parts the molecules will self-assemble into different geometries as illustrated in **e**. Packing parameter illustration reprinted with permission[1]*

cells are fabricated every second. In this section the self-assembling structures, which has been investigated throughout this project will be presented.

1.2.1 Entropically Driven System

According to the second law of thermodynamics entropy is not allowed to decrease. It can only increase or in special cases (adiabatic processes) remain unchanged. The entropy is a measure of the randomness of a system and hence nature will always try to increase the randomness of a system in order to ensure an increase in entropy. The hydrophobicity of materials is an effect of this particular thermodynamic principle, as will be explained below.

In figure 1.1 the general principle behind entropically driven self-assembly is illustrated. The driving force in the self-assembly process is the interaction between polar and non-polar molecules. In figure 1.1b and figure 1.1c a polar water molecule and a nonpolar heptane molecule is illustrated respectively. The difference in the polarity of these two molecules is an effect of the electronegativity of the individual atoms involved. The oxygen atoms in the water molecule is more electronegative than the hydrogen atoms and hence the shared electrons will spent more time around the oxygen

atoms than the hydrogen atoms resulting in a net negative charge on the oxygen atom and a net positive charge on the hydrogen atoms. Whereas in the case of the nonpolar heptane the carbon atoms and the hydrogen atoms have similar electronegativity and hence the electron will be divided equally and no polarity will exist.

The polar water molecules are able to form hydrogen bonds between neighboring water molecule, so that a hydrogen atom of a water molecule interacts with the oxygen atom of another water molecule. In liquid water the water molecules are free to move and hydrogen bonds are continuously formed and broken up over time. A nonpolar molecule submerged in water will induce order, to ensure charge neutrality in its surroundings as illustrated by the red water molecules in figure 1.1a, and hence lower the entropy locally. To maximize the entropy of the system nonpolar or hydrophobic molecules will stick together in order to reduce the contact area between the nonpolar molecules and the polar water molecules, as seen when you try to mix oil (nonpolar molecules) and water (polar molecules). If a molecule with a polar end and a nonpolar end, illustrated in blue and green in figure 1.1d respectively, is submerged in water the water molecules are free to move and interact through hydrogen bonds with the polar part of the molecule whereas the water molecules around the nonpolar part are forced into an induced order lowering the entropy locally. When the concentration of such molecules increases they will interact to shield the nonpolar part from contact with the water molecules, as illustrated in the lower part of figure 1.1d, to ensure a higher entropy of the system overall. Depending on the relative size of the polar and nonpolar parts, also known as the packing parameter, the molecules will assembly into a range of different geometries as illustrated in figure 1.1e. The most well known of such self-assembled structures are the cell membranes which consist of a self-assembled double layer of phospholipids. All molecules with a hydrophillic side and a hydrophobic side will to a certain degree attempt to shield of their hydrophobic parts when submerged in water and thereby only expose the hydrophobic side to the water molecules. As explained below this is also the case for the self-assembly of diphenylalanine monomers into the peptide nanotubes.

1.2.2   Factors Stabilizing Self-Assembled Structures

As mentioned above the initial self-assembly process is an entropically driven process and hence the formed structure will without any further stabilizing factors be a dynamic entity of monomers assembling and disassembling based on thermal fluctuations. To stabilize self-assembled structures such as proteins in the body a range of different stabilizing factors exists. In this section a short description of a few of these stabilizing entities will be given.

The hydrophobic packing of the self-assembly process provides a certain level of stability for the structure. However, thermal energy (even at room temperature) is in some cases enough to break up such a structure if no other stabilizing factors are present. In this case the assembly and disassembly of the structure will be a dynamic process as mentioned above. Of course the larger the hydrophobic part of the molecule, the better the packing and hence the more stable the structures will be.

The most well known stabilizing factor is hydrogen bonds between hydrogen atoms in hydrogen bond donor groups and electronegative ions (hydrogen bond acceptors) such as oxygen or nitrogen. It is in general stronger than the hydrophobic packing of monomers discussed above, but not as strong as covalent or polar bonds. The hydrogen bond is one of the main stabilizing bonds in the self-assembled structures in our body. In fact the double helix of the DNA molecules is held together by hydrogen bonds between the individual base pairs.

An even stronger bond can be formed between two thiol groups present in for instance the amino acid cystine. This bond is known as a disulfide bridge where the two thiol groups react and form the bond. This is a covalent bond and therefore a very strong chemical bond, which stabilize the entire self-assembled structure. In this case the role of the initial self-assembly process is to

move the thiol groups close together to enable the formation of the disulfide bridges, which in turn stabilize the entire structure (such disulfide bonds are often encountered in larger protein structures).

In the peptide nanotubes the stabilizing factors are the hydrophobic packing of the sidegroups and the π - π interaction arising from the stacking of the aromatic phenyl rings in the hydrophobic core of the self-assembled PNT's. In other words no chemical bonding between the individual monomers are present and the stability of the self-assembled structures relies solely on non covalent interactions.

1.3 Diphenylalanine Peptide Structures and Applications

1.3.1 A Historical Note on the Diphenylalanine Monomers

The diphenylalanine (FF) dipeptide has historically been related to the Alzheimer's disease. The connection arises from the notion that the two neighboring phenylalanine aminoacids are the central structural recognition element of the β-Amyloid (Aβ) peptide of Alzheimer's[2](in Alzheimer's patients this peptide forms amyloid fibrils in the brain tissue). All short polypeptide capable of binding the Aβ peptide had this central structural motif as the only recurring part. Therefore the FF monomer is often referred to as the central structural motif of the Aβ peptide. This origin initially led to the interpretation that the structures formed from this monomer also were amyloid like structures and hence very stable and difficult to dissolve.[3–5]

The FF monomers are produced in standard linear peptide synthesis and are commercially available and it has a molecular weight of 312.37 g/mol. Below an overview of the different structures that can be formed from the diphenylalanine monomer and its analogues is provided. The most used structure formed by the FF monomers is the peptide nanotubes that are the topic of the current work. In fact this structure has given name to a whole class of self-assembling structures (assembling in the samme way as the FF monomers). This class is referred to as the phe-phe class and includes dipeptide with bulky hydrophobic side groups such as leucine, isoleucine, tryptophane and of course phenylalanine.[6]

1.3.2 Self-Assembled Diphenylalanine Structures

The FF monomer is an interesting molecule since depending on the formation condition it is able to form very different structures as illustrated in figure 1.2. Other aromatic hydrophobic dipeptides have been reported to form both different and similar structures. A full discussion of these materials is out of the scope of the current work. I will refer the interested reader to consult some of the previous published work on this specific topic.[6, 10–13]

In figure 1.2 an overview of the pathways for the formation of the self-assembled FF structures is seen. Below the different pathways will be presented individually and previous applications of the formed structures will briefly be noted. In the final parts of the present chapter previous applications of the PNT's will be described.

Peptide Nanofibers

From the FF monomer a forrest of peptide nanofibers attached to the surface can be formed, as illustrated in pathway A in figure 1.2. The initial step in this pathway is the formation of a stock solution. The lyophilized form of the FF monomer is dissolved in 1,1,1,3,3,3 hexaflouroisopropanol (HFP) at a high concentration. In this alcohol high concentrations (above 200 mg/ml) of the peptide monomer can be dissolved without the formation of aggregates.The peptide nanofibers are formed by spreading the stock solution on a surface which is then dried under vacuum condition.
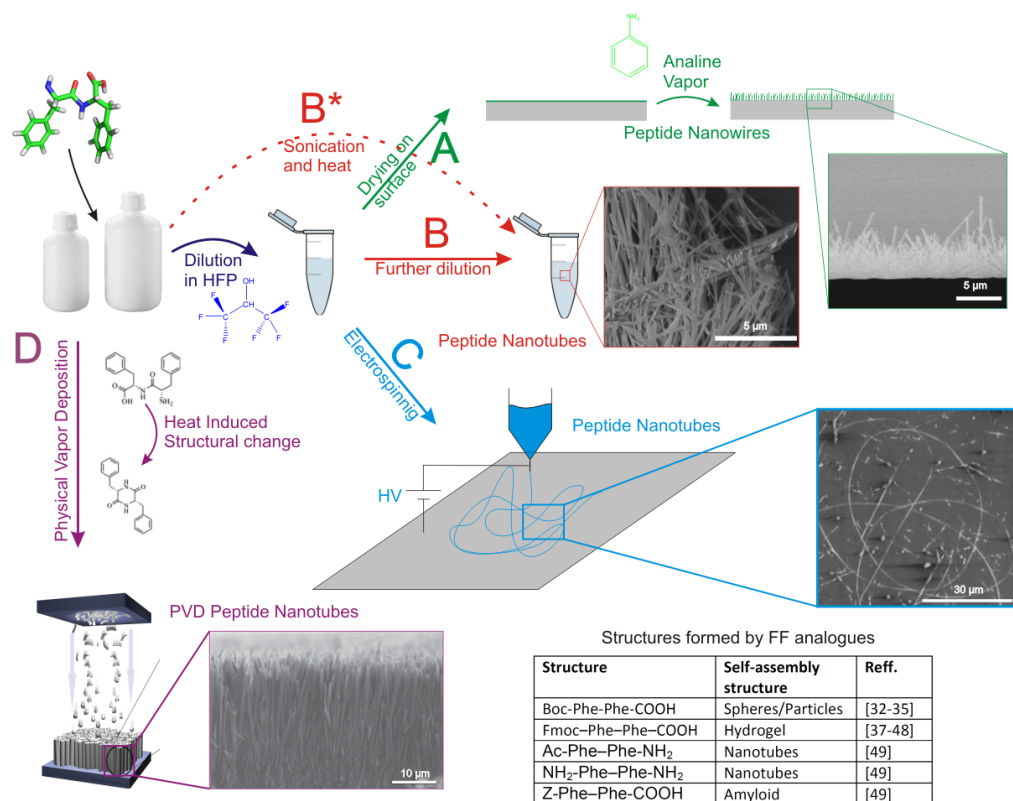
Figure 1.2: *Illustration of different pathways for the formation of the diverse structures that can be formed from the diphenylalanine peptide monomer (illustrated in the top left corner). In most (pathway A-C) applications the peptide monomer is initially dissolved in 1,1,1,3,3,3 hexaflouroisopropanol (HFP) to form a stock solution. If the HFP solution is dried on a substrate to form a peptide film, which is then treated with analine vapor at an elevated temperature, the formation of a peptide nanofiber forrest is observed as illustrated in pathway A. The peptide nanotubes that are the central structure in this thesis are formed upon a dilution of the stock solution in water as illustrated in pathway B and finally the peptide nanotubes can be electro spun directly from the HFP solution as indicated in pathway C. An alternative approach for the formation of peptide nanotubes can be seen in pathway D where a physical vapor deposition technique is utilized for the direct growth of peptide nanotubes attached to the surface of the growth substrate. Note that in this process the monomers undergoes a structural change as indicated in the figure. In the lower right corner of the figure structures formed by analogues of the peptide monomer is summarized. reprinted with permission from.[7–9]*

When the film is heated in the presence of aniline vapor the growth of the peptide wires will be initiated.[14] The gradient of the aniline vapor away from the surface will ensure the vertical alignment of the formed peptide wires. The diameter of the formed wires are rather consistent at approximately 200 nm and the length is controlled by the time of growth although it is typically in the order of a few microns.[14] The growth of the peptide wires can be grown in specific pattern by limiting the peptide film in the initial spreading by for instance PDMS structures whereby the growth of the peptide wires can be limited to specific areas of interest.[14, 15] The peptide wires have shown a high stability against thermal, chemical and proteolytic attacks[16] and have been grown on many different solid substrates such as silicon[14] and gold electrodes.[17]

The peptide nanofibers have been utilized in electrochemistry as an autoclavable alternative to laminin in order to increase the cell viability on metal electrode surfaces,[15, 18] for the formation of super hydrophobic surfaces[19] and as a scaffold for the formation of hybrids between the peptide material and cobalt oxide,[20] hydroxyapatite,[21] polyalanine[17] and palladium nanoparticles.[22]

Solution Formed Peptide Nanotubes

The solution based assembly of the PNT's is the simplest and most used approach for the formation of structures from the diphenylalanine monomers. In this approach illustrated as pathway B in figure 1.2 the lyophilized peptide monomer is initially dissolved in HFP to form the stock solution as explained above. This stock solution is then diluted in water or other polar solvents in which process the PNT's are formed.[3] The assembly is an entropically driven process where the hydrophobic side groups of the phenylalanine are rotated so that they are present on the same side of the peptide backbone.[23] The hydrophobic packing of the amino acid side groups (after rotation of the sidegroups to position them on the same side of the peptide backbone) results in the formation of the PNT's. The water molecules will in this conformation mainly be in contact with the hydrophillic peptide backbone which is entropically highly favorable also illustrated by the fast assembly of the PNT's. There is an alternative pathway for the formation of peptide nanotubes denoted as pathway B*. Rather than dissolving the peptide in the HFP, it can be dissolved in a water solution heated to 65°C, followed by 30 mins. of equilibration and finally cooling the solution to room temperature.[24] The peptide nanotubes will form during cooling of the solution once the concentration of the peptide monomers reaches a critical concentration. A different approach for the formation of the PNTs involved the mixing of the peptide stock solution and water in a laminar flow regimen. For this a microfluidic chip was fabricated allowing the introduction of the separated solutions and its mixing in a merging channel.[25]

The peptide nanotubes formed by the diphenylalanine monomer all share the same overall structural properties being that they are straight, stiff structures with no branches. The exact organization of the peptide monomers in the assembled structure will be discussed below.

In the present work focus has been on the PNT's formed upon dilution in pure water. However, the PNT's can be formed in other polar solvents to gain structures with different characteristics.[26–29]

Electrospinning of Peptide Nanotubes

PNT's can also be formed in an electrospinning procedure as illustrated in pathway C in figure 1.2. A high voltage difference is applied between the needle from the reservoir, containing the stock solution, and the substrate. This high voltage forms a jet of solution in which the peptide monomers are present. Upon the evaporation of the HFP the peptide nanotubes are formed. The formed structure shows the same characteristic Raman spectra as the solution based peptide nanotubes and hence has the same chemical composition.[8] The diameter of the electrospun fibers are much more consistent than the diameter of the PNT's formed in solution. The length of the

PNT's formed by the electrospinning process is also much longer than the tubes formed in solution. The diameter and length of the PNT's can be controlled to a certain degree by the electrospinning parameters such as the applied voltage and the concentration of the monomers.[8] The PNT's formed in the electrospinning process have currently not been utilized in any applications. This might be due to the fact that the peptide tubes formed in solution is easier to form than the PNT's formed by electrospinning.

Physical Vapor Deposition Based Nanotubes

In pathway D in figure 1.2 an approach for the formation of peptide nanotubes attached to the surface of a substrate is illustrated. This process is based on a physical vapor deposition (PVD) technique where the FF monomers in powder form is heated in a vacuum chamber at 220°C which evaporates the monomers. During the evaporation phase the peptide monomer attains a cyclic structure and finally assembles in peptide nanotubes on the surface of the substrate which is maintained at a lower temperature of 80°C.[9] The formed peptide nanotubes are vertically aligned as a function of the formation process as seen in figure 1.2 where a SEM image of the formed structures is shown. The peptide nanotubes formed in the PVD approach show a different conformation than the PNT's formed in solution due partly to the cyclic nature of the monomers and partly due to the absence of water. The peptide nanotube array can be formed at wafer scale and can be patterned as described by Shklovsky *et al.*[30]

 The peptide nanotubes formed by the physical vapor deposition technique have been utilized as super capacitor structures,[9,31] as surface modification for increased hydrophobicity[9] and as electrode modification in electrochemistry[30]

Structures Formed from Diphenylalanine Analogues

A slight chemical modification of the peptide monomer can as noted in the table in figure 1.2 lead to the formation of different peptide structures.[32] When a *tert*-butoxycarbonal(boc) group is attached to the amino terminated end of the dipeptide it is possible to form peptide spheres or particles. The modified peptide monomer is dissolved in HFP at a concentration of 100 mg/ml. When diluted in water this monomer forms peptide tubes as was the case for the native structure.[33] However when diluted in ethanol rather than water the monomers form nanospheres with diameter between 30 nm and 2 μm micrometers with an average diameter of 1 μm.[32] The formed structures have been reported as a unique material with a stiffness comparable to that of steel.[32] However, recently the hollowness of the structures has been questioned as assumed in the previous reports.[34] Furthermore they can be printed directly onto the surface of substrates using an ink jet printer.[33] The boc modified peptide stock solution has recently been combined with a stock solution of the native peptide for the formation of nano necklaces.[35] Another modified version of the diphenylalanine monomers, that forms hydrogel upon the dilution of the HFP stock in acidic solutions,[36,37] is the Fmoc version of the monomer where the amino group is protected by a fluorenylmethoxycarbonyl group.[38–42] These hydrogels have been used as cell culture platforms,[38–40,43–45] optical biosensors,[46] drug delivery candidates[47] and batteries.[48] An overview of the different analogues can be found in the review by Reches *et al.*[49]

1.3.3   Application of Diphenylalanine Peptide Nanotubes

Many applications of the peptide nanotubes have been inspired by previous applications of better know wire geometries such as semiconducting nanowires[50–53] and carbon nanotubes.[54–58] The applications presented below will be divided into direct applications, where the PNT is present in the final product, and indirect applications, where the PNT's are only used as a fabrication tool.

Bare in mind that many of the applications presented below were designed when the PNT's were still believed to be stable in most solutions. The issue with stability will be addressed in chapter 3.

One of the main advantages of the PNT's compared to the traditional wire structures mentioned above is beside the mild fabrication conditions the availability of both amino groups and carboxylic groups that decorates the surface of the PNT's. The presence of these groups allow a very simple and direct functionalization procedure with a possibility to use the two groups for two different functional molecules providing a simpler approach for multiple functionalization schemes.

Direct Incorporation

In direct applications the material properties of the self-assembled structures is a key parameter for the functionality of the finished product. The easy access to both amino groups and carboxylic groups on the surface of the nanowire enables, as mentioned above, a very easy functionalization scheme. This combined with the fact that the PNT's were believed to be stable under most conditions made them excellent candidates for electrode modification inspired mainly by the electrode modification with CNT's.[59–62] The purpose of such an electrode modification is to increase the surface area of the electrode and at the same time provide a pathway for functionalization. The central idea is illustrated in figure 1.3a where the enzymatically active molecule is chemically linked to the surface of the PNT's and hence the effective surface area of the electrode is increased[63] as first demonstrated by Yemini *et al.*[64] This effect has been utilized for the detection of glucose using glucose oxidase molecule,[66,72] dopamine using a PNT-Copper complex in a nafion film[73] and as an immunosensor for the detection of Escherichia coli bacteria.[65] In the electrochemical detection of glucose the PNT's are utilized in two different approaches. Initially the PNT's are simply used to increase the surface area of the working electrodes.[72] In the later approach the they are also utilized as a carrier for the glucose oxidase molecules, which is positioned in the cavity of the PNT's. The presence of the PNT increases the long term stability of the glucose oxidase[67,74] that retained a larger part of its functionality compared to glucose oxidase molecules stored directly in solution. The PNT's have in several applications been utilized as a scaffold for the immobilization of different active groups. As seen in figure 1.3b functionalized PNT's have been utilized for the detection of neurotoxins[69] and as carriers for photosynsitive active molecules.[68]

Another demonstrated direct application of the peptide nanotubes is the formation of coaxial nanocables, where the nanotube served the role as the isolating middle layer.[71] In this approach an extra amino acid containing a thiol group that enabled the attachment of discrete gold nanoparticles was introduced in the monomers. After the reduction of silver inside the cavity of the PNT's the reduction of gold from the solution formed a continues layer of gold on the outside of the nanotube from the discrete nanoparticles as illustrated in figure 1.3c.

The PNT's have furthermore been utilized in the fabrication of composite materials as a filler to achieve better material properties corresponding to the native polymer. PNT's have for instance been utilized to enhance the ion transport properties of solid polymer electrolytes[75] and increase the mechanical strength of an epoxy.[76]

Indirect Applications

In indirect applications the material properties and long term stability is of minor importance since the PNT's are only utilized as a scaffold structure in a fabrication process. In one of the first reports on the use of PNT's[3] the formed tubular structures were utilized as a template for the reduction of silver ions which eventually formed a silver nanowire.[3] However, the process behind the formation of the silver wire has been questioned in recent yars.[77] In another work the PNT's have been utilized as a scaffold material for the realization of hollow TiO_2 nanotubes.[78]
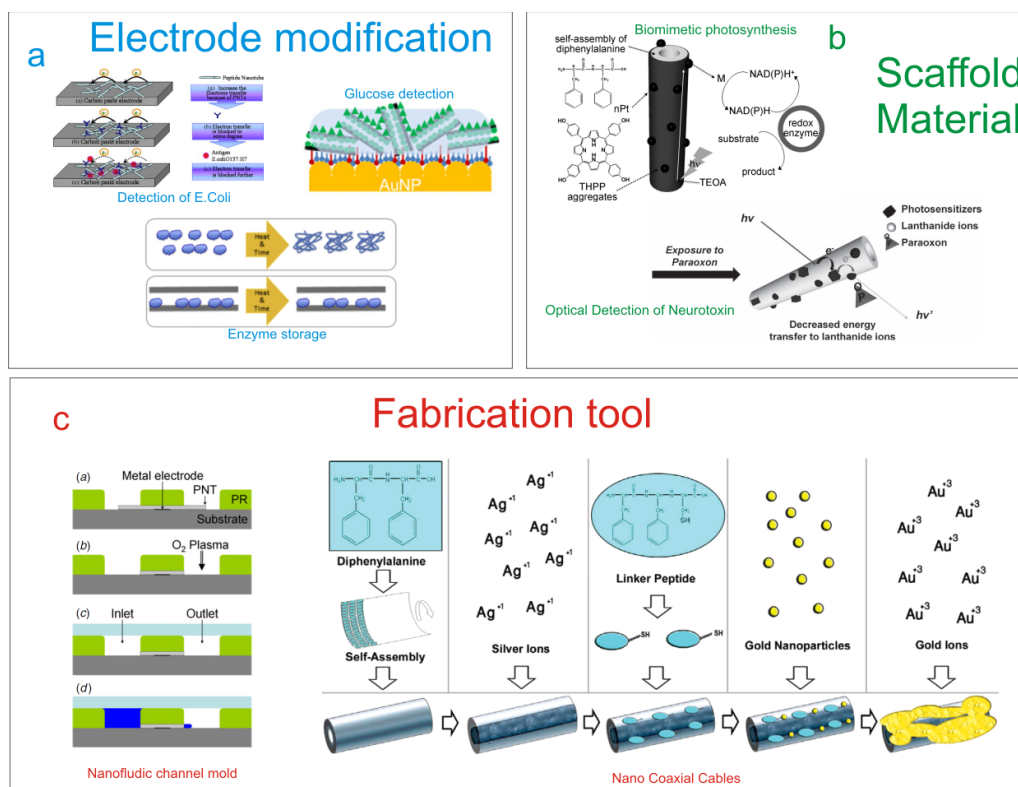
Figure 1.3: *Illustration of different applications of the FF PNT's. The most widely used direct application of the PNT's is as an electrode modification material to increase the surface area of the electrode and hence increase the sensitivity of the electrochemical measurements as illustrated in a. Another direct application of the PNT's is as a scaffold material for a biomimetic photosynthesis system and an optical biosensor is illustrated in b. Finally examples of the PNT's as a fabrication tool are illustrated in c. Reprinted with permission from.*[65–71]

Finally PNT's has been utilized as a scaffold for the fabrication of nanofluidic channels directly in a photoresist polymer as seen in figure 1.2c.[70]

The PNT's provide an easy and quick way of realizing nanostructured objects in a low cost approach. Therefore they have also been utilized as a template material to transfer the nanostructure geometry to other materials. However, before one is able to rely on the PNT's as a fabrication tool a controlled way of manipulating the structures must be developed. This will be the focus of chapter 4.

Diphenylalanine Peptide Nanotubes

The dipeptide FF can, as presented in the previous chapter, form a range of different structures with very different characteristics and properties depending on the formation conditions. When dissolved in water either directly using sonication[79] or from a stock solution in HFP[3,71] the dipeptide self-assemble into nanotubes with a hydrophilic core and outer shell.[6,77] On the other hand, when grown from a thin film in the present of analine vapor in the absent of water, the dipeptide form a forrest of nanofibers[14,20] with distinct different properties and characteristics than the corresponding nanotubes.[79]

In the present work focus has been placed on the nanotubes and the applications of these. Therefore in this chapter and the remainder of the thesis focus will be on the characteristics of the PNT's and the aggregates formed from these. The peptide nanowires will only be introduced to highlight the diversity of the structures formed from identical monomers.

2.1 Structure

The overall properties of the assembled PNT's and the larger microcrystals are strongly depended on the organization and interactions of the individual FF monomers. Therefore before the properties of the structure are investigated in more details the internal structure of these assemblies will be discussed.

2.1.1 Structural Organization

Originally it was proposed that the peptide monomers in the self-assembled PNT's were arranged in β sheets[3] similar to the assemblies of traditional amyloid fibrils.[4,5] This was supported by experimental data from Fourier transform infrared spectroscopy and congo red staining experiments.[3] The assumption arose from the original notion that the FF dipeptide was the central structural motif of the amyloid fibril Aβ42.[3] The presence of these fibrils in the brain is as mentioned above related to the Alzheimer's disease.

The FF monomers consist as previously mentioned of two phenylalanine amino acids as seen in figure 2.1a. The two side groups are highly hydrophobic and the peptide backbone is highly hydrophilic. Therefore if the hydrophobic side chains arrange so that they are at the same side
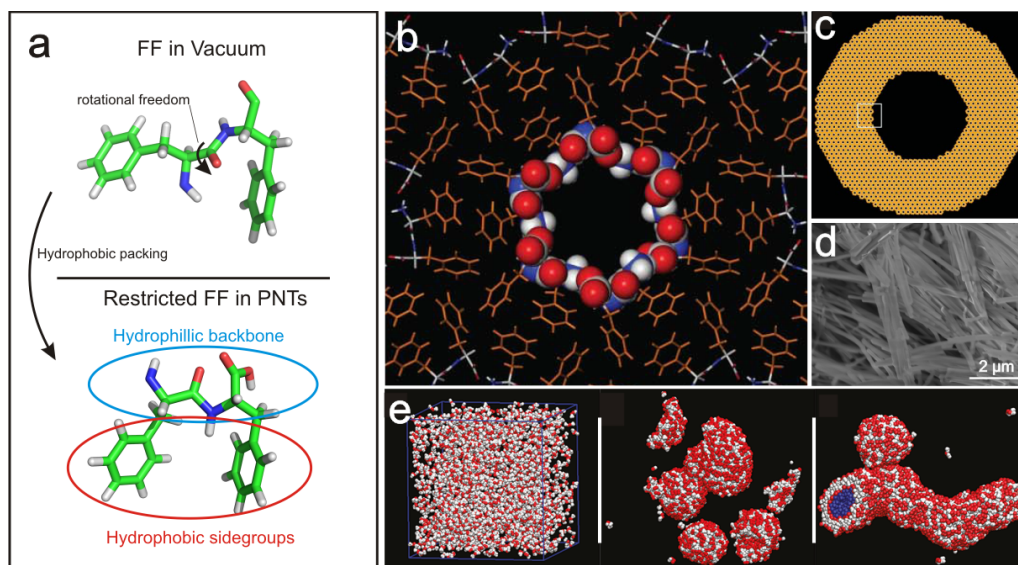
Figure 2.1: *In vacuum the two side groups of the FF molecule will be located on either side of the peptide backbone as illustrated in the top part of a. However, there is rotational freedom around the peptide bond indicated with θ in the figure so that the side groups can rotate to the same side of the backbone. This configuration gives rise to a molecule with a larger hydrophobic part and a smaller hydrophilic part. When submerged in a polar solvent this configuration is entropically favorable since the hydrophobic sidegroups can be shielded from the polar solution by the formation of double layered nanotubes as seen in b and e. The further aggregation of these nanotubes to increase the shielding effectiveness leads to the formation of the PNT's illustrated in c. In d a SEM image of these formed structures is shown. b and c is adapted from [77] and e is adapted from. [23]*

of the backbone the monomer will have a hydrophobic side and a hydrophilic side. When diluted in water the hydrophobic parts of the monomers would prefer to be shielded away from the polar water molecules forming structures similar to micelles. Due to the packing parameter the peptide monomers will be arranged in nanotubes with a hydrophilic core and surface. The hydrophobic sidechains are packed inside the wall of the individual PNT's as illustrated in figure 2.1b and confirmed by molecular dynamic (MD) simulation as seen in 2.1e.[23] This organization theory has been supported by single crystal x-ray diffraction experiments,[10] x-ray powder diffraction experiments[77] and molecular dynamics simulations.[23] The position of the two sidechain on the same side of the backbone results in an unusual torsion angle between the two amino acids (The rotational angle around the amide bond linking the two amino acids shown as θ in figure 2.1a) in the order of 0° representing a higher energy state than the ground level. However this is compensated by the possibility of limiting the contact between the hydrophobic sidechains and the polar water molecules and therefore an overall increase in entropy.[6] In fig. 2.1b an illustration of the suggested organization of the peptide monomers is shown which illustrates how the sidechains on the PNT's are shielded away from the hydrophilic core of the individual nanotubes and the core of the larger super assembly. This information was supported in molecular dynamics simulations where the FF monomers were randomly placed in a box with periodic boundary conditions as seen in figure 2.1e. In less than two μs the formation of the PNT's was observed[23] underlining the fast formation process also observed experimentally. In fig. 2.1c it is illustrated how the formed PNT's pack further together in the formation of the larger nanotubes and microstructures. This later aggregation of the individual PNT's into larger microstructures is a slower process than the formation of the individual nanotubes. The further aggregation of the individual PNT's is confirmed in the MD simulation shown in fig. 2.1e in this case through the interaction of a formed
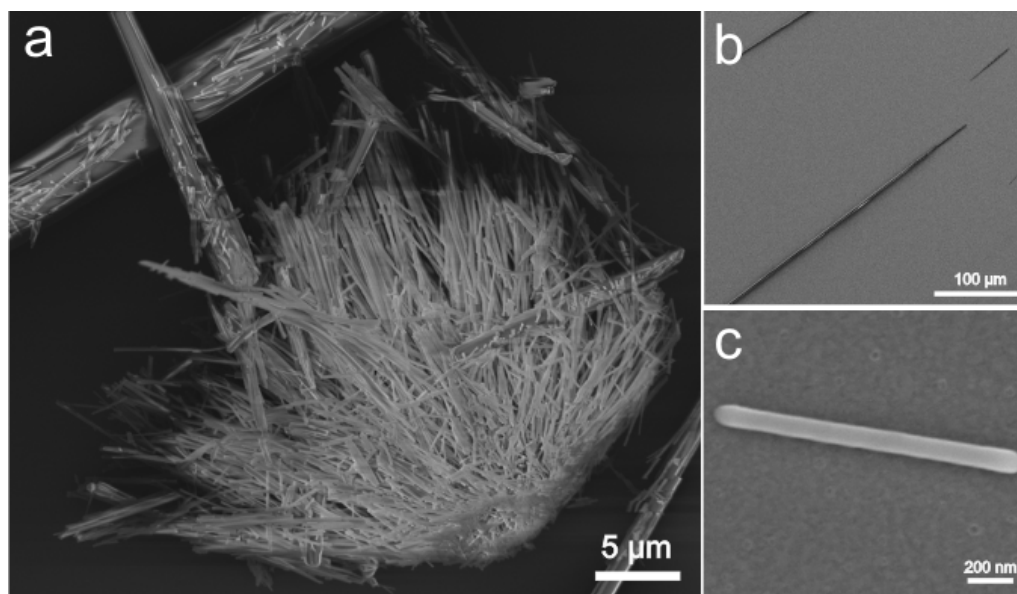
Figure 2.2: *Images of the FF PNT's. In a an assembly of the PNT's is shown. In this SEM image both the smaller PNT's (also seen in c) and the larger supra assemblies of these (also seen in b) is shown. In this image also the interaction between the smaller PNT's in the formation of the larger structures can be seen. Regardless of their size the tubes formed from the FF peptide appear strong and stiff evident by the straight nature of the structures.*

nanotube and a spherical structure. The aggregation of the formed PNT's further reduces the entropy of the system since the shielding of the hydrophobic sidechains in the individual PNT's is not sufficient. Therefore energy can be gained by fussing two or more of these individual nanotubes into larger supramolecular structures, while the water columns inside the individual PNT's remains.

2.1.2 Dimensions

As stated above the FF monomers initially assemble into individual PNT's that further aggregate into larger nano and microstructures. The diameter of these individual nanotubes is less than 2 nm. These structures are however not observed under dried conditions and therefore all of the characterization conducted and the suggested application is based on the larger supra assemblies and not the individual nanotubes. By tradition these supramolecular structures are referred to simply as PNT's regardless of their size. For simplicity this notion will be adopted in the present thesis.

The fact that the structures seen in SEM and TEM analysis are the larger supra assemblies also explains the wide range of different sizes and tubular shapes reported, ranging from the smallest structures like the one seen in figure 2.2c with a diameter around 100 nm to the larger giant structures with diameters of several μm's as seen in figure 2.2b. Despite the difference in size all of these structures show the same overall conformation indicating that they share the same building block namely the individual nanotubes. The internal van der Valls diameter of the individual nanotubes has been determined by x-ray crystallography to be 0.92 nm.[6] The water inside these central coloumns is crystallographic water meaning that it is an integral part of the structure and hence cannot be removed easily from the structures either by heating or vacuum. The larger supramolecular structures in fact consist to a large degree of such water columns. The formation of these supramolecular structures is a dynamic process, where over time, the average size of the structures in a given solution tend to increase. The presence of the central water columns has

furthermore been confirmed using electrostatic force microscopy,[34] where a change in the electrical signal indicates a local change in the dielectric properties of the material.

In figure 2.2a-c SEM images of the different sized FF PNT's are seen. From this figure it is obvious that the PNT's tend to be rigid and straight indicating that the stiffness of these structures is very high. Furthermore no branching has been observed in the PNT's at any point in contrast to many other self-assembled structures.

The dimension of the supramolecular structures is, as mentioned above, governed by the incubation time, namely the age of the solution. To obtain smaller peptide structures one should be sure to prepare fresh solution prior to experiments. The formed structures furthermore vary with relation to the central core of the microtubes. This behavior underlines the organizational theory proposed and verified by Görbitz.[6, 10, 77]

2.2   Physical Characteristics

In this section the physical characteristics of the assemblies will be presented and discussed. Some of the characteristic properties inherited from the individual monomers, some from the individual PNT's and some from the interplay between all of these components. Again as mentioned above the focus of this characterization will be on the larger assemblies rather than on the individual PNT's, since these will not be observed in experiments and hence will not have any practical applications.

2.2.1   Mechanical properties

The appearance of the PNTs in for instance SEM, as seen in figure 2.2, suggests that the PNT's are strong and rigid structures. In two different experiments the mechanical properties of the PNT's have been investigated.[80, 81] The two independent experiments both conducted with an AFM yielded rather similar results. In[7] a general introduction to these different characterization approaches can be found. In the studies a the stiffness of the tube was estimated to 160 N/m[80] independent on the tube dimensions and a Young's modulus of 19 GPa[80] and 27 GPa.[81]

The modulus was estimated for a range of temperatures and at temperatures beneath 100°C the modulus dropped with increasing temperatures. Above this temperature the nanotubes lost their structural confirmation probably due to reorganization of the peptide backbone in the individual monomers as reported elsewhere.[82, 83] The thermal stability of the formed nanotubes will be discussed in more details below. The humidity did not seem to change the properties of the nanotubes in any predictable manner.

2.2.2   Electrical Characteristics

The main application of the PNTs in previous reports has been as an electrode modification material for the increase of the active surface area and hence increase the sensitivity of the sensor. Therefore the electronic properties of the PNT's are highly relevant to study and have been the subject of previous work.

Initially the direct conductivity of the formed structures has been measured in a two electrode setup indicating that the PNT's as most biological materials are somewhat isolating.[84] In this work the PNT's were immobilized on gold electrodes and the current-voltage relationship for both single peptide tubes and bondles of tubes was recorded. In both cases only a few pA's were recorded at a potential difference of a few volts.[85] A slightly higher conductance has been observed for the peptide nanowires.[86] The charge transfer in the individual peptide monomers has been reported to be on the order of the transfer in inorganic structures such as CNT's.[87] However the weak link

in the PNT's is the coupling between the individual monomers in the PNT's and therefore the conductance of these structures is not comparable to that of the inorganic structures such as the CNT's.

Stability of the Peptide Nanotubes

3.1 Introduction

The initial focus of the present project was the development of biosensors, such as Biological Field Effect Transistors (BioFET), and drug delivery systems based on the PNT's. In this context the stability of the PNT's in liquid is vital. In a previous report the chemical and thermal stability of the PNT's was investigated.[83] However, in this work only dried samples of the PNT's were investigated and hence no real information regarding the stability in solution is gained. In the article below the stability of the PNT's in solution is investigated using a combination of optical microscopy, mass spectrometry and high pressure liquid chromatography experiments. To compare these results with the previously published work[83] it is important to keep the structures and the fast formation of the PNT's, described in the previous chapter, in mind.

3.1.1 A Note on Thermal Stability

The ability of the peptide nanotubes to handle elevated temperatures greatly depends on whether the peptides are in a dried condition or in a solution. The concentration at which the peptide nanotubes form is affected by the temperature of the solution, when the solution is heated the critical concentration increases and the already formed peptide nanotube structures start dissolving until the critical concentration of the monomers in solution is reached, whereby equilibrium once again is established. Therefore the thermal stability of the structures in solution is simply a question of the critical concentration of the monomers in that particular solution at a given temperature. This is also evident from the alternative formation process of the peptide nanotubes in which the peptide monomers are dissolved in a heated water solution under sonication.[24] The critical concentration of the monomers is higher at this elevated temperature and the PNT's form once the solution is cooled and the critical concentration as an effect of this decreases. Previously the thermal stability in solution has been studied and it has been published that the peptide nanotubes remain stable even at elevated temperatures (up to 120°C).[83] However as the peptide nanotubes are only studied in a dried state the peptide nanotubes are able to form in the evaporation process even if it is very rapid. Keep in mind that the peptide nanotubes form in less than a second.[23,77] Therefore in principle only the chemical stability of the individual monomers have been studied
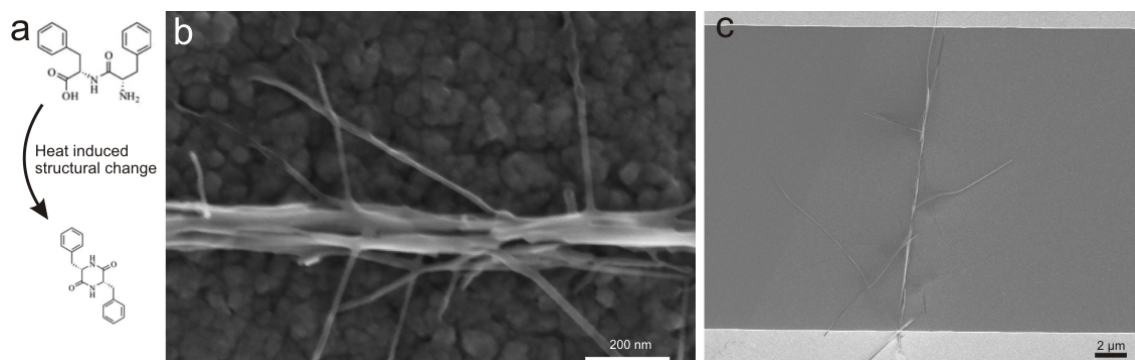
Figure 3.1: *Illustration of the structure formed when heating a dried peptide nanotube. The structural conformation change of the FF monomer, illustrated in **a**, induces a difference in the geometry of the peptide nanotube splitting the PNT's into smaller entities as seen in the SEM images shown in **b**. The dimensions of the newly formed structures are orders of magnitude smaller than that of the unmodified PNT's.*

in the previous work.[83] In agreement with the studies of dried structures they remain stable at temperatures of 121°C and below.

In the article below the stability of the peptide nanotubes in solution is investigated. In dried conditions the situation is different. In fact several studies has investigated the thermal stability of the formed and dried peptide nanotube structures. When the nanotubes are in a dried state their properties are remarkably different. At temperatures below 100°C the peptide nanotubes remain stable and the structural conformation is not affected by the heating procedure. However at elevated temperatures changes are observed even below the melting point of the structure, which is around 300°C,[83] as seen from the SEM images in Figure 3.1. The change in structural conformation seen in these images arize from a cyclization of the linear peptide backbone in the individual monomers as illustrated in Figure 3.1a. In this process the carboxylic - and the amino group reacts. The structural change was originally demonstrated with a range of x-ray techniques by Amdursky *et al.*[88] and later confirmed by 1D and 2D NMR studies by Jaworsky *et al.*[89] The structural change of the peptide monomers split the larger aggregates up into smaller entities as seen in the figure.

Stability of diphenylalanine peptide nanotubes in solution†

Karsten Brandt Andersen,[a] Jaime Castillo-Leon,[a] Martin Hedström[b] and Winnie Edith Svendsen*[a]

Over the last couple of years, self-organizing nanotubes based on the dipeptide diphenylalanine have received much attention, mainly as possible building blocks for the next generation of biosensors and as drug delivery systems. One of the main reasons for this large interest is that these peptide nanotubes are believed to be very stable both thermally and chemically. Previously, the chemical and thermal stability of self-organizing structures has been investigated after the evaporation of the solvent. However, it was recently discovered that the stability of the structures differed significantly when the tubes were in solution. It has been shown that, in solution, the peptide nanotubes can easily be dissolved in several solvents including water. It is therefore of critical importance that the stability of the nanotubes in solution and not after solvent evaporation be investigated prior to applications in which the nanotube will be submerged in liquid. The present article reports results demonstrating the instability and suggests a possible approach to a stabilization procedure, which drastically improves the stability of the formed structures. The results presented herein provide new information regarding the stability of self-organizing diphenylalanine nanotubes in solution.

1. Introduction

Self-organizing peptide nanotubes can be employed in a large number of intriguing applications ranging from building blocks in the fabrication of new types of biosensors, such as a Biological Field Effect Transistor (BioFET), over drug delivery systems, to the chemical modification of electrodes.[1–6]

Peptide nanotubes based on the self-organization of the dipeptide diphenylalanine (FF) have received much attention as a promising nanostructure. Previously, it has been shown that self-organizing nanotubes based on these particular dipeptides display a high Young's modulus and bending stiffness.[7,8] Recently, their electrical and structural properties were investigated in our group.[9,10] Furthermore it has been published that they are thermally stable up to 80 °C[11,12] and that they are also chemically very stable.[13] However, the latter result was obtained based on a study of *dried* samples of peptide nanotubes, for which reason investigation did not reveal information concerning the chemical stability of the peptide nanotubes when submerged in solution.

This article presents recent results demonstrating that peptide nanotubes can be dissolved in most liquids, including water. In contrast, peptide nanotubes have previously been found to be stable in most solvents. However, the previous data was obtained from the observation of dried droplets of peptide solutions and, therefore, any knowledge of the stability of the nanotubes in a liquid environment was lost. Hence, new investigations of the stability of the peptide nanotubes in solution are required. Within the framework of the present study, tests were performed on the stability of the nanotubes in various solutions ranging from organic solvents to buffer liquids, including Phosphate Buffered Saline (PBS), which is a commonly employed biological buffer and therefore highly relevant for biomedical applications.

Various descriptions of the self-organizing process for the peptide nanotubes exist in literature. The two governing hypotheses include the dipeptide monomers first forming a sheet and then rolling up to form nanotubes,[5,6,14] and the dipeptides arranging themselves into hydrophobic-hydrophilic rods which interact to form larger superstructures.[15–17] The information gained from the study of the dissolution process can assist in the understanding of the formation process since it is easier to monitor the former rather than the latter.

An interesting application involving the peptide nanotubes is the possibility of reducing silver within the nanotubes to increase their ability to conduct current.[5,6] However, the layer of peptides covering the silver nanowire after the reduction process significantly raises the contact resistance between the silver wire and the contact pads. Dry etching clean room processes have been suggested as a possible means for removing the dipeptide nanotubes from the contact area.[2] At the end of the paper we will suggest a simpler method for the removal of the peptide nanotubes.

2. Experimental section

2.1. Materials and chemicals

The FF peptide was purchased from Bachem (Cat. no. G-2925, Germany). All other chemicals were purchased from Sigma-Aldrich.

The optical microscope images were obtained using an inverted microscope (Olympus IX51) and all the dissolving experiments were conducted in 1.5 ml microwells purchased from Nunc A/S.

[a]DTU - Nanotech, Technical University of Denmark, Lyngby, Denmark. E-mail: winnie.svendsen@nanotech.dtu.dk; Fax: +45 4588 7762; Tel: +45 4525 5731
[b]Department of Biotechnology, Lund University, Lund, Sweden

2.2. Preparation of the peptide nanotubes

The peptide nanotubes were all formed from a stock solution of FF monomers. The stock solution was prepared by dissolving the FF peptide powder in the alcohol 1,1,1,3,3,3-hexafluoro-2-propanol (HFP) at a concentration of 100 mg/ml. A fresh stock solution was prepared prior to the experiments. In order to form the nanotubes, the stock solution was further diluted in water to a final concentration of 2 mg/ml and aged for a day during which period the nanotubes were formed. The peptide structures were formed in acidic conditions in diluted hydrochloric acid.

2.3. Fixation of the nanotubes

An important part of the study was the possibility of observing the nanotubes when placed in a solution. Such a controlled monitoring of the nanotubes in a liquid environment was enabled by fixing them to the substrate before introducing the solvent in question. In these experiments, a 10 μl drop of the peptide solution at a concentration of 2 mg/ml was dried in a microwell under vacuum conditions at room temperature. Control experiments showed that tubes dried under atmospheric pressures showed similar results, see the supplementary material. The microwell containing the dried sample was then placed under an inverted microscope and the peptides were monitored continuously as fresh solution was dispersed on top of the dried nanotubes.

2.4. Optical observation of the dissolving process

In these experiments a 10 μl drop of peptide solution (2 mg/ml) was dried as described above. To test the stability of the peptides in various solvents, 1 ml of the solvent was added to the microwell and the peptide structure was monitored using an optical microscope. To verify that the heat generated by the light from the inverted microscope did not influence the obtained results, parallel experiments were performed outside the inverted microscope. These experiments showed equivalent results, and it could thus be concluded that the generated heat in the liquid did not affect the results presented below.

2.5. HPLC experiments and mass spectrometry

To confirm observations from the optical microscopy, high pressure liquid chromatography (HPLC) as well as mass spectrometry (MS) analysis was performed on small samples of the fresh solution dispersed on top of the dried nanotubes at different times succeeding the addition of the solvents. If the peptide nanotubes became dissolved, the corresponding peak should increase over time. The solutions analyzed using HPLC were taken during the dissolution experiments as explained above. MS determinations of the peptide nanotubes (PNTs) were performed using turbo ion ® spray MS (QSTAR ®,-i-Q-TOF tandem mass spectrometer, PE Sciex, Toronto, Canada) connected in series to a HPLC system from Perkin Elmer (Boston, USA). The samples (≈ 10 μl) containing the FF monomers having gradually increased contact times with the solvents studied were serially injected *via* the LC autosampler. The mass spectrometer was set to positive ion mode with a needle voltage of +5500V and the quadrupole system was set to scan m/z 200–

1000 in TOF-MS mode whereas for product ion mode (*i.e.* MS/MS) a range of m/z 50–1000 was chosen. Analysis of the MS data was performed using the software Analyst ®,QS (PE Sciex, Toronto, Canada).

3. Results

The diphenylalanine dipeptide will form two different structures when mixed with water. In the solution both peptide nanotubes and larger microcrystals consisting of these peptide nanotubes will form. In Fig. 1 the two structures formed by this material are illustrated. In this figure also the interaction between the nanotubes and the larger microcrystal structures can be seen, as the nanotubes tend to attach to the sides of the larger microcrystals. In the inset an image of a single peptide nanotube is shown in order to better distinguish its size.

In the initial experiments, the stability of the peptide nanotubes in solution was investigated using solvents in which the nanotubes have previously been shown to be stable.[13] The microcrystals were monitored under the microscope immediately after the solvents had been added to the dried samples. In order to better be able to visualize the dissolution process the dissolving of the larger microcrystals was monitored in this part of the investigation. However, later the dissolution of the nanotubes will be followed by the monitoring of the concentration of the dipeptide monomers. Images of the nanotubes were taken at fixed intervals during the dissolution process, and Fig. 2 displays optical images from some of these experiments. As can be seen, the stability of the nanotubes was very different in solution as compared to previously published results. The nanotubes were found to dissolve in most of the tested solvents. Furthermore, the dissolution time of the peptide nanotubes differed drastically between the solutions. Images from long-term monitoring of the peptide tubes are available in the supplementary material. It was found that the peptide nanotubes seemed stable only in acetonitrile and PBS saturated with peptide monomers. Nevertheless, it should be noted that the peptide structures should be stable in
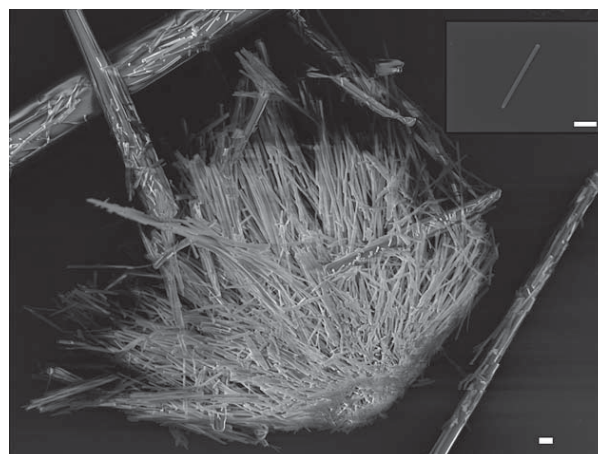

Fig. 1 SEM image to show the different structures that the dipeptide diphenylalanine is able to form. In this image the larger microcrystals also formed by diphenylalanine are visible along with a pile of peptide nanotubes. The inset shows a single peptide nanotube. The scale bars in both images correspond to 1 μm.
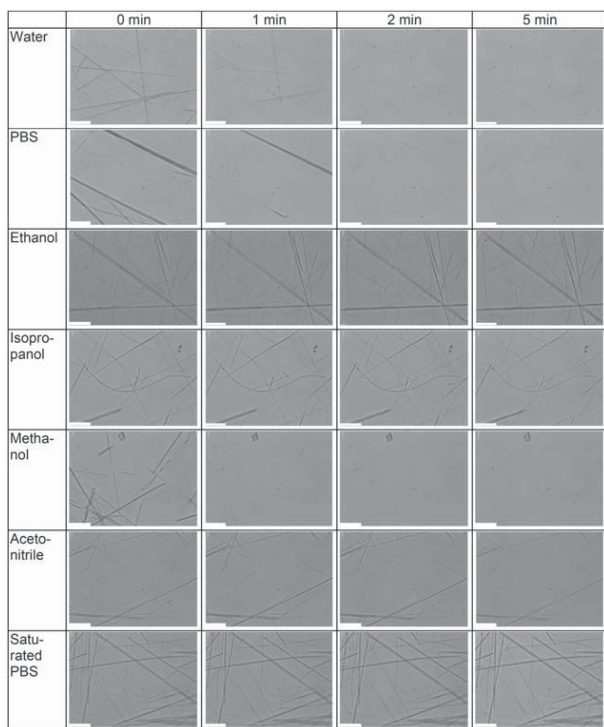
Fig. 2 Microscopy images of the dissolving peptide nanotubes in distilled water, PBS (pH 7,4), ethanol, isopropanol, methanol, acetonitrile and a PBS (pH 7,4) solution saturated with peptide monomers. From these images, the nanotubes were found to dissolve in many of the solutions in which it has been claimed that they were stable. All scale bars in the images correspond to 20 μm.

any saturated solution; PBS was merely used for illustrative purposes since the peptide tubes dissolved quickly in the non-saturated solution.

To confirm the results from the optical investigation, HPLC/MS experiments were conducted. If the results presented above were correct and the peptide nanotubes indeed dissolve when submerged in solution, the concentration of peptide monomer should increase over time from zero to a saturated concentration level in the liquid covering the dried nanotubes. Therefore, a way to confirm the results presented above would be to monitor the concentration of the peptide monomers as a function of time. Fig. 3 plots the amplitude of the HPLC peak corresponding to the peptide monomers dissolved in solution as a function of time. From this figure, it was clear that the amplitude of the peak and hence the concentration of the monomers did in fact increase over time and hence that the peptide nanotubes dissolves. By using MS, it was confirmed that the HPLC peak increasing in intensity over time corresponded to the FF monomers. The data from these experiments can be seen in the supplementary material online.

In order for the peptide tubes to be successfully incorporated into a variety of sensor systems, it is essential that their stability in solution becomes increased so that they remain intact longer when submerged in the liquid. Thus, it was studied how a change in the formation conditions affected the stability of the formed structures. The results showed that the structures formed in an acidic environment demonstrated an increase in stability over
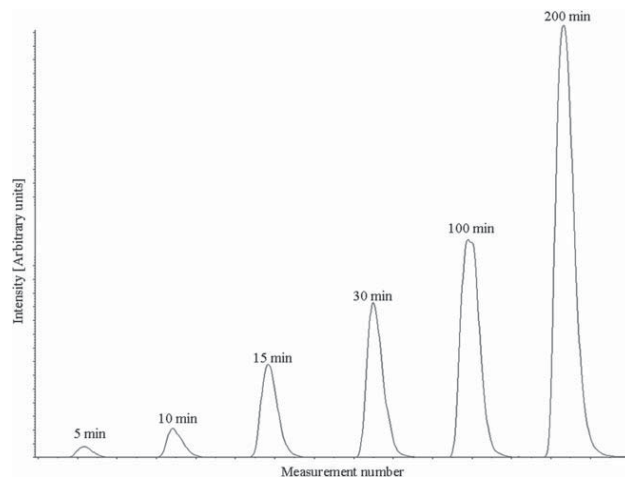
Fig. 3 An example of data from the HPLC experiments, performed to confirm the results presented in Fig. 2. Here the concentration of the FF monomers was monitored in an aqueous solution. The horizontal axis should not be seen as an expression of the dissolution time (but rather as the actual duration of the measurements). However, from the above figure, it is clear that the concentration of the FF peptide monomers increased as the peptides were dissolved in the fresh solution.
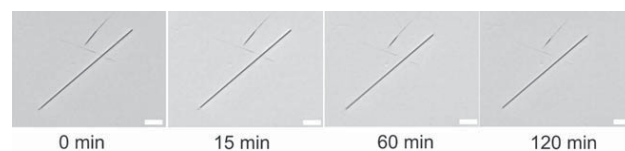
Fig. 4 Optical images of the dissolution process of peptide structures, formed at pH 3, submerged in PBS. It was clear that the tubes showed a tendency to be more stable when formed in a more acidic environment. All scale bars corresponds to 20 μm.

time. However, it should be noted that the exact structural conformation of these is still not known. Fig. 4 presents a number of optical images of the dissolution process of peptide structures formed at pH 3 submerged in PBS. This dissolution process should be compared to standard tubes becoming dissolved in PBS, as presented in Fig. 2. As can be seen from these images, the tubes showed a tendency of being more stable when formed in a more acidic environment. When formed in the most acidic environment, the tubes were found to be stable in the solution for up to several hours. It should be noted that the number of tubes formed in a given solution was strongly dependent on the pH of that particular solution. From the performed experiments, one can see that when formed at a pH between 5 and 6 the density of tubes is highest. In more acidic solutions, much fewer peptide tubes were formed and the formation process was significantly slower. At pH 3, for instance, the peptide solution had to age for several days before the tubes were completely formed.

4. Discussion

The results presented above have revealed new information with regard to the chemical stability of the peptide nanotubes. It was demonstrated that the peptide nanotubes could be dissolved in

most solvents including water and PBS. Many of the applications in which nanotubes are planned to play a central role involve their submersion in a solvent. An example of such use could be BioFET or cargo vehicles designed for drug delivery.

The dissolution effect observed in the optical microscope was confirmed by HPLC/MS experiments. Here, it was seen that the concentration of FF monomers increased over time in a fresh solution added to the dried peptide structures. The fact that the concentration of the monomers increased continually over time confirmed that the peptide structures became dissolved; otherwise, the concentration of monomers would be constant as a function of time. Through MS analysis, it was determined that it was the concentration of the FF monomers that increased over time.

The above mentioned results suggest that the formation of self-organizing peptide nanotubes was a question of solubility of the peptide monomers in the various solutions. When the concentration of the peptide monomers exceeded the solubility limit of peptide monomers, peptide nanotubes were formed. Naturally, the solubility of the peptide monomers varied with the type of solution. When a fresh solution was added to a dried sample of peptide nanotubes, the latter became dissolved due to the same effect. Initially, the concentration of peptide monomers in the fresh solution was zero, and as long as the concentration of monomers remained below the solubility of peptide monomers, the nanotubes continued to dissolve and eventually disappeared.

The previous section demonstrated that it was possible to drastically increase the stability of the peptide tubes by altering the formation process. This represents a means of obtaining a sufficient stabilization of the peptide tubes in order for them to be useful in a variety of applications. We have shown tubes that remained unaffected by the dissolution process for more than two hours in a PBS solution, whereas tubes formed in the standard approach disappeared after only a couple of minutes, as evidenced in the experiments. This was indeed very promising since a further optimization of the parameters involved in the formation process might result in even more stable tubes.

The time it took to form the peptide tubes varied significantly with pH, as was mentioned above. This might prove useful in future applications since the formation of peptide tubes in distilled water might lead to additional peptide tubes forming in the evaporation phase. This, in turn, could give rise to tubes at unwanted places after a completed manipulation. However, for the tubes formed in the acidic solution, the formation process would be so slow that no new tubes should form in the evaporation phase. Hence, when a tube in solution has been positioned at the place of interest, no formation of new tubes occurs when the solution is evaporated, thus rendering the manipulation of the peptide far more simple. It should be noted that the structural details of the structures formed in the acidic environment is still unknown. Therefore whether they are in fact nanotubes or rather nanowires is a subject for further investigation.

In this work, only the pH of the solution was varied, however many other parameters in the formation process may influence the properties of the tubes. When the peptide monomers are dissolved in distilled water, as described in the standard process for tube formation,[6] the pH of the solution actually dropped to around pH 5. It was demonstrated that the tubes formed at this pH were the most unstable (even though the amount of formed tubes was much larger), which indicates that the standard production approach results in the most unstable structures. Therefore, it is strongly suggested that the parameters of the formation process be investigated further and in particular that a new standard fabrication process be developed.

The results presented by Adler-Abramovich et al.[13] can also be explained by this description of nanotube formation. These authors mainly studied peptides after solvent evaporation. In this case, the peptide nanotubes will form in the evaporation phase even though they are not present in the solution. This is due to the concentration of the monomers increasing as the solvent evaporates. Our experiments also confirmed that nanotubes reformed in the evaporation phase.

The results presented in this article may explain some of the difficulties with these peptide nanotubes according to prior publications. In the work by Ryu et al.,[18] the authors stated that the stability of the peptide nanotubes could not be investigated as a result of the nanotubes detaching from the surface they were placed on when emerged into the solvent. These observations can be explained by the fact that the nanotubes simply dissolved in the different solutions in which they were submerged. The fact that the peptide nanotubes dissolved in nearly all solutions can actually also be used in a wide variety of new and innovative applications. For instance, water could be used instead of the dry etching machines, as suggested previously,[2] in the process of achieving electrical contact between the contact pads and the silver wires reduced inside the peptide nanotube. Furthermore, the nanotubes could be employed as a mold in the fabrication of a nanofluidic channel connecting two reservoirs.

5. Conclusion

This article has presented the stability of diphenylalanine peptide nanotubes in solution, which differed significantly from previously published results regarding the stability under dried conditions. In particular, images of the peptide nanotubes dissolving in distilled water, PBS, ethanol, methanol, isopropanol and acetonitrile were shown.

It was argued that the dissolution of these peptides could be due to the final solubility of the peptide monomers in the respective solutions. In particular, the nanotubes were found to be stable in a saturated solution, which confirms this hypothesis.

In many potential applications, the peptide nanotubes will be exposed to a solvent. The present investigation is thus of great importance since it proves that the stability of the peptide nanotubes in solution differs from that of the same structure under dry conditions. From this, it is clear that an emphasis should be put on the stabilization of the peptide nanotubes in order to expand the field of possible applications for this material.

The present article has also shown that the stability of the peptide tubes could be increased by simply forming them under, for instance, varying pH conditions of the solution. In particular, it was demonstrated that tubes formed at low pH were more stable than their counterparts formed in the standard fabrication approach used previously. Such a dramatic increase in peptide stability is indeed a promising result. However, room for optimization remains with regard to the formation parameters, which may result in even longer stabilization.

Acknowledgements

References

1 A. L. Briseno, S. C. B. Mannsfeld, S. A. Jenekhe, Z. Bao and Y. Xia, *Mater. Today*, 2008, **11**, 38–47.
2 N. B. Sopher, Z. R. Abrams, M. Reches, E. Gazit and Y. Hanein, *J. Micromech. Microeng.*, 2007, **17**, 2360–2365.
3 M. Yemini, M. Reches, E. Gazit and J. Rishpon, *Anal. Chem.*, 2005, **77**, 5155–5159.
4 E. C. Cho, J.-W. Choi, M. Lee and K.-K. Koo, *Colloids Surf., A*, 2008, **313–314**, 95–99.
5 M. Reches and E. Gazit, *Science*, 2003, **300**, 625–627.
6 O. Carny, D. E. Shalev and E. Gazit, *Nano Lett.*, 2006, **6**, 1594–1597.
7 N. Kol, L. Adler-Abramovich, D. Barlam, R. Z. Schneck, E. Gazit and I. Rousso, *Nano Lett.*, 2005, **5**, 1343–1346.
8 L. Niu, X. Chen, S. allen and S. J. B. Tendler, *Langmuir*, 2007, **23**, 7443–7446.
9 C. H. Clausen, J. Jensen, J. Castillo, M. Dimaki and W. E. Svendsen, *Nano Lett.*, 2008, **8**, 4066–4069.
10 J. Castillo, S. Tanzi, M. Dimaki and W. Svendsen, *Electrophoresis*, 2008, **29**, 5026–5032.
11 V. L. Sedman, L. Adler-Abramovich, S. Allen, E. Gazit and S. J. B. Tendler, *J. Am. Chem. Soc.*, 2006, **128**, 6903–6908.
12 V. L. Sedman, S. Allen, X. Chen, C. J. Roberts and S. J. B. Tendler, *Langmuir*, 2009, **25**, 7256–7259.
13 L. Adler-Abramovich, M. Reches, V. L. Sedman, S. Allen, S. J. B. Tendler and E. Gazit, *Langmuir*, 2006, **22**, 1313–1320.
14 M. Reches and E. Gazit, *Nano Lett.*, 2004, **4**, 581–585.
15 C. H. Görbitz, *Chem.–Eur. J.*, 2001, **7**, 5153–5159.
16 C. H. Görbitz, *Chem. Commun.*, 2006, 2332–2334.
17 C. H. Görbitz and F. Rise, *J. Pept. Sci.*, 2008, **14**, 210–216.
18 J. Ryu and C. B. Park, *Biotechnol. Bioeng.*, 2010, **105**, 221–230.

3.2 Summary and Perspectives

In the article above the stability of the PNT's in solution was investigated and in contrast to previous study where only the dried samples of the PNT's were investigated it was demonstrated that the PNT's in fact dissolve in most liquids including water. This has tremendous effect on the current project since structures that are not stable under liquid conditions cannot be relied upon as the central component in a BioFET or similar biosensor as was the original goal of the project. Nor can it be used as a drug delivery system considering that in the blood stream the PNT's would dissolve within seconds (assuming it did not dissolve in the preparation process). Even though it seemed possible to increase the stability of the peptide nanotubes in solution by the formation of the structures in an acidic environment they still dissolved only in this case slower. In the remainder of the thesis focus will be on the application of the PNT's in situations where the solubility of the PNT's in water will be an advantage.

Initially after the publication of this article focus in the project was turned to the stabilization of the PNT's based on the approach described in the article and the crosslinking of the individual peptide monomers in the formed PNT's with molecules such as glutaraldehyde. However, despite the effort it was not possible to stabilize the structures completely. Instead of pursuing the route of changing the material properties of the PNT's it was decided to pursue new applications in which the material properties of the PNT's can be utilized. The first step in this was to fully understand the stability of the peptide nanotubes as described in the chapter below.

Clean Room Fabrication Tool

4.1 Introduction

In the previous chapter the stability of the PNT's in liquid was investigated. It was demonstrated that the formed PNT's dissolve in most liquids including water, rendering the use of such structures in direct applications challenging. This also explains why an external polymer matrix was required to keep the covalently linked structures in place at the electrode surfaces during the electrochemical measurements described in chapter 1. Despite the issue with the stability in liquid, PNT's still are a very interesting alternative as reinforcement to enhance the mechanical properties of a hybrid material.[75, 76] One should keep the solubility in mind when designing the hybrid materials. The solubility of the PNT's in water might in some cases actually be an advantage - namely when utilizing the structures indirectly as a sacrificial scaffold material or as a fabrication tool to transfer the geometry and dimensions of PNT's to other materials. In the remainder of the thesis focus will be on such indirect applications of the PNT's and the potential of the formed structures.

In the article below the stability of the PNT's under a bombardment with heavy ions is investigated to explore the potential use of the PNT's as a water soluble clean room masking material. In the final part of the paper the fabrication of silicon microwires based on a PNT mask is demonstrated as an example of the possibilities of this new type of masks.

Self-Assembled Peptide Nanotubes as an Etching Material for the Rapid Fabrication of Silicon Wires

**Martin B. Larsen · Karsten B. Andersen ·
Winnie E. Svendsen · Jaime Castillo-León**

Abstract This study has evaluated self-assembled peptide nanotubes (PNTS) and nanowires (PNWS) as etching mask materials for the rapid and low-cost fabrication of silicon wires using reactive ion etching (RIE). The self-assembled peptide structures were fabricated under mild conditions and positioned on clean silicon wafers, after which these biological nanostructures were exposed to an RIE etching process. Following this treatment, the structure of the remaining nanotubes and nanowires was analyzed by scanning electron microscopy (SEM). Important differences in the behavior of the nanotubes and the nanowires were observed after the RIE process. The nanotubes remained intact while the nanowires were destroyed by the RIE process. The instability of the peptide nanowires during this process was further confirmed with focused ion beam milling experiments. The PNTS could stand energetic argon ions for around 32 s while the PNWS resisted only 4 s before becoming milled. Based on these results, self-assembled PNTS were further used as an etching mask to fabricate silicon wires in a rapid and low-cost manner. The obtained silicon wires were subjected to structural and electrical characterization by SEM and I–V measurements. Additionally, the fabricated silicon structures were functionalized with fluorescent molecules via a biotin–strepta-vidin interaction in order to probe their potential in the development of biosensing devices.

1 Introduction

Biological nanostructures based on self-assembled peptides have been highlighted as very promising materials for various applications, including drug delivery, electronics, and energy storage, among others [1–3]. Compared to nanomaterials such as carbon nanotubes or silicon nano-wires, self-assembled peptides can be fabricated outside the clean room, under mild conditions, and in a rapid, low-cost process [4]. Their preparation in a microfluidic device was recently reported [5]. Diphenylalanine, (FF), the core recognition motif of Alzheimer's β-amyloid peptide, is a short dipeptide that self-assembles into 3D nanostructures (i.e., nanotubes, nanowires, or hydrogels) [4]. The manipulation, electrical and structural characterization, and the stability under liquid conditions of nanotubes formed by FF peptides were recently studied in our group [6–8]. These nanostructures can be easily functionalized [9]; FF nanotubes present extraordinary mechanical properties, and FF nanowires are resistant to thermal, chemical, and proteolytic attacks [10, 11]. All these properties make them promising materials to be used in micro- and nanofabrication processes.

Due to their optical, electrical, photonic, and mechanical properties, silicon wires are extensively used in electronics

M. B. Larsen · K. B. Andersen · W. E. Svendsen · J. Castillo-León (✉)
Department of Micro and Nanotechnology,
Technical University of Denmark,
Building 345 east, 2800 Kgs,
Lyngby, Denmark
e-mail: jaic@nanotech.dtu.dk
URL: www.nanotech.dtu.dk/Research/nanoSOM/nabis

🖄 Springer

Fig. 1 Comparison of the stability of self-assembled PNWS and PNTS after 1 min under an RIE process. SEM image after RIE of **a** a PNW and **b** a PNT
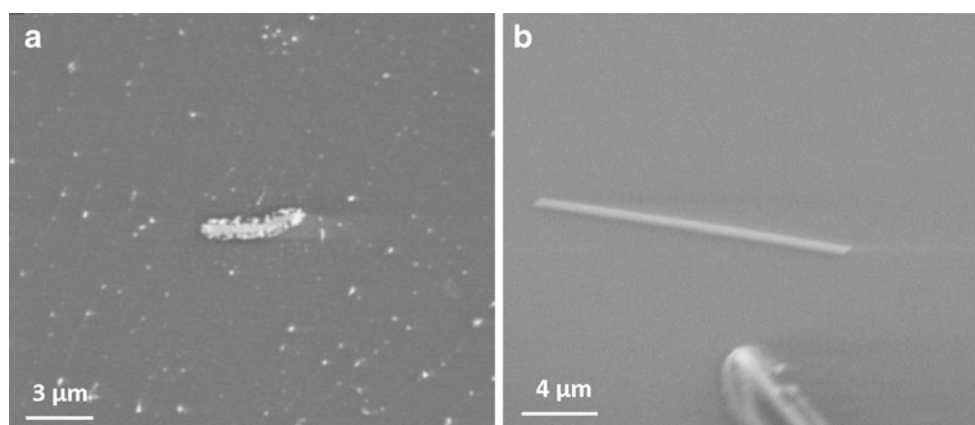
[12, 13], chemical and biosensor development [14], photonics [15, 16], and microelectromechanical systems [17, 18], among many other applications. Standard techniques for the preparation of silicon wires include top-down and/or bottom-up approaches [19–21]. These methods may include several steps, the use of specialized equipment and in some cases the application of high temperatures and/or pressures [22, 23]. All these conditions increase the fabrication time and costs.

A more simple and low-cost fabrication process that reduces the fabrication time is highly sought after. In this work, peptide nanotubes (PNTS) and peptide nanowires (PNWS) were used as etching mask materials to fabricate silicon wires in a less complicated and low-cost fashion by deep reactive ion etching (RIE). Deep RIE is a powerful top-down fabrication method extensively used to prepare 3D silicon structures [24–31]. The resultant materials were evaluated to prove that functional silicon structures could indeed be obtained using this technique, which thus

constitutes a simple, fast, and low-cost method for the preparation of silicon wires.

2 Materials and Methods

Fabrication of self-assembled peptide nanotubes and nanowires Diphenylalanine peptide was purchased from Bachem (cat. no. G-2925, Germany). Fresh stock solutions were prepared by dissolving the lyophilized form of the peptide in 1,1,1,3,3,3-hexafluoro-2-propanol (HFP) (Sigma-Aldrich) at a final concentration of 100 mg/mL. Fresh solutions were prepared before each experiment. Amyloid peptide nanotubes, PNTS, were obtained by dissolving aliquots of a concentrated diphenylalanine peptide stock solution in water.

Peptide nanowires, PNWS, were synthesized following a previously reported method [32]. In short, 10-μL drops of peptide solutions in HFP of concentrations ranging from 0.05
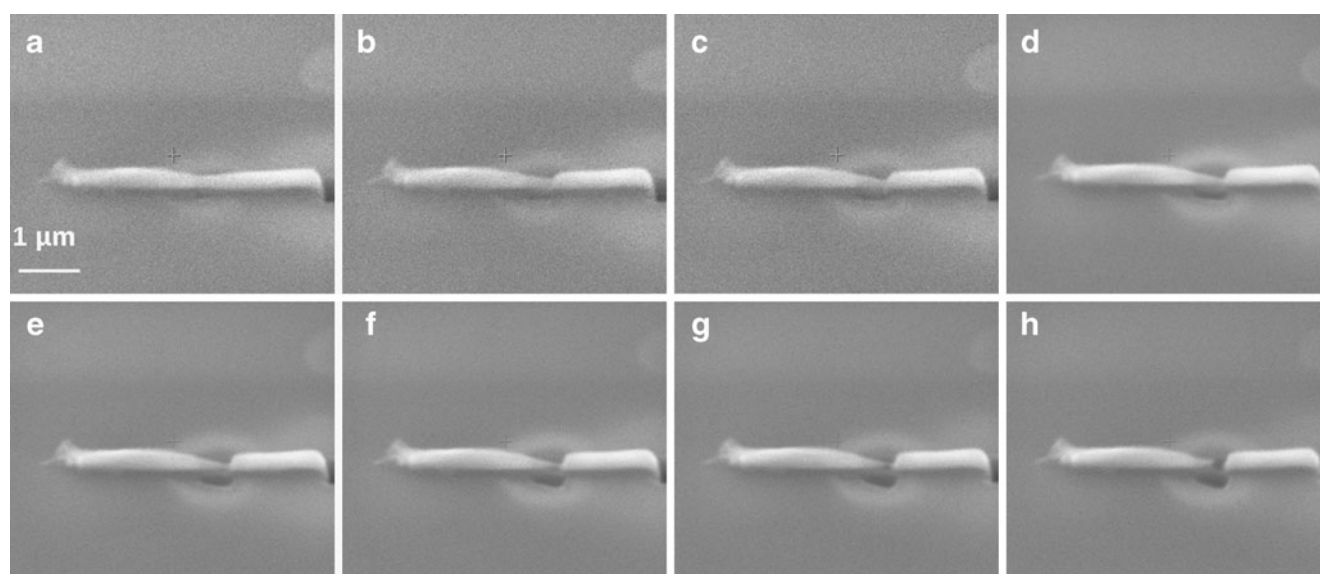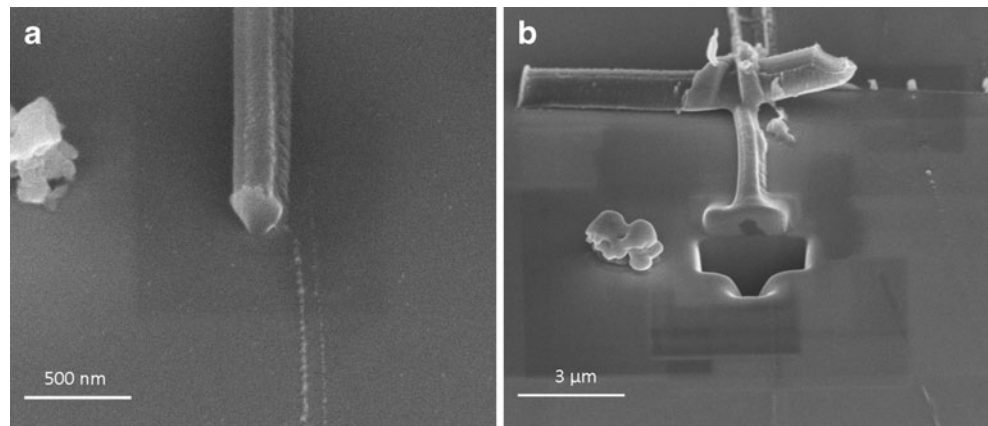

Fig. 2 An SEM image of a PNT being milled using FIB with steps of 2 s; from **a** to **h**

Fig. 3 SEM image of a PNW **a** before and **b** after milling with FIB during 4 s

to 25 mg/mL were pipetted onto the working surface of commercial gold electrodes. The samples were allowed to dry under anhydrous conditions in a vacuum desiccator in order for an amorphous film to form. The aniline vapor treatment was carried out in a Petri dish containing two separate compartments, one for the sample and one for the aniline solvent, in order to allow only the solvent vapor to reach the film. The chamber system was sealed with an aluminum sealing film and placed in the oven for 16 h at 100°C.

Production of polysilicon wafers For the preparation of the polysilicon structures, custom-made silicon nitride SOI wafers, with the insulation layer being silicon nitride, were used. On the wafers, a layer of polysilicon and a layer of insulating silicon nitride, both 100-nm thick, were deposited.

An ultraviolet lithography process was used to define interdigitated electrodes on the surface of the polysilicon wafers. These electrodes were later used as contact pads to connect the fabricated polysilicon structures. A 100-nm aluminum layer was deposited onto the wafers using electron beam evaporation. The remaining aluminum was removed in a lift-off process together with the remained photoresist.

Immobilization of the PNTS and PNWS on the polysilicon wafers The PNTS and PNWS were manually positioned on the polysilicon wafers by placing a droplet of the peptide solution on top of the aluminum electrodes located at their surface.

RIE process An STS C010 Multiplex Cluster System for reactive ion etching was used during this study. During the etching process, SF_6 and O_2 gases with flow rates of respectively 32 standard cubic centimeters per minute (sccm) and 8 sccm were employed. The pressure inside the vacuum chamber was adjusted to 80 mTorr and the RF power to 30 W.

Fig. 4 Process steps for the fabrication of silicon nanostructures using self-assembled peptide nanotubes as an etching mask. **a** 100 nm of polysilicon on a 100-nm silicon nitride wafer. **b–d** Photolithography and metallization steps to define the electrodes. **e–f** Manual peptide tube placement and flushing with DI water. **g** Reactive ion etching of the structures to define the polysilicon wires. **h** Removal of PNTS using distilled water
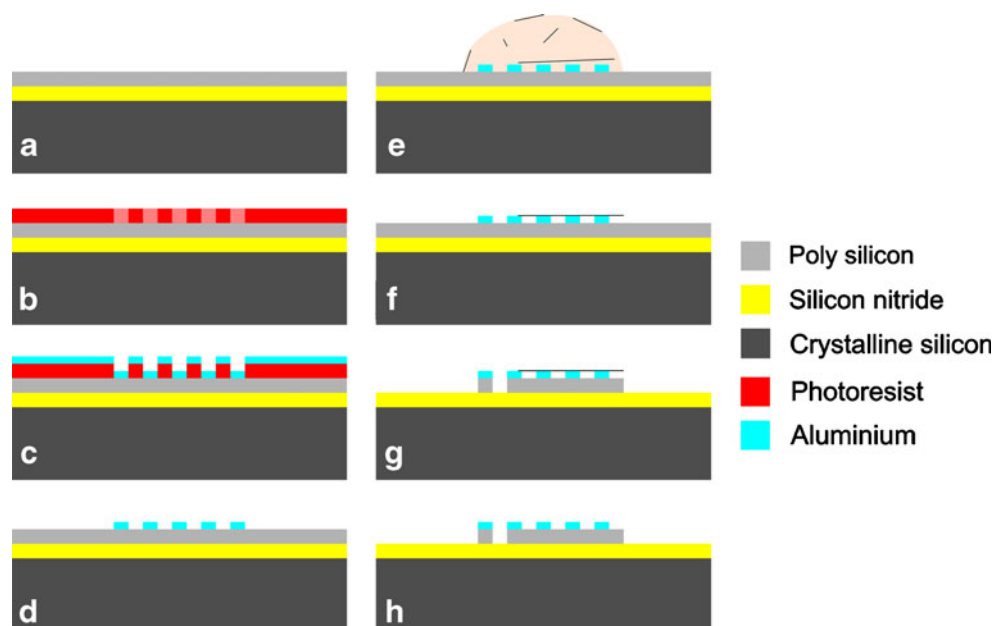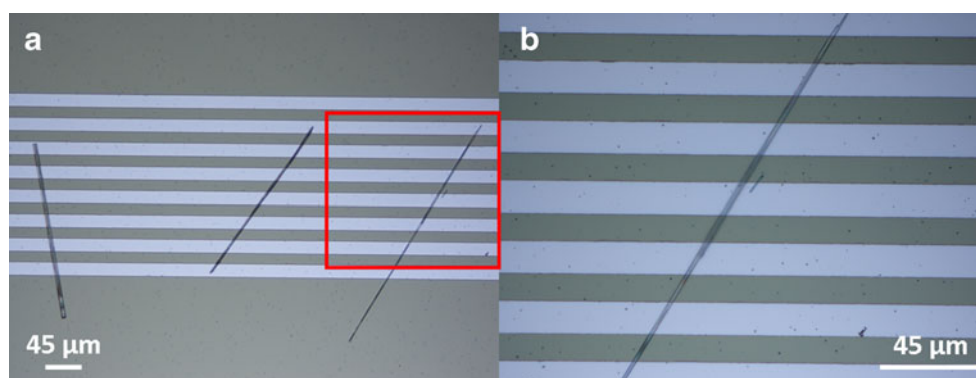

Poly silicon
Silicon nitride
Crystalline silicon
Photoresist
Aluminium

Fig. 5 a Optical image of PNTS immobilized on a polysilicon wafer. b Zoom of one of the PNTS connecting the aluminum electrodes

Focused Ion Beam For the focused ion beam (FIB) milling experiments on the PNTS and PNWS, a Quanta™ dual-beam scanning electron microscope and focused ion beam work station was utilized. The samples were covered with a layer of gold to avoid charge build up and thus obtain better images and a more precise control during the milling process. The samples were bombarded with Ga ions during several exposure times, after which they were evaluated using scanning electron microscopy (SEM). The milling procedure was conducted in steps of 2 s.

Electrical characterization A current preamplifier (Stanford Research SR570) was used to obtain the I–V curves.

Functionalization of the polysilicon wire The polysilicon wire was thoroughly washed with ethanol to remove any organic contaminant. Subsequently, the wire was immersed in a 2% (3-aminopropyl)triethoxysilane (APTES) ethanol solution for 30 min. The polysilicon wire was washed with ethanol and heated to 120°C for 10 min to completely remove the ethanol. The APTES-modified polysilicon wire was incubated in 1 mg/mL of sulfo-NHS-biotin for 3 h. Following this, the modified wire was incubated with an Atto 610 streptavidin solution during 30 min, and the functionalized wire was finally evaluated using a fluorescent microscope.

3 Results and Discussion

Stability of the self-assembled PNTS and PNWS under RIE The stability of the self-assembled PNTS and PNWS in an RIE process was evaluated. For this, droplets of solutions containing self-assembled tubes and wires were deposited on a silicon wafer and then dried at room temperature. Subsequently, the wafer was placed in the RIE chamber and exposed to the process for 1, 2, and 3 min. At the end of the process, the samples were evaluated using SEM. As shown in Fig. 1, the structure of the self-assembled wires was severely damaged while that of the tubes was unaffected by the RIE process.

This difference in behavior between the two structures, which in this case was attributed to the dissimilarities in their structural conformation, has been previously noted and discussed by other researchers [11]. Ryu and co-workers observed differences in the stability of the same type of self-assembled structures as that investigated in our work when exposed to thermal, chemical, and proteolytic attacks. However, contrary to our findings, the nanowires demonstrated a better resistance to these attacks, and Ryu and co-workers suggested their use in future applications requiring harsh processing conditions. These findings obviously suggest the realization of a more detailed study on the differences in behavior between the two types of

Fig. 6 a SEM image of the PNTS located at the surface of the polysilicon wafer. b Zoom of the SEM image of the etched silicon wire, inside the *circles*, after removal of the PNTS
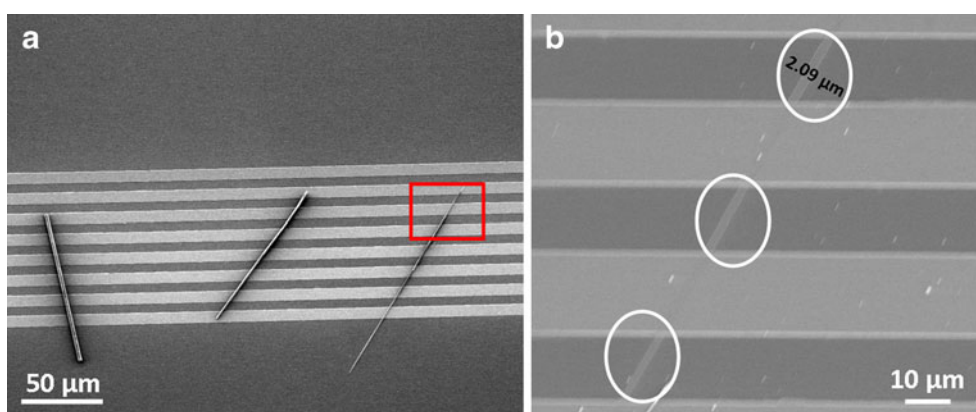
Fig. 7 SEM image of a polysilicon structure etched using two overlapping PNTS. The *inset* displays a zoom of the crossing point where clear ridges can be seen after removal of the PNTS with distilled water

self-assembled peptide structures, which is beyond the goal of the present investigation.

FIB milling FIB milling was used to further confirm the differences in stability between PNTS and PNWS. The FIB technique is very similar to RIE and has previously been used to modify a 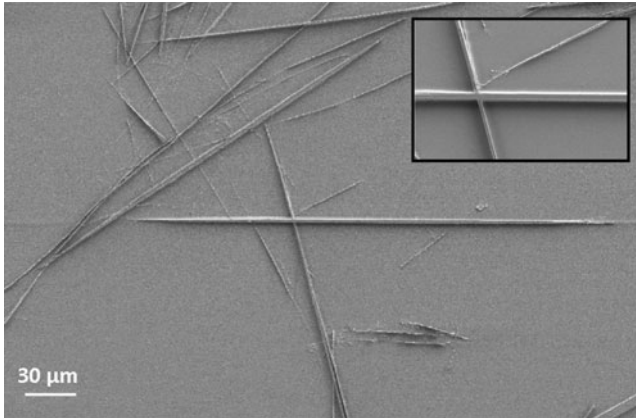wide variety of materials, including silicon [33–35]. The obtained results confirmed our previous observations using RIE. PNTS seemed to better resist the bombardment of ions as compared to PNWS. The time required to mill cross-sections of PNTS was longer than the corresponding time for the milling of PNWS. It took 32 s to mill through a peptide nanotube (PNT), cf.
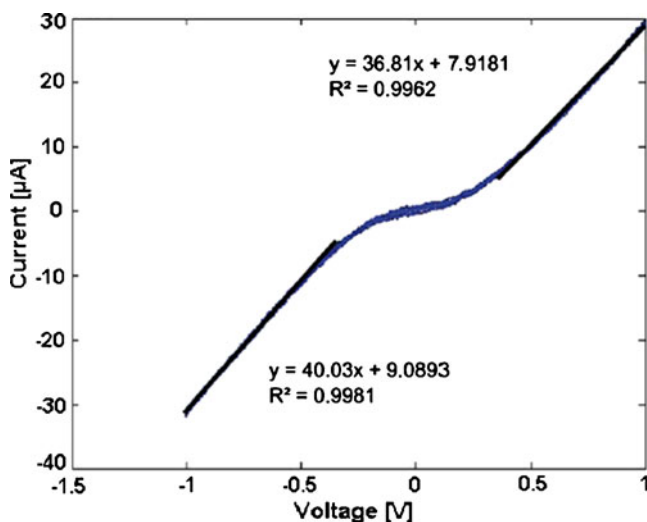

Fig. 8 Characteristic I–V curve of a polysilicon wire fabricated using PNTS as the etching mask material. The voltage was swept from −1 to 1 V. The measured resistance for the negative region was 27.1 MΩ, whereas it was 25.0 MΩ for the positive region

Fig. 2, while in the case of the PNW, the same process took only 4 s, cf. Fig. 3.

Fabrication of silicon structures using self-assembled PNTS as an etching mask Based on the results from the stability test, self-assembled PNTS were chosen as the etching material for the fabrication of silicon structures in an RIE process. For this, a solution of self-assembled PNTS was manually placed on a silicon wafer containing aluminum electrodes. Once the solvent had been allowed to evaporate at room temperature, the wafer was placed in an RIE chamber and etched for 5 min. The entire process is described in Fig. 4.

An optical image of the PNTS positioned on top of the aluminum electrodes before the RIE process is given in Fig. 5.

Subsequently, the wafer was evaluated with SEM. The PNT was still present after the RIE process, and the structure was found not to be affected by the RIE process, as evidenced in Fig. 6. Figure 6a displays an SEM image of the PNTS after the RIE process. As can be seen, the PNTS were located at the same positions as in Fig. 5, and their structure appeared unaffected by the RIE procedure. Figure 6b displays a zoom of Fig. 6a after removal of the PNT with distilled water. It can be observed that a silicon wire was etched exactly at the same location where the PNT was placed. The fabricated silicon structure displayed the same diameter as the PNT, and it connected the aluminum electrodes on the polysilicon wafer.

Different types of polysilicon structures can be etched based on the initial placement of the PNTS. Figure 7 displays a polysilicon structure etched using two overlapping PNTS as the etching mask. Clear ridges were exposed after rinsing the polysilicon wafer with distilled water to remove the PNTS.

Functionalization and electrical characterization of the etched polysilicon structures In order to evaluate the possibility of employing the fabricated polysilicon structures in the development of biosensing devices, their electrical properties were characterized. For this, an I–V curve was plotted for the etched polysilicon structure connecting the aluminum wires displayed in Fig. 6b. A voltage scan between −1 and 1 V was applied to the aluminum electrodes, and the current through the polysilicon wire connecting the metal electrodes was measured. The obtained I–V curve is given in Fig. 8.

As expected for a conductive silicon structure, the etched polysilicon wire was able to conduct a current after a potential was applied to the metal electrodes. The I–V curve displayed resistances of 27.1 and 25.0 MΩ at the negative and positive regions, respectively. These values indicate that the fabricated polysilicon structure

Fig. 9 Optical image of a poly-silicon wire fabricated using a self-assembled PNT **a** before the functionalization and **b** after the functionalization with a fluorescent molecule
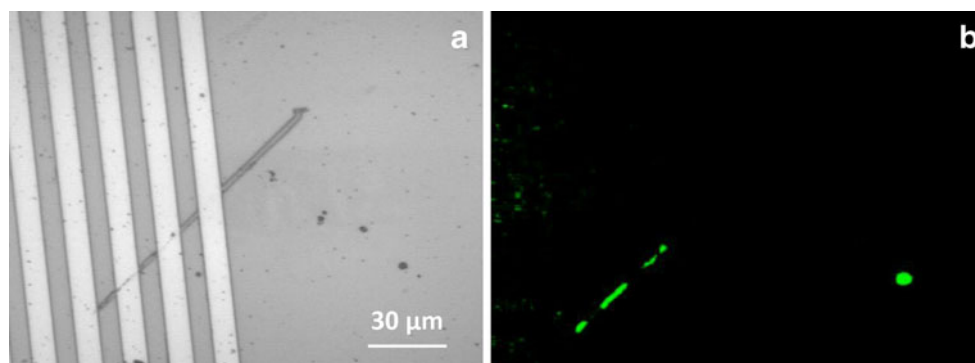
could be used for the development of a biosensing device such as a field effect transistor or an electrochemical biosensor. The diode behavior for small potential is due to Schottky barriers between the aluminum and the lightly doped polysilicon. In sensor applications, heavy-doped contact regions should be added below the aluminum electrodes.

In order to evaluate the functionalization of the fabricated polysilicon structure, a fluorescent molecule was attached to its surface through the biotin–streptavidin interaction. Figure 9 displays a polysilicon wire before, Fig. 9a, and after, Fig. 9b, the functionalization with Atto 610 streptavidin.

It was found to be possible to attach a fluorescent molecule to the surface of the fabricated polysilicon wire, thus suggesting that the latter could be further functionalized with other functional molecules such as enzymes or antibodies for the development of biosensing devices.

4 Conclusions

Self-assembled PNTS and PNWS were exposed to RIE etching and to an FIB milling process. The self-assembled structures differed in their behavior: the PNTS were more resistant in both cases. These behavioral differences should be further explored in future studies. Nevertheless, based on the obtained results, functional polysilicon wires were fabricated using self-assembled PNTS as an etching mask material. The presented fabrication procedure was fast, simple, and low-cost compared to traditional methods for preparing silicon nanowires. The etched polysilicon structures displayed sizes that were similar to those found when self-assembled PNT were used as an etching mask. Moreover, the conductivity of the fabricated polysilicon structure was evaluated as well as its functionalization through the attachment to a fluorescent molecule. The obtained results suggested that the fabricated polysilicon

structure has the potential to be used in the development of biosensing devices.

References

1. de la Rica, R., & Matsui, H. (2010). Applications of peptide and protein-based materials in bionanotechnology. *Chemical Society Reviews, 39*(9), 3499–3509. doi:10.1039/b917574c.
2. Scanlon, S., & Aggeli, A. (2008). Self-assembling peptide nanotubes. *Nano Today, 3*(3–4), 22–30.
3. Yan, X. H., Zhu, P. L., Li, J. B. (2010). Self-assembly and application of diphenylalanine-based nanostructures. *Chemical Society Reviews, 39*(6), 1877–1890. doi:10.1039/b915765b.
4. Reches, M., & Gazit, E. (2006). Designed aromatic homo-dipeptides: formation of ordered nanostructures and potential nanotechnological applications. *Physical Biology, 3*(1), S10–S19. doi:10.1088/1478-3975/3/1/s02.
5. Castillo-León, J., Rodriguez-Trujillo, R., Gauthier, S., Jensen, A. C. Ø., Svendsen, W. E. (2011). Micro-"factory" for self-assembled peptide nanostructures. *Microelectron Eng*. doi:10.1016/j.mee.2010.12.023.
6. Andersen, K. B., Castillo-Leon, J., Hedstrom, M., Svendsen, W. E. (2011). Stability of diphenylalanine peptide nanotubes in solution. *Nanoscale, 3*(3), 994–998. doi:10.1039/C0NR00734J.
7. Castillo, J., Tanzi, S., Dimaki, M., Svendsen, W. (2008). Manipulation of self-assembly amyloid peptide nanotubes by dielectrophoresis. *Electrophoresis, 29*(24), 5026–5032. doi:10.1002/elps.200800260.
8. Clausen, C. H., Jensen, J., Castillo, J., Dimaki, M., Svendsen, W. E. (2008). Qualitative mapping of structurally different dipeptide nanotubes. *Nano Letters, 8*(11), 4066–4069. doi:10.1021/nl801037k.
9. Reches, M., & Gazit, E. (2007). Biological and chemical decoration of peptide nanostructures via biotin-avidin interactions. *Journal of Nanoscience and Nanotechnology, 7*(7), 2239–2245. doi:10.1166/jnn.2007.645.
10. Diaz, J. A. C., & Cagin, T. (2010). Thermo-mechanical stability and strength of peptide nanostructures from molecular dynamics: self-assembled cyclic peptide nanotubes. *Nanotechnology*. doi:10.1088/0957-4484/21/11/115703.
11. Ryu, J., & Park, C. B. (2009). High stability of self-assembled peptide nanowires against thermal, chemical, and proteolytic

attacks. *Biotechnology and Bioengineering, 105*(2), 221–230. doi:10.1002/bit.22544.

12. Hayden, O., Agarwal, R., Lu, W. (2008). Semiconductor nanowire devices. *Nano Today, 3*(5–6), 12–22.

13. Yang, P., Yan, R., Fardy, M. (2010). Semiconductor nanowire: what's next? *Nano Letters, 10*(5), 1529–1536.

14. Patolsky, F., Zheng, G. F., Lieber, C. M. (2006). Fabrication of silicon nanowire devices for ultrasensitive, label-free, real-time detection of biological and chemical species. *Nature Protocols, 1* (4), 1711–1724. doi:10.1038/nprot.2006.227.

15. Weiss, S. M., & Fauchet, P. M. (2006). Porous silicon one-dimensional photonic crystals for optical signal modulation. *IEEE Journal of Selected Topics in Quantum Electronics, 12*(6), 1514–1519. doi:10.1109/jstqe.2006.884083.

16. Weiss, S. M., Haurylau, M., Fauchet, P. M. (2004). Silicon-based photonic bandgap modulators. In 2004 First IEEE International Conference on Group IV Photonics. pp. 171–173.

17. Arnold, S. P., Prokes, S. M., Zaghloul, M. E. (2005). Localized growth and functionalization of silicon nanowires for MEMS sensor applications. In Oregan, F., Wegemer, C. (Eds.), Proceedings of the 2005 European Conference on Circuit Theory and Design, vol 3. pp. 397–400.

18. Englander, O., Christensen, D., Kim, J., Lin, L. W. (2006). Post-processing techniques for the integration of silicon nanowires and MEMS. In MEMS 2006: 19th IEEE International Conference on Micro Electro Mechanical Systems, Technical Digest. Proceedings: IEEE Micro Electro Mechanical Systems Workshop. pp. 930–933.

19. Bandaru, P. R., & Pichanusakorn, P. (2010). An outline of the synthesis and properties of silicon nanowires. *Semiconductor Science and Technology, 25*(2), 10.1088/0268-1242/25/2/024003.

20. Ozsun, O., Alaca, B. E., Leblebici, Y., Yalcinkaya, A. D., Yildiz, I., Yilmaz, M., et al. (2009). Monolithic integration of silicon nanowires with a microgripper. *Journal of Microelectronic Systems, 18*(6), 1335–1344. doi:10.1109/jmems.2009.2034340.

21. Weber, J., Singhal, R., Zekri, S., Kumar, A. (2008). One-dimensional nanostructures: fabrication, characterisation and applications. *International Materials Reviews, 53*(4), 235–255. doi:10.1179/174328008x348183.

22. Colli, A., Fasoli, A., Pisana, S., Fu, Y., Beecher, P., Milne, W. I., et al. (2008). Nanowire lithography on silicon. *Nano Letters, 8*(5), 1358–1362. doi:10.1021/nl080033t.

23. Fellahi, O., Hadjersi, T., Maamache, M., Bouanik, S., Manseri, A. (2010). Effect of temperature and silicon resistivity on the elaboration of silicon nanowires by electroless etching. *Applied Surface Science, 257*(2), 591–595. doi:10.1016/j.apsusc.2010.07.039.

24. Abe, H., Yoneda, M., Fujlwara, N. (2008). Developments of plasma etching technology for fabricating semiconductor devices. *Japanese Journal of Applied Physics, 47*(3), 1435–1455. doi:10.1143/jjap.47.1435.

25. Barlian, A. A., Park, W. T., Mallon, J. R., Rastegar, A. J., Pruitt, B. L. (2009). Review: semiconductor piezoresistance for microsystems. *Proceedings of the IEEE, 97*(3), 513–552.

26. Esashi, M., & Ono, T. (2005). From MEMS to nanomachine. *Journal of Physics. D. Applied Physics, 38*(13), R223–R230. doi:10.1088/0022-3727/38/13/r01.

27. Fu, Y. Q., Colli, A., Fasoli, A., Luo, J. K., Flewitt, A. J., Ferrari, A. C., et al. (2009). Deep reactive ion etching as a tool for nanostructure fabrication. *Journal of Vacuum Science and Technology B, 27*(3), 1520–1526. doi:10.1116/1.3065991.

28. Han, X. L., Larrieu, G., Dubois, E. (2010). Realization of vertical silicon nanowire networks with an ultra high density using a top-down approach. *Journal of Nanoscience and Nanotechnology, 10* (11), 7423–7427. doi:10.1166/jnn.2010.2841.

29. Hirai, Y., Yabu, H., Matsuo, Y., Ijiro, K., Shimomura, M. (2010). Biomimetic bi-functional silicon nanospike-array structures prepared by using self-organized honeycomb templates and reactive ion etching. *Journal of Materials Chemistry, 20*(48), 10804–10808. doi:10.1039/c0jm02423f.

30. Mehran, M., Sanaee, Z., Mohajerzadeh, S. (2010). Formation of silicon nanograss and microstructures on silicon using deep reactive ion etching. *Micro and Nano Letters, 5*(6), 374–378. doi:10.1049/mnl.2010.0111.

31. Strobel, S., Kirkendall, C., Chang, J. B., Berggren, K. K. (2010). Sub-10 nm structures on silicon by thermal dewetting of platinum. *Nanotechnology, 21*(50), 7. doi:10.1088/0957-4484/21/50/505301.

32. Ryu, J., & Park, C. B. (2008). High-temperature self-assembly of peptides into vertically well-aligned nanowires by aniline vapor. *Advanced Materials, 20*(19), 3754–3758.

33. Giannuzzi, L. A., & Stevie, F. A. (1999). A review of focused ion beam milling techniques for TEM specimen preparation. *Micron, 30*(3), 197–204.

34. Korotcenkov, G., & Cho, B. K. (2010). Silicon porosification: state of the art. *Critical Reviews in Solid State and Materials Sciences, 35*(3), 153–260. doi:10.1080/10408436.2010.495446.

35. Tseng, A. A. (2004). Recent developments in micromilling using focused ion beam technology. *Journal of Micromechanics and Microengineering, 14*(4), R15–R34. doi:10.1088/0960-1317/14/4/r01.

4.2 Summary and Perspectives

In this article the potential use of the PNT's as a dry etching mask was demonstrated. The fact that the PNT's despite being very stable during the ion bombardment dissolve rapidly in water after processing makes it possible to pattern materials not compatible with acetone which is used to remove traditional masking material such as photoresist or e-beam resist.

Other 1D structures such as silicon dioxide nanowires has previously been utilized as etching masks for the formation of silicon nanowires.[90,91] However, in this case the removal of the masking material is often more complicated than the removal of traditional photoresists in acetone. Furthermore the formation of these inorganic nanowires is a more complicated and slower process than the formation of the peptide nanotubes that are the topic of this work. The PNT's provides new possibilities both with the simple formation and with due to the water solubility makes it possible to pattern organic materials.

CHAPTER 5

Manipulation Techniques

5.1 Introduction

In the article presented in the previous chapter the PNT's were pipetted on top of aluminum electrodes and by chance a few were aligned across the electrodes. The geometry of the PNT's was in the etching procedure transferred to the thin silicon layer beneath providing a simple and low cost nanolithography mask. To utilize the possibilities of this new fabrication technique a manipulation method capable of positioning the PNT's between electrodes on wafer scale must be developed. The purpose of such a manipulation method is to position the PNT's at the prober location(s) or with the proper orientation(s) to enable contact between the nanostructures defined by the nanotube geometry and the macroscopic contact pads.

Manipulation methods can be divided into two overall groups depending on whether single structures are moved individually in a serial approach, in this context referred to as a serial manipulation technique, or a parallel manipulation technique, where several or preferably all structures are positioned in a single step. In the development of prototypes one often relies on a serial manipulation technique such as pick and place using micro tweezers,[94–98] AFM probes[99–101] or optical tweezers,[102–104] etc. For an in depth description of these the interested reader is referred to some of the many reviews on this topic.[105–108]

In this work focus has been on the development of a parallel manipulation technique capable of positioning the PNT's in a single step process at wafer scale to utilize the dry masking capabilities of the PNT's at large scale. A whole range of different parallel manipulation methods for the positioning of nanowire structures have also been developed based on very different techniques such as inkjet printing,[33] magnetic and electric fields fields,[109–111] hydrophobic-hydrophillic interactions,[112] blown bubble,[113,114] etc. Again a number of review exists on this topic.[93,115,116]

In fig. 5.1a an overview of an the manipulation methods considered in this project are provided along with references for further reading. In this introduction only the manipulation methods, that provided the best results and lead to the development of the final manipulation method will be discussed. The principle behind the manipulation methods discussed below is illustrated in figure 5.1b-d.

a

Seriel
- μ-tweezers [94-98]
- **DEP*** [84]
- Probe manipulation [99-101]
- Optical tweezers [102-104]

Parallel
- DEP [110,111]
- **Magnetic [109]**
- **Langmuir-Blodgett*,c** [127-130]
- **Fluidic*,d** [131-134]
- **Spin casting*** [137,138]
- Blown Bubble [113,114]
- **Inkjet Printing [33]**
- **Acustophoresis***

Bold: Demonstrated with FF PNT's   *: Investigated in this work   [ ]: Refference for the work   b,c,d: Example included below

Dielectrophoresis (DEP)   **Langmuir-Blodgett**   **Microfluidic Alignment**

b   c   d

Figure 5.1: *Overview of the different manipulation techniques considered to orient and position the PNT's. In* **a** *a list of the different techniques considered is provided. The techniques highlighted in bold has been demonstrated with the FF PNT's. An asterix furthermore indicates that the principle was investigated in this work. Finally after each manipulation techniques references are given for further reading. In b-d the principle behind the techniques that was investigated further in this project(dielectrophoresis, Langmuir-Blodgett, and flow based manipulation) is illustrated along with an image of PNT's aligned with this method. Reprinted with permission from.* [84, 92, 93]

5.1.1 Dielectrophoresis

Dielectrophoretic (DEP) manipulation of the PNT's has been demonstrated previously in our group as a serial manipulation approach as seen in figure 5.1b.[84] By proper design of the electrodes the DEP manipulation approach can be utilized in large scale parallel manipulation on wafer scale.[110, 111] Therefore in the current project the first manipulation approach that was investigated further was the parallel DEP manipulation. The principle behind DEP is illustrated in figure 5.1b. In an asymmetric electrical field the structures will either be pushed towards (positive DEP) or pushed away (negative DEP) from the stronger field.[117] DEP has been extensively used for the manipulation of different nanowire geometries such as metal nanowires,[118, 119] carbon nanotubes,[110, 111, 120, 121] rhodium rods,[120] indium arsenide nanowires[122] and silicon nanowires.[123]

The force on the particle arises from the different properties (polarizability and conductivity) of structures and the medium in which the structures are suspended. Therefore if there is no difference or only very little difference between these parameters the forces will be equally small. The capture of the PNT's with DEP proved challenging partly due to the small forces exerted on the PNT's since a large part of the PNT is the water filled cavity and hence without change of medium (which would partly dissolve the structures) before the DEP manipulation the forces exerted on the PNT's would be smaller.

5.1.2 Langmuir-Blodgett

A Langmuir-Blodgett trough is traditionally used to form monolayer films of different molecules both directly on a water surface[124–126] or by a transfer process on other substrates.[125, 126] This manipulation method has been used for the alignment of silicon nanowires,[90, 92, 127, 128] ZnSe nanowires[129] and silver nanowires.[130] A Langmuir-Blodgett trough is a water bath, where floating sliding barrier can glide over the water surface pressing the molecules in the surface together until they form a complete monolayer. The structures forming the monolayer are suspended in a liquid with a low boiling point and carefully pippeted onto the water, where the low boiling point liquid evaporates leaving the molecules suspended on the water surface. The formation of the monolayer is monitored through the surface tension in the through between the sliding barriers (upon the formation of the monolayer the surface tension increases drastically). The monolayer can then be transferred to a substrate by pulling the substrate out of or pushing it into the water surface depending on the hydrophobicity of the substrate.[125]

As seen from figure 5.1c the moving barriers will force the wire like structures to orient parallel to the moving barriers.[90, 130] In the figure the best result obtained with the Langmuir-Blodgett manipulation method is shown, but such good results were rare. the biggest issue was the underlying water bath. After suspension on the water surface the PNT's started dissolving in the process of moving the barriers making it impossible to form the monolayer surface and prober orienting the PNT's. This issue could potentially be faced if the water in the trough was replaced with a saturated solution of the peptide monomers. This would prevent the dissolution of the PNT's on the water surface. However, it might also compromise the alignment in the surface through the formation of peptide nanotubes in the trough.

5.1.3 Flow Based

In another approach the fluidic motion in a microfluidic channel was utilized to orient the PNT's according to the direction of the flow. This form of manipulation of wire like structures has previously been demonstrated for the manipulation of silicon nanowires,[131] silver nanowires[132] and carbon nanotubes.[133, 134] In the flow based manipulation technique a microfluidic channel is placed on the surface of the receiving substrate as illustrated in figure 5.1d. The solution containing the

structures to be positioned is flushed through the microfluidic channel and some of the structures (aligned by the flow in the microfluidic channel) will come in contact with the substrate and remain in place after the removal of the fluidic channel due to van der Wals interaction between the PNT's and the substrate. In figure 5.1d, PNT's positioned using this technique can be seen. From this it is evident that the manipulation method in principle works. However, not seen in this figure is the major issue of clogging in the microfluidic channel caused by the PNT's.

The same effect that leads to the fast formation of the PNT's in the initial formation process also leads to the fact that the PNT's tend to stick together and once one is either attached to the wafer substrate, or more likely to the walls of the polymer microfluidic structures, additional PNT's flowing in the channel will pile up, ruin the alignment and eventually clog the channel and hence compromise the alignment. Even the addition of Tween, a polysorbate surfactant, to the PNT solution could not prevent the clogging of the microfluidic channel.

It was demonstrated that PNT's could successfully be oriented in a flow based manipulation approach. Inspired by the lab on a disc microfluidic systems,[135, 136] where the rotational motion of a spinning disk is used to drive the solution inside microfluidic channels, a system was designed where channels were milled into a plastic substrate (mimicking a silicon wafer with clamped or attached polymer channels). The idea behind the manipulation approach is to drive the PNT solution in open channels on the substrate by the rotational motion of the substrate. In the present work both channel oriented in the axial direction and channels spiralling out from the center of the wafer was investigated. The alignment of the PNT's worked very well and even with the spiralling channel the PNT's aligned according to the direction of the channel. If not for the success of the spin casting technique this could have been a promising candidate for the manipulation method utilized in the final fabrication procedure presented in the article below.

5.1.4   Spin Casting

With the modified version of the spin casting technique[137, 138] developed in this project the best compromises between the degree of manipulation and the time required to achieve this were found. In the article below this manipulation technique is presented along with a demonstration of the properties of the FF PNT's as a lift off material for the rapid, simple and inexpensive formation of nanoslits in metal surfaces.

REGULAR PAPER

Alignment and Use of Self-Assembled Peptide Nanotubes as Dry-Etching Mask

Karsten B. Andersen, Jaime Castillo-León*, Tanya Bakmand, and Winnie E. Svendsen

DTU Nanotech, Technical University of Denmark, Building 345B, Kgs. Lyngby 2800, Denmark

Self-assembled diphenylalanine peptide nanotubes provide a means of achieving nanostructured materials in a very simple and fast way. Recent discoveries have shown that this unique material, in addition to remaining stable under dry conditions, rapidly dissolves in water making it a promising candidate for controlled nanofabrication without organic solvents. The present work demonstrates how this unique structure can be aligned, manipulated and used as both an etching mask in a dry etching procedure and as a lift-off material. As a further demonstration of the potential of this technique, the peptide nanotubes were utilized to fabricate silicon nanowire devices and gold nanoslits in a rapid manner.
© 2012 The Japan Society of Applied Physics

1. Introduction

Self-assembling structures, such as different peptides, liposomes and block copolymers among others, have long been considered attractive options for the realization of low cost nanostructures.[1–5] However, despite the increased focus on these materials, few devices that rely solely on self-assembled structures have been widely adopted. One of the reasons for this is that many of these self-assembled structures cannot match traditional sensor materials such as silicon with regard to for instance conductivity[6] and stability.[7] Another challenge when working with self-assembling materials is the manipulation of the formed structures so that they can be placed at the desired location in a repeatable, fast and reliable manner. In order to realize low-cost nanostructures with self-assembling biomaterials while maintaining the material properties of for instance silicon, self-assembling structures have been utilized as a fabrication tool to transfer their nanostructures to more standard sensor materials.[8–10] However, this approach does not solve the second challenge of manipulating the formed structures.

To meet this challenge, many different manipulation methods have been investigated as is discussed below. The common goal of these approaches is to position the material in a controlled manner in large scale to enable parallel production. The peptide nanotubes (PNTs) formed by the dipeptide diphenylalanine are interesting due to their fast formation that takes place under mild conditions,[2,11,12] their large stiffness[13] and high Young's modulus,[14] their good stability under dry conditions[7,15] and finally the fact that they can be dissolved in most liquids including water.[7] The electrical and structural properties of PNTs were recently studied in our group.[6,16,17] The material has been utilized in a wide variety of applications such as for moulds for the fabrication of nanofluidic channels and coaxial nano-cables,[18,19] fabrication of silicon wires[20] and electrode modification for development of biosensors.[21–23]

The present work demonstrates how this self-assembled biological material can be used for fast, cheap and reproducible cleanroom processing. As will be shown, the peptide nanotubes can be employed as an etching mask in a dry etching procedure and their potential as a lift-off mask for the fabrication of gold nanoslits is demonstrated in another approach. Due the unique properties of the PNTs, both of these procedures can be realized without the use of

organic solvents, which is otherwise normally required in traditional fabrication techniques either to remove the masking material or to perform the lift off procedure. Furthermore, the present approach enables patterning of materials that are incompatible with solvents. Finally a manipulation method based on a modified spin casting technique capable of orienting the peptide nanostructures on wafer scale is presented. This simple method was optimized to position the peptide nanostructures individually across the entire wafer.

2. Experimental Methods

2.1 Peptide nanotubes fabrication
Peptide nanotubes were synthesised using diphenylalanine peptide (Bachem G-2925). Fresh stock solutions were prepared by dissolving the lyophilized form of the peptide in 1,1,1,3,3,3-hexafluoro-2-propanol (HFP; Sigma-Aldrich) at a final concentration of 100 mg/mL. Fresh solutions were prepared before each experiment. Peptide nanotubes, PNTS, were fabricated by dissolving aliquots of the stock solution in water.

2.2 Silicon wafer fabrication
Silicon nanowires were fabricated from a silicon-on-isolator (SOI) wafer, in this case a device layer of 50 nm and a buried oxide layer of 380 nm. A UV lithography process was used to define interdigitated electrodes on the surface of the silicon wafers. These electrodes were later used as contact pads to connect the fabricated silicon structures. A 100-nm aluminium layer was deposited onto the wafers using electron beam evaporation. The remaining aluminium was removed in a lift-off process together with the remaining photoresist.

2.3 Peptide nanotubes alignment
The peptide nanotubes solution was dropped on the wafer along with drops of isopropanol in an alternating manner, so that each drop of the PNTs suspension is immediately followed by a drop of isopropanol.

2.4 Reactive ion etching experiment
For the reactive ion etching (RIE) process a STS C010 Multiplex Cluster System was used during this study. During the etching process, SF_6 and O_2 gases with flow rates of respectively 32 and 8 sccm were employed. The pressure inside the vacuum chamber was adjusted to 80 mTorr and the RF power to 30 W.

---

*E-mail address: jaic@nanotech.dtu.dk

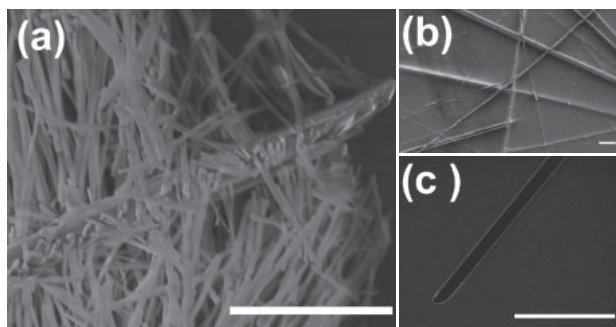© 2012 The Japan Society of Applied Physics

Fig. 1. Illustration of the properties of the peptide nanotubes as a fabrication tool: (a) A SEM image of the diphenylalanine peptide nanotubes. The image also portrays an example of the larger structures which the nanotubes tend to aggregate into. Both of these structures have shown excellent masking abilities for the patterning of materials in dry etching procedures. (b) A surface protected by peptide structures has been etched in a reactive ion etching process. Finally, the peptide nanotubes can be utilized as lift off materials. (c) A nanoslit fabricated in a lift-off process with the peptide nanotubes. All scale bars in the images correspond to 5 μm.

3. Results and Discussion

3.1 Peptide nanotubes as masking material

Many different preformed materials such as silicon dioxide nanowires have previously been utilized as masking materials in dry etching procedures for the fabrication of nanosized structures.[24,25] What makes the diphenylalanine PNTs unique, beside the fact that they are formed under mild conditions at low cost, is that they are more etch resistant than silicon while they at the same time dissolve in water, thus making the removal of the mask easier and more gentle.

Figure 1(a) shows a scanning electron microscopy (SEM) image where both types of structures, nanotubes and large bundles, are visible. The diameter of the smaller PNTs was on the order of 200 to 300 nm, and the diameter of the larger bundles can be more than 3 to 5 μm. In a previous study, we demonstrated the use of the bigger bundles for the fabrication of nanoribbons or larger silicon microwires.[20] However, silicon nanowires present a larger sensitivity than the corresponding nanoribbons. Consequently, this study has focused on investigating the performance of the smaller peptide nanotubes as a fabrication tool to achieve both silicon nanowires and nanoslits in metal surfaces. Furthermore, a controlled manipulation approach capable of orienting the PNTs, thus enabling a controlled and reproducible production of for instance silicon nanowire devices, has been developed.

To demonstrate that the PNTs displayed a similar etch resistance as the larger bundles in a dry etching procedure, a solution containing both PNTs and bundles was placed on a silicon substrate. After evaporation of the solvent, the wafer was dry-etched for 2 min and finally the PNTs and the bundles were dissolved by placing the wafer in pure distilled water. Figure 1(b) presents a SEM image of the now patterned silicon surface. From this figure, it is evident that both the PNTs and the bundles were able to act as a mask for the etching procedure and finally dissolve rapidly in water.

Another way of utilizing the characteristic properties of the peptide nanotubes in cleanroom processing is as lift-off materials for the patterning of for instance various metal films. In this approach, the peptide nanotubes are positioned

on the wafer before the material to be patterned is deposited. After metal deposition, the wafers are placed in a distilled water bath and the metal on top of the peptide nanotubes is lifted off as the underlying tubes dissolve, leaving a slit in the metal surface with the same dimensions as the dissolved PNT.

To demonstrate the potential of this application method, a nanoslit was patterned in a titanium gold double layer. After positioning of the peptide nanotubes on the wafer, a double layer of titanium and gold with a thickness of 10 and 50 nm, respectively, was deposited. As described above, the wafers were after the metal deposition placed in a Milli-Q water bath in which the titanium gold double layer became patterned through the lift-off process. An example of a patterned nanoslit in the gold titanium double layer is given in the SEM image of Fig. 1(c). The darker area in the image corresponds to the silicon wafer and the lighter area is the titanium gold double layer. In cleanroom processing, titanium is often used as an adhesive layer between the gold and, in this case, the underlying silicon layer.

3.2 Manipulation of peptide nanotubes

As described above, the PNTs are formed within seconds and therefore provide a fast approach for achieving nanostructured materials at low cost. However, before the structures can be utilized in the controlled and reproducible fabrication of different devices, such as silicon nanowires in cleanroom processing, a manipulation method capable of transferring them from the liquid in which they are formed to the substrate must be developed. For this purpose many different manipulation methods capable of performing wafer scale alignment exist, ranging from techniques based on Langmuir Blodgett films to bubble bursting.[26–30] For the PNTs in this work, an alignment method based on a modified version of a spin casting approach gave the best result. The procedure is described below.

The approach renders it possible to align the PNTs on the wafer surface pointing radially away from the centre of the wafer, and is based on the spin casting manipulation technique described elsewhere.[31,32] In the original method,[31] the solution is simply dropped on the spinning substrate drop by drop and the wafer is allowed to dry between the droplets. When applying this technique to the PNTs, they tended to bundle up in larger piles around the wafer, thus disturbing the flow and thereby compromising the alignment results. An illustration of these piles of peptides can be seen in the inset of Fig. 2. It is believed that these larger piles were formed when the PNTs of a subsequent drop came into contact with the few nonaligned tubes from the previous drop and got stuck. Consequently, when the next droplets arrived, the obstruction to the flow was even larger, increasing the probability of a new tube getting captured and causing piles to build up. Such a build-up of PNT piles naturally compromised the effectiveness of the alignment procedure and hence the yield of the fabrication process.

A simple modification of the above procedure has proven to drastically reduce the issues of piling and nonaligned PNTs as seen in Fig. 2. In this approach, each drop of the PNT solution is immediately followed by a drop of isopropanol. The isopropanol ensures that the non-aligned
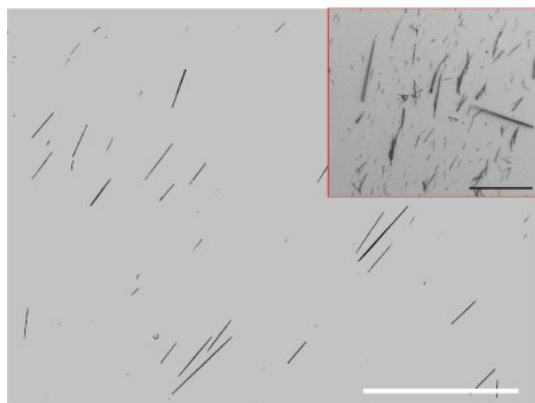
Fig. 2. (Color online) Example of the advantages of using the modified spin casting manipulation approach: Illustration of the alignment procedure utilized in this work. The inset shows a typical surface result after alignment using the standard spin casting procedure. In this image, a larger pile of peptide nanotube bundles is visible. The presence of these bundles compromises the effectiveness of the alignment procedure. Nevertheless, the bundles of peptide tubes can be avoided using the manipulation approach described in this article, as can be seen from a comparison of the two images. The scale bars correspond to 200 μm.
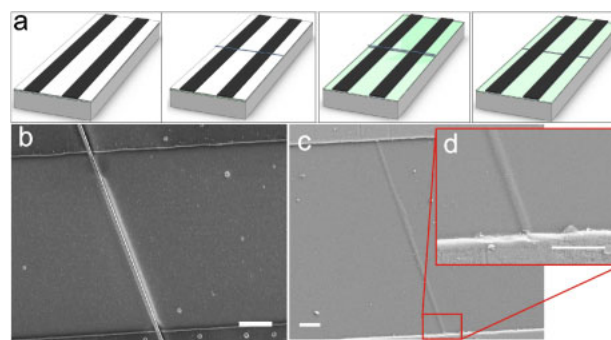

Fig. 3. (Color online) Fabrication sequence for silicon nanowire devices: Illustration and results of the fabrication of silicon nanowire devices. (a) An illustration of the fabrication procedure for the fabrication of a single silicon nanowire between two electrodes. (b)–(d) SEM images of the devices during the fabrication process. In this case the fabricated silicon nanowire is on the order of 250 nm. All scale bars in the images correspond to 2 μm.

tubes or potential bundles of tubes are flushed off the wafer since they will represent a larger cross sectional area for the isopropanol than their corresponding aligned structures. Hence these will be more likely to be flushed off the substrate during the flushing spinning process, since a larger radial force will be exerted on these structures compared to the aligned. The wafers were allowed to dry before the next double droplet as in the original approach.

Combining the above-presented results opens the possibility for a low-cost and rapid fabrication of silicon nanowires based on the masking properties of PNTs. As a demonstration of the potential of such an alignment procedure combined with the unique properties of the PNTs, silicon nanowires for biosensing purposes were fabricated.

Finally it is important to mention that using the described approach it is possible to control the orientation of the PNTs but not the exact position of them. However by prober design it is possible to overcome this so that only the PNTs at the electrodes are relevant, whereas the distance between the wires connecting the electrodes and contact pads should be much larger that the average peptide nanotube length. In this way the PNTs will only be able to bridge the gap between two connections in the electrode area. The number of nanotubes bridging the gap can be adjusted by changing either the concentration of the peptide solution or by increasing the spin casting time.

3.3 Rapid fabrication of silicon nanowires using peptide nanotubes as etching mask

Silicon nanowires have in recent times been shown to perform in an excellent manner as a sensor platform for label-free detection of various biomarkers ranging from cancer markers over DNA to whole viruses.[10,33] However, the fabrication costs of such devices is relatively high due to the requirement of e-beam or another nanolithography process.[34] Our work presents an alternative fabrication approach that can be utilized for a fast and cheap fabrication of silicon nanowire devices.

Silicon nanowire devices were fabricated from a SOI wafer, in this case with a device layer of 50 nm and a buried oxide layer of 380 nm. The fabrication process is illustrated in Fig. 3(a). The metal electrodes were first patterned using standard photolithography, and after deposition of the electrodes, the peptide nanotubes were positioned according to the procedure described above. The silicon nanowires were then etched in a reactive ion etching process masked by the positioned peptide nanotubes. Finally, the peptide nanotubes were dissolved by placing the now processed wafers in a pure distilled water bath.

Figure 3(b) presents a SEM image of a PNT positioned between two metal electrodes. After alignment of the PNT, the wafers were placed in the RIE where the PNT acted as a mask for the dry etching procedure leaving behind a silicon nanowire with a width of the same size as the PNT diameter. Finally, the PNT was removed by dipping the wafer in pure distilled water whereby the PNT dissolved, leaving behind a silicon nanowire as shown in Figs. 3(c) and 3(d). The silicon nanowire fabricated in this experiment had a width on the order of 250 nm — well below the limitations of standard photolithography.

As an additional evidence of our suggestion of the use of PNTs as dry-etching mask SEM images showing PNTs before and after the dry etching are included in Figs. 4 and 5. In Fig. 4(a) the area containing PNTs is seen after the etching procedure and in Fig. 4(b) the same area is seen after water rinsing (dissolving the peptide mask). Figure 5 shows a SEM image of a fabricated silicon nanostructure cross from where it can be verify that the even the slits between the PNTs were etched away.

To verify the complete removal of the PNTs after the etching procedure, the fabricated silicon nanowire devices were functionalized using a fluorescent compound. In this approach the native oxide covering the silicon nanowire was removed using a hydrofluoric acid etch. Followed by a functionalization procedure in which silicon was selectively marked with a fluorescent compound. The fluorescent image is shown in Fig. 6(a). One should note that the functionalization experiments were conducted on the larger nanoribbons defined using the bigger bundles as described previously[19] for a clearer visualization of the results.
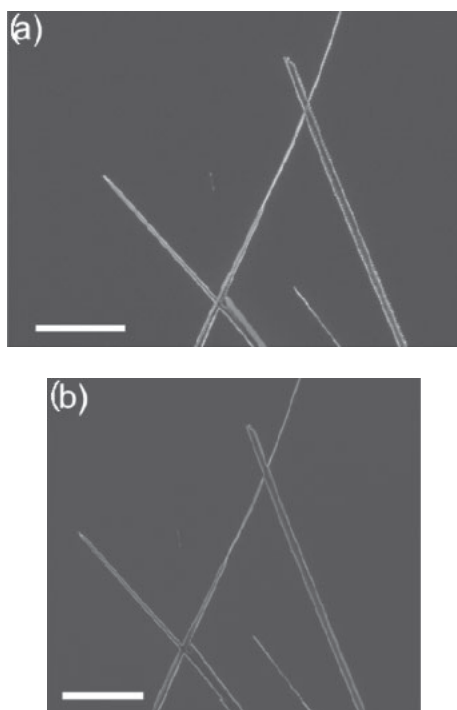
Fig. 4. SEM images of an area containing PNTs (a) before and (b) after the dry-etching process. Scale bar in these images correspond to 20 μm.
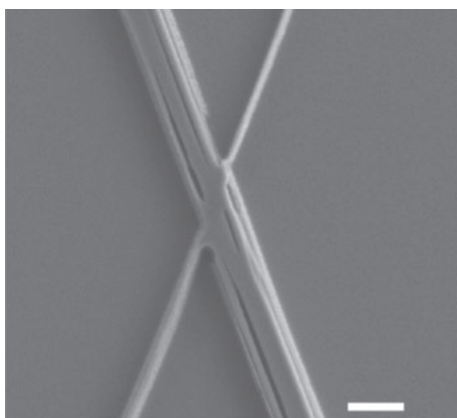

Fig. 5. SEM image of silicon nanostructures forming an intersecting point fabricated using PNTs as dry-etching mask. Even the slits between the PNTs were etched as is displayed here. Scale bar in this image correspond to 20 μm.

The final test involved verifying whether an electrical contact could be established between the metal electrodes and the silicon nanowires. Figure 6(b) displays the electrical characteristics of a silicon nanowire. The current–voltage (I–V) curves were measured using a custom-built experimental setup. Due to the lack of a highly doped region between the metal electrodes and the lightly doped silicon nanowire, the curve showed features that were slightly non linear as is also evident from the plots. The high resistance of the two nanowires was due partly to small dimensions and partly to the light doping (the sheet resistance of the wafers was between 9 and 23 Ω/cm). The latter can be changed according to demand.
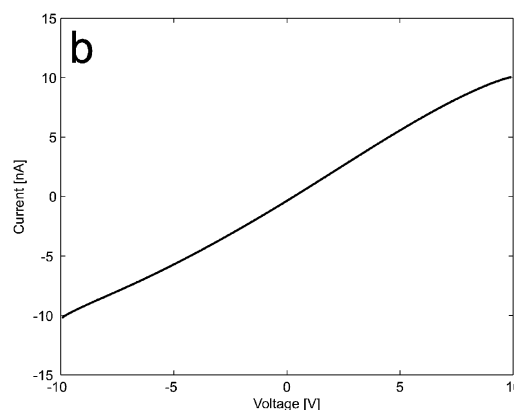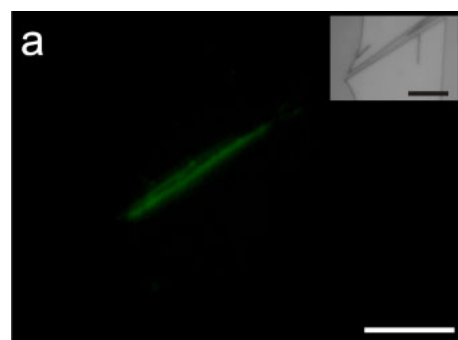

Fig. 6. (Color online) Characterization of fabricated silicon nanowires: To verify that the result of the fabrication process is in fact a silicon nanowire, the surface of the structure is first functionalized with a fluorescent streptavidin through a silanization approach where only silicon dioxide and hence the native oxide covering the silicon nanowire is marked. The results are seen in (a) and the inset shows an optical image of the same area. (b) The I–V curve for the silicon nanowire. The slightly nonlinear behavior of the device is due to poor electrical contact.

4. Conclusions

This work has demonstrated how newly discovered properties of diphenylalanine PNTs make them excellent candidates as the next nanotechnology fabrication tool. The fact that the formed nanotubes dissolve in distilled water while remaining stable under prolonged ion bombardment in a dry etching procedure allows for an easy and fast processing of fragile materials, where organic solvents for the removal of the masking layer can be avoided. In particular, it was demonstrated how the PNTs could be utilized for a low-cost and fast fabrication of silicon nanowires. Furthermore, the PNTs could be used as lift-off masks for the patterning during deposition of materials. The lift off procedure could be conducted in pure distilled water due to the unique properties of the PNTs, and the need for organic solvents could again be avoided. This rendered possible the patterning of fragile materials. Finally, a method for aligning the PNT structures on a wafer scale based on a modified spin casting technique avoiding the use of pumps was also presented as an alternative for the alignment and manipulation of these biological nanostructures on desired locations.

1) C. Allen, D. Maysinger, and A. Eisenberg: Colloid Surf. B **16** (1999) 3.
2) E. Gazit: Chem. Soc. Rev. **36** (2007) 1263.
3) I. W. Hamley: Angew. Chem., Int. Ed. **42** (2003) 1692.
4) C. Park, J. Yoon, and E. L. Thomas: Polymer **44** (2003) 6725.
5) S. Scanlon and A. Aggeli: Nano Today **3** (2008) 22.
6) J. Castillo, S. Tanzi, M. Dimaki, and W. Svendsen: Electrophoresis **29** (2008) 5026.
7) K. B. Andersen, J. Castillo-Leon, M. Hedstrom, and W. E. Svendsen: Nanoscale **3** (2011) 994.
8) J. P. Lee, B. M. Bang, S. Choi, T. Kim, and S. Park: Nanotechnology **22** (2011) 275305.
9) J. S. Park, T. H. Han, J. K. Oh, and S. O. Kim: J. Nanosci. Nanotechnol. **10** (2010) 6954.
10) G. J. Zhang, L. Zhang, M. J. Huang, Z. H. H. Luo, G. K. I. Tay, E. J. A. Lim, T. G. Kang, and Y. Chen: Sens. Actuators B **146** (2010) 138.
11) J. Castillo-León, R. Rodriguez-Trujillo, S. Gauthier, A. C. Ø. Jensen, and W. E. Svendsen: Microelectron. Eng. **88** (2011) 1685.
12) M. Reches and E. Gazit: Science **300** (2003) 625.
13) N. Kol, L. Adler-Abramovich, D. Barlam, R. Z. Shneck, E. Gazit, and I. Rousso: Nano Lett. **5** (2005) 1343.
14) L. Niu, X. Chen, S. Allen, and S. J. B. Tendler: Langmuir **23** (2007) 7443.
15) L. Adler-Abramovich, M. Reches, V. L. Sedman, S. Allen, S. J. B. Tendler, and E. Gazit: Langmuir **22** (2006) 1313.
16) C. H. Clausen, M. Dimaki, S. P. Panagos, E. Kasotakis, A. Mitraki, W. E. Svendsen, and J. Castillo-León: Scanning **33** (2011) 201.
17) C. H. Clausen, J. Jensen, J. Castillo, M. Dimaki, and W. E. Svendsen: Nano Lett. **8** (2008) 4066.
18) O. Carny, D. E. Shalev, and E. Gazit: Nano Lett. **6** (2006) 1594.
19) N. B. Sopher, Z. R. Abrams, M. Reches, E. Gazit, and Y. Hanein: J. Micromech. Microeng. **17** (2007) 2360.
20) M. Larsen, K. Andersen, W. Svendsen, and J. Castillo-León: BioNanoScience **1** (2011) 31.
21) E. C. Cho, J. W. Choi, M. Lee, and K. K. Koo: Colloid Surf. A **313–314** (2008) 95.
22) M. Yemini, M. Reches, E. Gazit, and J. Rishpon: Anal. Chem. **77** (2005) 5155.
23) M. Yemini, M. Reches, J. Rishpon, and E. Gazit: Nano Lett. **5** (2005) 183.
24) A. Colli, A. Fasoli, S. Pisana, Y. Fu, P. Beecher, W. I. Milne, and A. C. Ferrari: Nano Lett. **8** (2008) 1358.
25) D. Whang, S. Jin, and C. M. Lieber: Nano Lett. **3** (2003) 951.
26) S. Li, N. Liu, M. B. Chan-Park, Y. Yan, and Q. Zhang: Nanotechnology **18** (2007) 455302.
27) M. Liu, Y. Chen, Q. Guo, R. Li, X. Sun, and J. Yang: Nanotechnology **22** (2011) 125302.
28) G. Yu, A. Cao, and C. M. Lieber: Nature Nanotechnology **2** (2007) 372.
29) G. Yu, X. Li, C. M. Lieber, and A. Cao: J. Mater. Chem. **18** (2008) 728.
30) T. D. Yuzvinsky, A. M. Fennimore, A. Kis, and A. Zettl: Nanotechnology **17** (2006) 434.
31) A. R. Hopkins, N. A. Kruk, and R. A. Lipeles: Surf. Coatings Technol. **202** (2007) 1282.
32) B. Zheng, C. J. Gerdts, and R. F. Ismagilov: Curr. Opin. Struct. Biol. **15** (2005) 548.
33) G. Zheng, F. Patolsky, Y. Cui, W. U. Wang, and C. M. Lieber: Nat. Biotechnol. **23** (2005) 1294.
34) K. Balasubramanian: Biosens. Bioelectron. **26** (2010) 1195.

5.2 Summary and Perspectives

The fabrication method presented in the present article relies on a spin casting procedure, in which the PNT's are positioned on the wafer aligned with the axial direction. The spin casting procedure itself ensures the absence of larger piles of PNT's and that the structures are positioned individually on the wafer. To utilize this manipulation technique for a controlled fabrication of for instance silicon nanowires, as was the case here, or nanowires from different materials, the electrodes providing the electrical contact to the nanowires, must be designed so that they are oriented perpendicular to the PNT and hence nanowire orientation. To avoid unwanted short circuits elsewhere on the devices the mask must be designed so that the PNT's are only capable of bridging the gab between the electrodes and not between connecting wires. An in depth description of the design of the electrode mask is given in the fabrication procedure discussion in Appendix A.

As mentioned above the manipulation techniques must be changed and optimized for each structure to be positioned and each surface that the structures should be positioned on top. Therefore a manipulation technique providing excellent results for the manipulation of silicon nanowires on a silicon dioxide surface may be useless for the positioning of the biological structures. The method presented in the article is tailored towards the manipulation of FF PNT's on a hydrophillic native oxide covered silicon wafer with a thin electrode pattern as seen in the article. If the structure or the surface is changed some of the parameters in the manipulation methods will probably need to be changed accordingly in order to ensure prober alignment.

Silicon nanowire devices fabricated in this approach has been extensively used in the group in biosenser applications.[139, 140]

CHAPTER 6

PEDOT Nanowires

6.1 Introduction

In an attempt to fabricate biosensors at a lower cost effort has been invested in the development of nanowire devices in different conducting polymers as for instance polyalanine[141–143] and PEDOT.[144–146] The fabricated polymer nanowires has been utilized for both gas - and biosensors.[147–151] However, still issues remain in the development of such polymer nanowire devices. Namely that traditional micro and nano fabrication processes cannot be used in the realization of these devices due to the dependency of organic solvents for the removal of the photoresists.[152]

In the previous chapters the PNT's were utilized in the fabrication of silicon nanowire devices. One of the key aspects of the PNT based fabrication procedure is that the dry etching mask defining the nanowire geometry is water soluble. This allows the patterning of organic material traditionally incompatible with acetone or other organic solvents. In the present article PEDOT nanowire devices was realized in a fast and low cost procedure based on the PNT lithography approach. It was however necessary to change the electrode material since the aluminum oxide formed on aluminum electrodes prevented prober electrical contact between the electrodes and the spin coated PEDOT layer.

Note that the manipulation technique needs to be tailored towards this new surface in order to provide better alignment of the PNT's due to the different surface properties of PEDOT compared to silicon. In the final parts of the paper the functionality of the fabricated PEDOT nanowires is demonstrated in a temperature experiment.

Fabrication and Characterization of PEDOT Nanowires Based on Self-Assembled Peptide Nanotube Lithography

Karsten Brandt Andersen[a,b], Nikolaj Ormstrup Christiansen[a,b], Jaime Castillo-León[a],
Noemi Rozlosnik[a], Winnie Edith Svendsen[a]

[a]DTU Nanotech - Department of Micro- and Nanotechnology, Technical University of Denmark, Lyngby, Denmark
[b]These authors contributed equally

Abstract

In this article we demonstrate the use of self-assembled peptide nanotube structures as a masking material in a rapid, mild and low cost fabrication of PEDOT:TsO nanowire device. In this new fabrication approach the PEDOT:TsO nanowire avoids all contact with any organic solvents otherwise traditionally used in clean room fabrication. This can be achieved due to the intriguing properties of the self-assembled peptide nanotubes utilized as a dry etching mask for the patterning of the PEDOT:TsO nanowire. The peptide nanotubes, despite remaining stable during the reactive ion etching procedure, can be dissolved rapidly in water afterwards. The fabricated PEDOT:TsO nanowire devices exhibit excellent electrical characteristics. Finally the potential of these PEDOT:TsO nanowires as temperature sensors has been demonstrated and the high resolution of the sensor was illustrated.

1. Introduction

Since the original paper on silicon nanowire demonstrating the potential of these new type of biosensors was published more than a decade ago [1] the field of silicon nanowires has received a lot of attention and many articles exploring this specific field have been published [2, 3, 4, 5]. But the fabrication costs of the nanowire devices still are a challenge hindering the full exploration of the nanowire devices as biosensors for diagnostic use [6]. One of the approaches explored to face this challenge has been the realization of nanowires in cheaper materials, for instance conductive polymers such as polyanaline [7, 8, 9] and PEDOT [10, 11, 12]. The benefits of the cheaper nanowire devices have been demonstrated in various applications ranging from chemical gas and liquid sensors [13, 14] over temperature sensors [15] to biosensors [16, 17, 18]. However, the fabrication procedure for the polymer nanowire devices still is challenging and/or time consuming, due to the incompatibility of the polymers with organic solvents used in traditional nanofabrication techniques [19]. Recently we have demonstrated the use of self-assembled diphenylalanine peptide nanotubes (PNT's) as dry etching masks for the low cost, mild and rapid clean room fabrication of silicon nanowire devices [20, 21]. Diphenylalanine self-assembled peptide nanostructures are biological entities able to self-organize in a rapid way under mild conditions. Its on-chip fabrication, structural and electrical characterization, manipulation and application in the development of biosensors were recently reported [22, 23, 24, 25, 26]. In this work we have demonstrated the rapid fabrication of PEDOT:TsO nanowire devices (the whole process can be conducted in approximately 5 hours) based on the self-assembled PNT lithography. The benefit of this fabrication

procedure is that any contact between PEDOT:TsO and organic solvents, such as acetone, can be avoided since the PNT's dissolve rapidly in Milli Q water after the dry etching pattern transfer [27]. The potential of the fabricated PEDOT:TsO nanowire was demonstrated in a temperature experiments, in which the nanowire devices showed a high resolution with a fast response.

2. Materials and Methods

2.1. Chemicals

The Lyophilized diphenylalanine dipeptide powder was purchased from Bachem (product number: G-2925). All other chemicals utilized were purchased from Sigma-Aldrich.

2.2. PEDOT:TsO Preparation

260 μl Baytron C (40,% Fe^{III}tosylate in butanol), 80 μl butanol, 6 μl pyridine and 8.8 μl EDOT were thoroughly mixed and spun on the substrate wafer with 4000 rpm for 60 s. The coated wafers were heated to 70°C for 10 minutes to evaporate the inhibitor Pyradine and start the polymerization process. The wafers were finally rinsed in de-ionised water to wash away excess reactants. This procedure ensures a PEDOT:TsO film thickness of 75 nm.

2.3. Preparation of Diphenylalanine Peptide Nanotubes

The PNT's were prepared from a stock solution, where the lyophilized form of the peptide monomers was dissolved at a concentration of 100 mg/ml in $1, 1, 1, 3, 3, 3$ hexaflouro-2-propanol (HFP). The HFP stock solution was diluted to a final peptide concentration of 2 mg/ml in water in which process the PNT's are formed. Fresh stock solution were prepared prior to experiments to avoid pre aggregates.

2.4. Spin Casting Procedure

The PNT's were positioned across the electrodes in a spin casting procedure as described in [21]. In short the solution containing the newly formed PNT's is dropped in individual drops on the spinning substrate. This spin casting procedure ensures that the PNT's on the surface of the wafer are oriented along the axial direction. In this work a spinrate of 4000 rpm was utilized in all of the experiments.

2.5. Reactive Ion Etching Procedure

The reactive ion etching procedure was conducted in a STS Cluster System C010 with a pressure of 300mTorr and a power of 100W. For the patterning of the PEDOT:TsO an oxygen based plasma was used (98 SCCM O$_2$ and 20 SCCM N$_2$). The wafers were subjected to the plasma for 15 s, which was enough to etch through the thin PEDOT:TsO layer.

2.6. Visualization

All scanning electron microscopic (SEM) images were acquired using a Zeiss supra 40 VP operated in the in-lens mode with an acceleration voltage of 3 kV. The atomic force microscopy (AFM) measurements were conducted using a PSIA XE 150 in both tapping (for topography imaging) and contact (for conductive recordings with a tip bias of 0.7 V) mode. The conductive AFM images was acquired with a Cr/Pt coated cantilever (ContE-Al, Budget Sensors) with a force constant of 0.3/m. The current between the AFM tip and sample was measured using an inverting current amplifier and one of the analogue-digital converter inputs of the AFM controller.

2.7. Electrical Readout

The impedance of the PEDOT:TsO nanowire device was recorded with a custom build lab view controlled experimental setup, as described in [5], where the current through the PEDOT:TsO nanowire is externally amplified using a low-noise current preamplifier model: SR570 from Stanford Research Systems and finally recorded using a National Instruments data acquisition card model BNC-2111.

2.8. Temperature Measurements

The initial temperature measurements were conducted in a water bath with a temperature controlled feedback loop. The real temperature of the water bath was measured using an external thermometer model VT5-S40 from VWR. To investigate the response time of the PEDOT:TsO nanowire to a change in temperature two water baths at different temperatures were prepared and the PEDOT:TsO nanowire devices were moved manually from one to the other while the impedance of the wire was continuously monitored.

3. Results and Discussion

3.1. Fabrication of PEDOT:TsO Nanowires

In a previous work we have demonstrated the use of the diphenylalanine PNT's as a dry etching mask for the fabrication of poly silicon nanowires[20, 21]. One of the benefits of utilizing the PNT's besides the low cost and rapid fabrication process is that they can be removed in Milli Q water after processing[27]. In this way acetone, traditionally required for the removal of photoresists, can be avoided. This enables the patterning of new types of materials normally incompatible with such organic solvents. In this work a modified version of this fabrication procedure has been utilized for the rapid and low cost fabrication of PEDOT:TsO nanowire devices. In fact the entire fabrication procedure can be conducted in approximately 5 hours yielding at the moment around 200 ready to use PEDOT:TsO nanowire devices. In figure 1 the fabrication steps in the process is illustrated. The first and the most time consuming part of the fabrication was the deposition and patterning of the gold electrodes and contact pads allowing electrical connection to the PEDOT:TsO nanowires. In this work 90 nm of gold was deposited on a 500 nm thick silicon dioxide layer grown from a bare silicon wafer utilizing a 10 nm Chromium adhesion layer. The metal layers were patterned in a traditional lift off procedure. The only difference being that the wafer was dipped in a 5% buffered hydrofluoric acid solution for 20 s prior to metal deposition in order to ensure a smooth corner on the edge of the gold electrodes to provide electrical connection between the electrodes and the PEDOT:TsO nanowire. In the second step the PEDOT:TsO layer was spin coated on the wafer with a spinrate of 4000 rpm followed by a post backing step as explained above. The PNT's forming the dry etching mask were positioned across the electrodes in a modified spin casting technique described in [21]. In this manipulation procedure the PNT's aligned according to the axial direction on the wafer. The gold electrodes were positioned perpendicular to this direction such that the aligned peptide nanotubes only were able to bridge the gab at the electrode position and not at other locations in order to avoid potential short circuits as described in our previous work[21]. The final step in the fabrication process was to transfer the pattern of the self-assembled peptide nanotubes to the spin coated PEDOT:TsO layer. After pattern transfer the PNT's were removed in pure Milli Q water.

3.2. Characterization of PEDOT:TsO Nanowires

The fabricated PEDOT:TsO nanowire devices were characterized using both SEM and AFM. A SEM image of a PEDOT:TsO nanowire spanning the gap between two gold electrodes is shown in figure 2a and 2in b a zoom of the contact between the PEDOT:TsO nanowire and the gold electrode illustrates the smooth step coverage of the PEDOT:TsO nanowire across the step from the oxide substrate to the top of the gold electrodes. The large contact area between the gold electrodes and the PEDOT:TsO nanowire and the smooth coverage of the step from the electrode to the substrate by the PEDOT:TsO, as seen in the figure, ensured proper electrical contact in the devices. This is also evident from the small impedance and linear current voltage characteristics even at room temperature of these devices as described below. In figure 2c a topography image of the surface of the PEDOT:TsO nanowire recorded with an AFM in tapping mode is seen and from the line profile shown in d the height of the PEDOT:TsO nanowire can be determined to 75 nm. In this image the surface roughness of the PEDOT:TsO nanowire is also clearly seen. This roughness of the surface introduces a larger surface to volume ratio than comparable flat nanowires and should therefore increase the sensitivity of the measurements. With conductive AFM the complete removal of the PNT's from the PEDOT:TsO surface after etching was verified as seen in figure 3c. From this AFM image it is seen that the surface of the PEDOT:TsO nanowire is highly conductive and hence the isolating PNT's must have dissolved.
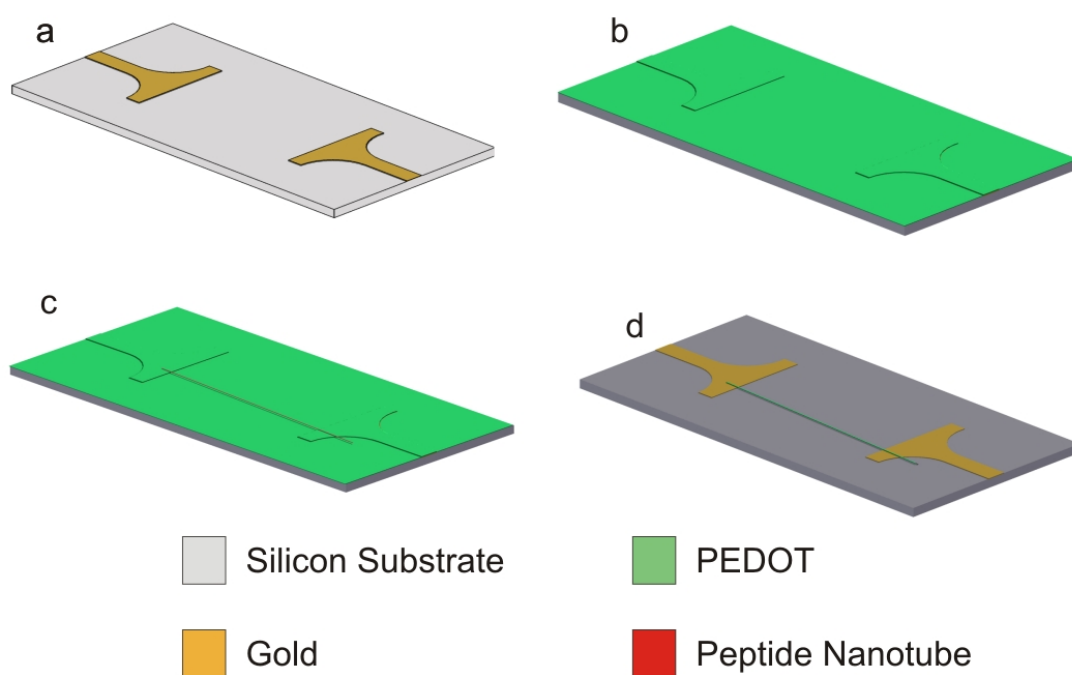
Figure 1. Illustration of the fabrication procedure developed and utilized in this article. In this approach the gold electrodes were initially defined by a lift off procedure. The PEDOT:TsO was spincoated on the wafer and finally the peptide nanotubes were spin casted on the coated wafer to ensure prober alignment of the structures to the electrodes. In the last step the pattern of the nanotubes was transferred to the PEDOT:TsO layer in a reactive ion etching procedure and finally the peptide nanotubes were dissolved in Milli Q water. The process can be completed in approximately 5 hours.

Figure 2. Visualization of the fabricated PEDOT:TsO nanowire structures with the gold contact pads visible. A SEM image of the whole PE-DOT:TsO nanowire spanning the gap between two of the gold electrodes is seen in a. And in b a zoom of the contact area between the PEDOT:Ts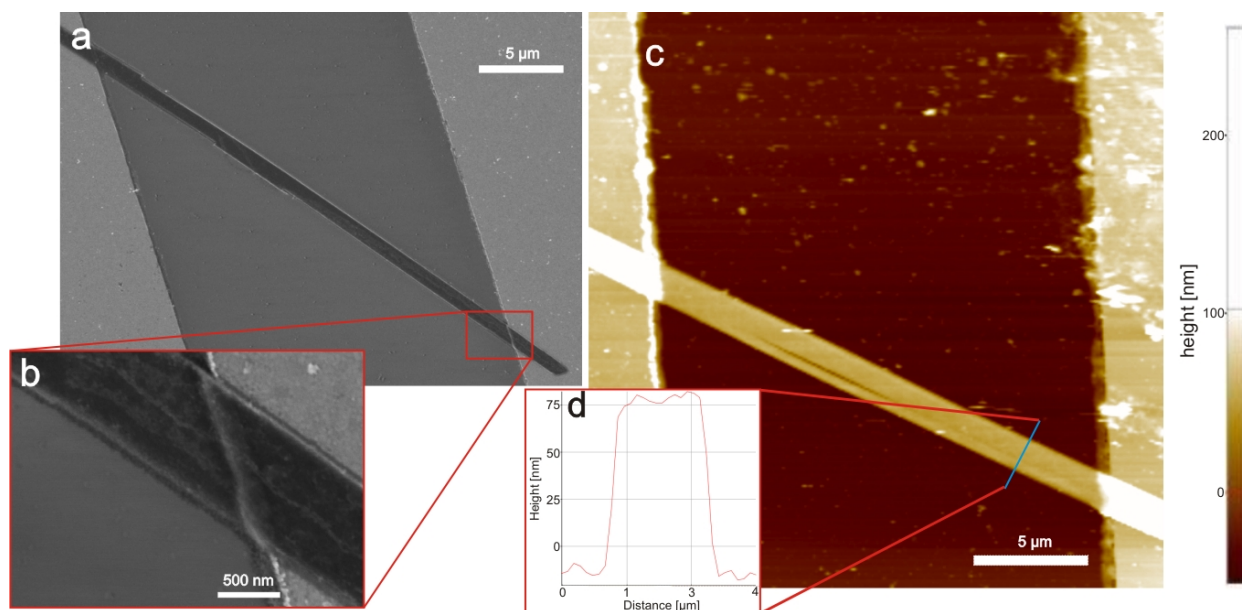O nanowire and the gold contacts is shown. In this image it is seen that the PEDOT:TsO nanowire covers the step of the gold contact very well, which is also evident in the electrical recordings presented below. In c an AFM image of the junction between the PEDOT:TsO nanowire and the gold contact pads is seen and in d a line scan covering the PEDOT:TsO wire is included to verify the height of the fabricated PEDOT:TsO nanowire. From this scan the thickness of the nanowire can be estimated to 75 nm.

3.3. Electrical Characterization

From the SEM image in figure 2a and 2b a continuous connection between that the PEDOT:TsO nanowire and the gold without any fracture in the structure can be seen, which indicates a good electrical connection. To verify this the current voltage relationship of a single PEDOT:TsO nanowire was recorded and plotted in figure 3a for a range of different temperatures. From this plot is is clear that an ohmic electrical contact between the gold contact pads and the PEDOT:TsO nanowires was established as the current voltage relation was linear. The proper electrical contact is ensured by the large contact area between the PEDOT:TsO nanowires and the gold electrodes combined with the smooth corner of the electrodes. The major difference, between this and previous fabrication approaches, is that the PEDOT:TsO in this case is first spin coated on the electrodes and patterned at the electrodes yielding the good electrical contact.

3.4. Temperature Measurements

Finally, to demonstrate the potential of the PEDOT:TsO nanowires they were used as temperature sensors. The impedance of the PEDOT:TsO nanowire was monitored as the temperature was changed. In figure 4a the impedance of the wire is plotted as a function of the temperature of the solution in which the PEDOT:TsO nanowires were submerged (determined by external temperature sensing). In this experiment a linear correlation between the impedance of the PEDOT:TsO nanowires and the external temperature was seen. From this plot it is also evident that the noise level in the PEDOT:TsO nanowire appears very small (corresponding to less than 0.05°C). This is further investigated in 4b where the impedance is monitored while the temperature is changed 0.4°C. As a result of this change in temperature the impedance of the PEDOT:TsO nanowire increased more than 8 times the noise level. Note that in this measurement no shielding of the signal was conducted to mimic the situation in real temperature sensing environments. Performing the measurements in a faraday cage would result in an even smaller noise level and hence higher sensitivity. During the experiments it was also noted that the response time of the PEDOT:TsO nanowire temperature sensor was shorter than that of the traditional external temperature sensor. Therefore in figure 4 the response time of the PEDOT:TsO nanowire device is investigated by the repeated change of external temperature of the wire. From this measurement it
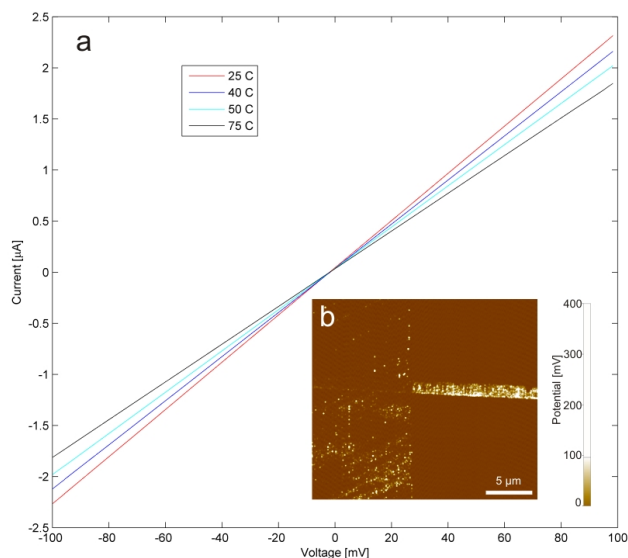
Figure 3. An image acquired with conductive AFM is shown in c demonstrating the complete removal of the isolating peptide nanotubes from the surface of the PEDOT:TsO nanowire. I-V curves for the nanowire devices at different temperatures is plotted to demonstrate the completely linear ohmic behavior of the PEDOT:TsO nanowire indicating a good contact between the gold electrodes and the PEDOT:TsO nanowire in a.

is seen that within 10 s the PEDOT:TsO nanowire device has equilibrated to the new temperature. The fast response of the PEDOT:TsO nanowire stem from the small thermal mass of the wire. In the specific experiments, in fact, the major part of the thermal mass and hence the major contribution to the response time stems from thermal mass of the substrate wafer on which the PEDOT:TsO nanowire is fabricated. The PEDOT:TsO nanowire itself has a thickness of 50 nm, a length of 10 μm and a width in the order of 500 nm and hence the volume of the wire is only 0.25 μm^3 compared to the $\approx 10^{17} \mu$m^3 of the substrate. In comparison with other temperature sensors such as strings and bimetallic geometries relying on optical readout [28, 29, 30], the PEDOT:TsO nanowire only requires a 2 point electrical readout that, due to the small impedance, in principle can be read using a multimeter depending on the desired precision. The very low contact resistance between the gold electrode and the PEDOT:TsO nanowire ensure very sensitive measurements since the dominant change to the impedance of the device is the impedance of the PEDOT:TsO nanowire and hence any smaller change in the impedance in the gold contact pads and electrodes due to the temperature change can be disregarded. In order to utilize the PEDOT:TsO nanowires as biosensors in liquid condition one will have to pattern a passivation layer covering the gold electrodes to ensure no parasitic current through the medium in which the sensors are operated, this will be the focus of future work.

4. Conclusion

In this work we have combined the benefits of bottom up fabrication using self-assembled peptide structures for the patterning of PEDOT:TsO nanowires with the benefits of top down fabrication of macroscopic gold electrode patterns to provide contact pads for reliable electrical contact. In this way we have demonstrated a rapid and low cost fabrication method for the preparation of PEDOT:TsO nanowire devices (The entire fabrication process can be conducted in approximately 5 hours). Note that in the fabrication procedure the PEDOT:TsO layer is never in contact with any organic solvents due to the easy removal of the peptide nanotubes in water. The fabricated PEDOT:TsO nanowires were demonstrated as sensitive to temperature changes (down to 0.05°C changes can be detected with the current setup) and with a fast response time (in this setup approximately 10 s).

References

[1] Y. Cui, Q. Wei, H. Park, C. M. Lieber, Nanowire nanosensors for highly sensitive and selective detection of biological and chemical species, Science 293 (2001) 1289–1292. doi:10.1126/science.1062711.
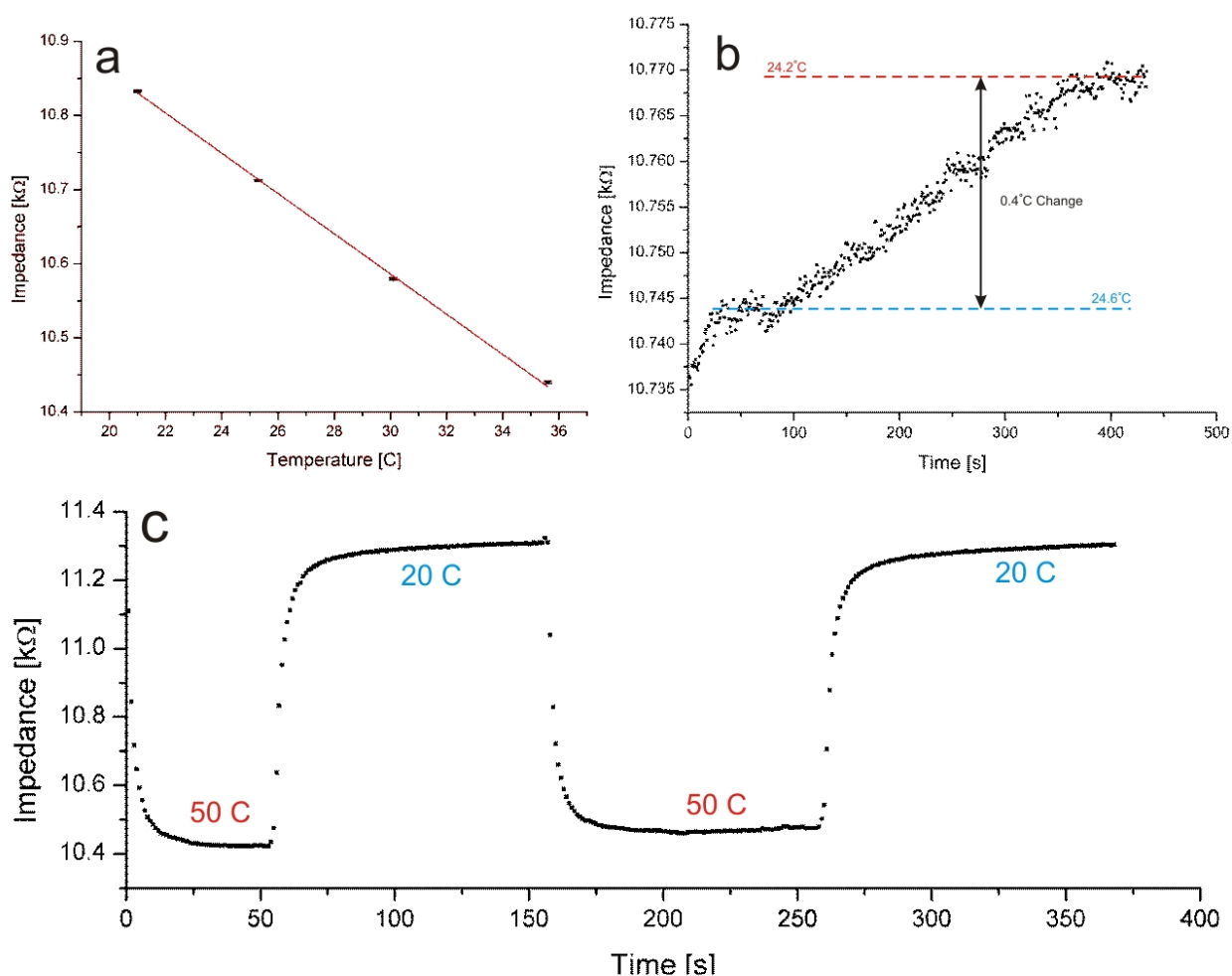
Figure 4. To demonstrate the potential of these PEDOT:TsO nanowire devices they have been utilized as temperature sensors. In a the relationship between temperature and impedance is plotted and from this plot it is seen that the temperature-impedance relation seems very linear. And in b the sensitivity of the PEDOT:TsO nanowire device to temperature changes is illustrated. In this case the temperature was changed with 0.4°C which resulted in a signal change of more than 8 times the noise flor. To determine the response time of the PEDOT:TsO nanowire devices to change in external temperatures the impedance of the nanowire was continuously monitored as the device was transferred between two water baths with different temperatures as seen in c. Within a few seconds the impedance has changed to the new value. Note that the major part of the response time in this setup stems from the thermal mass of the substrate on which the PEDOT:TsO nanowire is fabricated. The response time of the wire itself is much faster.

[2] G. Zheng, F. Patolsky, Y. Cui, W. U. Wang, C. M. Lieber, Multiplexed electrical detection of cancer markers with nanowire sensor arrays, Nature Nanotechnology 23 (2005) 1294–1301. doi:Zheng2005.

[3] G.-J. Zhang, L. Zhang, M. J. Huang, Z. H. H. Luo, G. K. I. Tay, E.-J. A. Lim, T. G. Kang, Y. Chen, Silicon nanowire biosensor for highly sensitive and rapid detection of dengue virus, Sensors and Actuators B: Chemical 146 (2010) 138–144. doi:10.1016/j.snb.2010.02.021.

[4] C.-Y. Hsiao, C.-H. Lin, C.-H. Hung, C.-J. Su, Y.-R. Lo, C.-C. Lee, H.-C. Lin, F.-H. Ko, T.-Y. Huang, Y.-S. Yang, Novel poly-silicon nanowire field effect transistor for biosensing application, Biosensors and Bioelectronics 24 (2009) 1223–1229. doi:10.1016/j.bios.2008.07.032.

[5] W. E. Svendsen, M. Jrgensen, L. Andresen, K. B. Andersen, M. B. B. S. Larsen, S. Skov, M. Dimaki, Silicon nanowire as virus sensor in a total analysis system, Procedia Engineering 25 (2011) 288–291. doi:10.1016/j.proeng.2011.12.071.

[6] K. Balasubramanian, Challenges in the use of 1d nanostructures for on-chip biosensing and diagnostics: A review, Biosensors and Bioelectronics 26 (2010) 1195–1204. doi:10.1016/j.bios.2010.07.041.

[7] I. Lee, X. Luo, X. T. Cui, M. Yun, Highly sensitive single polyaniline nanowire biosensor for the detection of immunoglobulin g and myoglobin, Biosensors and Bioelectronics 26 (2011) 3297–3302. doi:10.1016/j.bios.2011.01.001.

[8] I. Lee, X. Luo, J. Huang, X. T. Cui, M. Yun, Detection of cardiac biomarkers using single polyaniline nanowire-based conductometric biosensors, Biosensors 2 (2012) 205–220. doi:10.3390/bios2020205.

[9] X. Luo, I. Lee, J. Huang, M. Yun, X. T. Cui, Ultrasensitive protein detection using an aptamer-functionalized single polyaniline nanowire, Chemical Communications 47 (2011) 6368–6370. doi:10.1039/c1cc11353d.

[10] A. Das, C. H. Lei, M. Elliott, J. E. Macdonald, M. L. Turner, Non-lithographic fabrication of pedot nano-wires between fixed au electrodes, Organic Electronics 7 (2006) 181–187. doi:10.1016/j.orgel.2005.12.006.

[11] Y.-Z. Long, J.-L. Duvail, Z.-J. Chen, A.-Z. Jin, C.-Z. Gu, Electrical conductivity and current-voltage characteristics of individual conducting polymer pedot nanowires, Chinese Physics Letters 25 (2008) 3474–3477.

[12] Y. Z. Long, J. L. Duvail, Z. J. Chen, A. Z. Jin, C. Z. Gu, Electrical properties of isolated poly(3,4-ethylenedioxythiophene) nanowires prepared by template synthesis, Polymers for Advanced Technologies 20 (2009) 541–544. doi:10.1002/pat.1379.

[13] Y. Chen, Y. Luo, Precisely defined heterogeneous conducting polymer nanowire arrays fabrication and chemical sensing applications, Advanced Materials 21 (2009) 2040–2044. doi:10.1002/adma.200803292.

[14] C. M. Hangarter, S. C. Hernandez, X. He, N. Chartuprayoon, Y. H. Choa, N. V. Myung, Tuning the gas sensing performance of single pedot nanowire devices, Analyst 136 (2011) 2350–2358. doi:10.1039/c0an01000f.

[15] Y. Z. Long, J. L. Duvail, M. M. Li, C. Gu, Z. Liu, S. P. Ringer, Electrical conductivity studies on individual conjugated polymer nanowires: Two-probe and four-probe results, Nanoscale Research Letters 5 (2010) 237–242. doi:10.1007/s11671-009-9417-y.

[16] J. A. Arter, D. K. Taggart, T. M. Mcintire, R. M. Penner, G. A. Weiss, Virus-pedot nanowires for biosensing, Nano Letters 10 (2010) 4858–4862. doi:10.1021/nl025826.

[17] J. A. Arter, J. E. Diaz, K. C. Donavan, T. Yuan, R. M. Penner, G. A. Weiss, Virus-polymer hybrid nanowires tailored to detect prostate specific membrane antigen, Analytical Chemistry 84 (2012) 2776–2783. doi:10.1021/ac203143y.

[18] B. Kannan, D. E. Williams, C. Laslau, J. Travas-Sejdic, A highly sensitive, label-free gene sensor based on a single conducting polymer nanowire, Biosensors and Bioelectronics 35 (2012) 258–264. doi:10.1016/j.bios.2012.02.058.

[19] R. H. Farahi, A. Passian, L. Tetard, T. Thundat, Critical issues in sensor science to aid food and water safety, American Chemical Society Nano 6 (2012) 4548–4556. doi:10.1021/nn204999j.

[20] M. B. B. S. Larsen, K. B. Andersen, W. E. Svendsen, J. Castillo-León, Self-assembled peptide nanotubes as an etching material for the rapid fabrication of silicon wires, BioNanoScience 1 (2011) 31–37. doi:10.1007/s12668-011-0005-6.

[21] K. B. Andersen, J. Castillo-León, T. Bakmand, W. E. Svendsen, Alignment and use of self-assembled peptide nanotubes as dry-etching mask, Japanese Journal of Applied Physics 51 (2012) 06FF13. doi:10.1143/JJAP.51.06FF13.

[22] C. H. Clausen, J. Jensen, J. Castillo, M. Diamki, W. E. Svendsen, Qualitative mapping of structurally different dipeptide nanotubes, Nano Letters 8 (2008) 4066–4069. doi:10.1021/nl801037k.

[23] J. Castillo-León, S. Tanzi, M. Dimaki, W. E. Svendsen, Manipulation of self-assembly amyloid peptide nanotubes by dielectrophoresis, Electrophoresis 29 (2009) 5026–5032. doi:10.1002/elps.200800260.

[24] C. H. Clausen, M. Dimaki, S. P. Panagos, E. Kasotakis, A. Mitraki, W. E. Svendsen, J. Castillo-Len, Electrostatic force microscopy of self-assembled peptide structures, Scanning 33 (2011) 201–207. doi:10.1002/sca.20231.

[25] J. Castillo-León, R. Rodriguez-Trujillo, S. Gauthier, A. C. . Jensen, W. E. Svendsen, Micro-factory for self-assembled peptide nanostructures, Microelectronic Engineering 88 (2011) 1685–1688. doi:10.1016/j.mee.2010.12.023.

[26] J. J. Castillo, W. E. Svendsen, N. Rozlosnik, P. Escobar, F. Martnez, J. Castillo-León, Detection of cancer cells using a paptide nanotube-folic acid modified graphene electrode, Analystdoi:10.1039/c2an36121c.

[27] K. B. Andersen, J. Castillo-León, M. Hedström, W. E. Svendsen, Stability of Diphenylalanine Peptide Nanotubes in Solution, Nanoscale 3 (2011) 994–998. doi:10.1039/c0nr00734j.

[28] A. K. Pandey, O. Gottlieb, A. Shtempluck, E. Buks, Performance of an aupd micromechanical resonator as a temperature sensor, Applied Physics Letters 96 (2010) 203105. doi:10.1063/1.3431614.

[29] T. Larsen, S. Schmid, L. Grnberg, A. O. Niskanen, J. Hassel, S. Dohn, A. Boisen, Ultrasensitive string-based temperature sensors, Applied Physics Letters 98 (2011) 121901. doi:10.1063/1.3567012.

[30] H. Kang, D. Kim, M. Song, Sensitivity enhancement of fbg temperature sensor, OPTICAL SENSING AND DETECTION II 8439 (2012) 84392C. doi:10.1117/12.923271.

6.2   Summary and Perspectives

In the current article PEDOT nanowires were realized based on the PNT mask to demonstrate the patterning of organic materials. Note that the fabrication technique described in this paper is very fast. In fact the entire process from the isolated substrate wafer to the final PEDOT nanowire devices can be realized in less than a day. This work was the first demonstration where the water solubility of the peptide nanotubes was of vital importance. In the fabrication of silicon nanowires it was merely convenient that the nano lithography masking material could be removed in water rather organic solvents. In this work it was key.

Due to the temperature sensitivity of the PEDOT nanowires demonstrated in this report it will in future applications be necessary to either ensure a constant temperature or have a reference PEDOT wire for monitoring the change in impedance caused by changes in external temperatures.

In the previous article we demonstrated that the PEDOT nanowires had a high sensitivity to temperature changes. Currently we are working on the exploitation of this sensitivity for biosensing purposes. However, Before the fabricated PEDOT nanowire devices can be utilized for biosensing purposes a passivation layer covering the gold electrodes connecting the gold contact pads and the PEDOT nanowires must be passivated to avoid leakage current running through the analyte solution rather than through the nanowire.

CHAPTER 7

Conclusion

The main aim of the current project was to investigate and demonstrate different applications of the self-assembling peptide nanotubes based on the dipeptide diphenylalanine. When the project started the structures were believed to be both conducting and stable in most solutions. However, in the initial characterization experiments I have demonstrated that in fact when carefully examined the peptide nanotubes dissolve in most liquids over time. The misinterpretations in former reports arise from an underestimation of how fast the PNT's were able to self-assemble. In the previous work only dried samples was investigated and the PNT's are able to form in the evaporation phase.

In the present study I have performed an in depth study of the stability of the peptide nanotubes when submerged in liquid. In this study I demonstrated that when formed peptide nanotubes were submerged in liquid the concentration of monomers in that particular liquid increased continuously over time. This confirmed the dissolution of the larger peptide nanotubes observed by optical microscopy. We demonstrated that it was possible to increase the stability of the formed structures by changing the formation conditions. In fact when formed in acidic solutions the peptide nanotubes proved significantly more stable (they did still dissolve but proved stable in solution for a few hours). However, the low conductivity of the peptide nanotubes renders them not suited for the implementation as the central component in biological field effect transistors as was the original idea.

In a further investigation of the stability of the peptide nanotubes the structures were taken to a dual beam scanning electron microscope. In this experiment it was demonstrated that the peptide nanotubes, despite the fact that they dissolve in most liquids, remain remarkable stable during prolonged bombardment with heavy ions. This effect was further utilized to demonstrate the potential use of the peptide nanotubes as an inexpensive water soluble mask to be used in standard cleanroom fabrication of silicon nanowires instead of the traditional and very expensive electron beam lithography. In this report also the potential use of the peptide nanotubes as a lift off mask for the fabrication of nanoslits in metal surfaces was demonstrated. Note that in this process the lift off procedure is conducted in water instead of acetone.

In order to utilize the full potential of the peptide nanotubes as a cleanroom fabrication tool a method for the controlled manipulation of the peptide nanotubes must be developed. This manipulation technique should enable a proper positioning of the peptide nanotubes in fast and reliable manner preferably at wafer scale. Different manipulation techniques were considered,

57

but the solubility of the peptide nanotubes rendered many traditional manipulation techniques useless. With a modified version of the spin casting technique developed in this project the best compromises between the results and the time required for the manipulation were achieved. By proper electrode design it was possible to increase the yield of this fabrication process to 80 % with very few short circuits.

The water solubility of the peptide nanotube dry etching mask allows the patterning of organic materials, which are not compatible with acetone or other organic solvents used to remove the traditional photoresists. In the final parts of the project the rapid (entire process could be conducted in approximately 5 hours) and low cost fabrication of conductive polymer (PEDOT:TsO) nanowire devices based on the peptide nanotube lithography approach was demonstrated. The potential of the fabricated nanowire devices as temperature sensors was demonstrated. In the experiments it was shown that the nanowire devices were capable of detecting a temperature change of $0.05°C$.

CHAPTER 8

Final Thoughts and Outlook

Self-assembling structures will continue to intrigue scientists in years to come. Due to advances in peptide synthesis and a better understanding of the biological structures new self-assembling structures will be discovered and they will initially be surrounded by the same hype as for the diphenylalanine peptide nanotubes. However, it is important first to properly characterize the material and to keep these material properties in mind when designing applications for the new and fascinating structures. The water solubility of the diphenylalanine peptide nanotubes does not make them less interesting. In fact they may even prove more valuable as a fabrication tool than in the various direct application previously reported.

In this work I have demonstrated the potential of the peptide nanotubes as a fabrication tool. I might have just scratched the surface of the opportunities for the peptide nanotubes in an alternative fabrication approach, where top down fabrication approach for the patterning of the interconnections is combined with the self-assembled peptide nanotube based lithography allowing a vast amount of nanostructures in a rapid and mild manner. In fact the water solubility of the peptide nanotubes allows the patterning of new polymer materials incompatible with the organic solvents used in traditional photolithography. However, a number of challenges for the full exploitation of this fabrication approach still exists: 1) The formation process of the peptide nanotubes leads to a large distribution in size ranging from the smallest nanotubes in the order of 100 nm up to several microns. A smaller size variation can be achieved if the peptide tubes are prepared immediately before the spin casting procedure, but the size variation is still significant. The formed peptide nanotubes also vary in length, which further complicate the design of the electrodes and contact pads. Recently we have seen that with a point sonicator it was possible to break up the PNT's into smaller much more uniform entities. The sonication of the PNT solution could be performed immediately prior to the spin casting procedure whereby smaller and more uniform PNT's would be positioned on the wafer. This would further allow an optimization of the electrode structure to fit these smaller PNT's providing smaller nanowires and less short circuits. 2) The spin casting procedure does still not ensure a perfect yield. In fact only a few chips were realized with all the five electrode pairs connected by nanowires. As mentioned in chapter 5 a whole range of different parameters affect the spin casting procedure and to ensure better alignment a detailed study on how the individual parameters affect the alignment should be conducted. A simple way of increasing the yield of the manipulation approach would be to increase

59

the affinity between the peptide nanotubes and the substrate at the electrode locations by a surface modification and vice versa at the contact pad positions (most short circuits are experienced in this area).

If the challenges mentioned above could be met a number of very interesting applications for the peptide nanotubes could be explored. Below I will briefly mention a few that from my point of view should be explored. 1) In the same way as PEDOT:TsO nanowires were realized one could be able to fabricate graphene nanoribbons either directly on the electrodes or (due to the water solubility of the peptide nanotubes) on the polymer sacrificial layer, used to transfer the graphene from the copper growth substrate to the device substrate, providing the user with a graphene nanoribbon stamp. 2) In chapter 3 it was seen how the structure changed upon heating of a formed and dried peptide nanotube. If the heated structures could be used as a dry etching mask in the same way as the non heated structures one would be able to produce nanowire devices with much smaller dimension and at the same time with a much larger surface to volume ratio. Both of these should result in a sensor with a larger sensitivity. The benefit of the heated structures is that the smaller entities of the PNT's remain in the same position and therefore the heated structure often still bridge the gaps between the electrodes and could still potentially be used as an etching mask. It would result in a nanowire structure with a much higher surface to volume ratio and at the same time smaller dimension of the fabricated nanowire and hence a higher sensitivity.

Bibliography

[1] Luc Wasungu and Dick Hoekstra. Cationic lipids, lipoplexes and intracellular delivery of genes. *Journal of Controlled Release*, 116:255–264, 2006.

[2] Ehud Gazit. A possible role for π-stacking in the self-assembly of amyloid fibrils. *The FASEB Journal*, 16:77–83, 2002.

[3] Meital Reches and Ehud Gazit. Casting Metal Nanowires Within Discrete Self-Assembled Peptide Nanotubes. *Science*, 625:625–627, 2003.

[4] R. Nelson, M. R. Sawaya, M. Balbirnie, A. Ø. Madsen, C. Riekel, R. Grothe, and D. Eisenberg. Structure of the cross-β spine of amyloid-like fibrils. *Nature*, 435:773–778, 2005.

[5] M. R. Sawaya, S. Sambashivan, R. Nelson, M. I. Ivanova, S. A. Sievers, M. I. Apostol, M. J. Thompson, M. Balbirnie, J. J. W. Wiltzius, H. T. McFarlane, A. Ø. Madsen, C. Riekel, and D. Eisenberg. Atomic structures of amyloid cross-β spines reveal varied steric zippers. *Nature*, 447:453–457, 2007.

[6] Carl Henrik Görbitz. Microporous organic materials from hydrophobic dipeptides. *Chemistry an European Journal*, 13:1022–1031, 2007.

[7] Jaime Castillo-León, Karsten B. Andersen, and Winnie E. Svendsen. *Self-assembled peptide nanostructures for biomedical applications: advantages and challenges.* Intech, 2011.

[8] Gurvinder Singh, Alexander M. Bittner, Sebastian Loscher, Nikola Malinowski, and Klaus Kern. Electrospinning of diphenylalanine nanotubes. *Advanced Materials*, 20:2332–2336, 2008.

[9] Lihi Adler-Abramovich, Daniel Aronov, Peter Beker, Maya Yevnin, Shiri Stempler, Ludmila Buzhansky, Gil Rosenman, and Ehud Gazit. Self-assembled arrays of peptide nanotubes by vapour deposition. *Nature Nanotechnology*, 4:849–854, 2009.

[10] Carl Henrik Görbitz. Nanotube formation by hydrophobic dipeptides. *Chemistry an European Journal*, 7:5153–5159, 2001.

[11] Carl Henrik Görbitz. Nanotubes from hydrophobic dipeptides: pore size regulation through side chain substitution. *New Journal of Chemistry*, 27:1789–1793, 2003.

[12] Meital Reches and Ehud Gazit. Designed aromatic homo-dipeptides: formation of ordered nanostructures and potential nanotechnological applications. *Physical Biology*, 3:10–19, 2006.

[13] Xuehai Yan, Pengli Zhu, and Junbai Li. Self-assembly and application of diphenylalanine-based nanostructures. *Chemical Society Reviews*, 39:1877–1890, 2010.

[14] J. Ryu and C. B. Park. High-temperature self-assembly of peptides into vertically well-aligned nanowires by aniline vapor. *Advanced Materials*, 20:3754–3758, 2008.

[15] Mehmet B. Taskin, Luigi Sasso, Indumathi Vedarethinam, Winnie E. Svendsen, and Jaime Castillo-León. Vertically aligned patterned peptide nanowires for cellular studies. *proceeding of: TechConnect World*, 3:64–67, 2012.

[16] Jungki Ryu and Beum Park. High stability of self-assembled peptide nanowires against thermal, chemical, and proteolytic attacks. *Biotechnology and Bioengineering*, 105:221–230, 2010.

[17] Jungki Ryu and Chan Beum Park. Synthesis of diphenylalanine/polyaniline core/shell conducting nanowires by peptide self-assembly. *Angewandte Chemie International Edition*, 48:4820–4823, 2009.

[18] Luigi Sasso, Indumathi Vedarethinam, Jenny Emnéus, Winnie E. Svendsen, and Jaime Castillo-León. Self-assembled diphenylalanine nanowires for cellular studies and sensor applications. *Journal of Nanoscience and Nanotechnology*, 12:3077–3083, 2012.

[19] Joon Seok Lee, Jungki Ryu, and Chan Beum Park. Bio-inspired fabrication of superhydrophobic surfaces through peptide self-assembly. *Soft Matter*, 5:2717–2720, 2009.

[20] Jungki Ryu, Sung-Wook Kim, Kisuk Kang, and Chan Beum Park. Synthesis of diphenylalanine/cobalt oxide hybrid nanowires and their application to energy storage. *Amarican Chemical Society Nano*, 4:159–164, 2010.

[21] Jungki Ryu, Sook Hee Ku, Minah Lee, and Chan Beum Park. Bone-like peptide/hydroxyapatite nanocomposites assembled with multi-level hierarchical structures. *Soft Matter*, 7:7201–7206, 2011.

[22] Hyang-Im Ryoo, Joon Seok Lee, Chan Beum Park, and Dong-Pyu Kim. A microfluidic system incorporated with peptide/pd nanowires for heterogeneous catalytic reactions. *Lab on a Chip*, 11:378–380, 2010.

[23] Pim W. J. M. Frederix, Rein V. Ulijn, Neil T. Hunt, and Tell Tuttle. Virtual Screening for Dipeptide Aggregation: Toward Predictive Tools for Peptide Self-Assembly. *Physical Chemistry Letters*, 2:2380–2384, 2011.

[24] Yujiang Song, Sivakumar R. Challa, Craig J. Medforth, Yan Qiu, Richard K. Watt, Donovan Peña, James E. Miller, Frank van Swol, and John A. Shelnutt. Synthesis of peptide-nantube platinum-nanoparticle composites. *Chemical Communications*, 9:1044–1045, 2004.

[25] Jaime Castillo-León, Romén Rodriguez-Trujillo, Sebastian Gauthier, Alexander C. Ø. Jensen, and Winnie E. Svendsen. Micro-"factory" for self-assembled peptide nanostructures. *Microelectronic Engineering*, 88:1685–1688, 2011.

[26] Priyadharshini Kumaraswamy, Rajesh Lakshmanan, Swaminathan Sethuraman, and Uma Maheswari Krishnan. Self-assembly of peptides: influence of substrate, ph and medium on the formation of supramolecular assemblies. *Soft Matter*, 7:2744–2754, 2011.

[27] Gokhan Demirel and Fatih Buyukserin. Surface-induced self-assembly of dipeptides onto nanotextured surfaces. *Langmuir*, 27:12533–12538, 2011.

[28] Karsten B. Andersen, Jaime Castillo-Léon, Martin Hedström, and Winnie E. Svendsen. Stability of Diphenylalanine Peptide Nanotubes in Solution. *Nanoscale*, 3:994–998, 2011.

[29] Minjie Wang, Lingjie Du, Xinglong Wu, Shijie Xiong, and Paul K. Chu. Charged diphenylalanine nanotubes and controlled hierarchical self-assembly. *Amarican Chemical Society Nano*, 5:4448–4454, 2010.

[30] J. Shklovsky, P. Beker, N. Amdursky, Ehud Gazit, and G. Rosenman. Bioinspired peptide nanotubes: Deposition technology and physical properties. *Materials Science and Engineering B*, 169:62–66, 2010.

[31] P. Beker, I. Koren, N. Amdursky, Ehud Gazit, and G. Rosenman. Bioinspired peptide nanotubes as supercapacitor electrodes. *Journal of Material Science*, 45:6374–6378, 2010.

[32] L. Adler-Abramovich, N. Kol, I. Yanai, D. Barlam, R. Z. Shneck, E. Gazit, and I. Rousso. Self-assembled organic nanostructures with metallic-like stiffness. *Angewandte Chemie International Edition*, 49:9939–9942, 2010.

[33] Lihi Adler-Abramovich and Ehud Gazit. Controlled patterning of peptide nanotubes and nanospheres using inkjet printing technology. *Journal of Peptide Science*, 14:217–223, 2007.

[34] Casper H. Clausen, Maria Dimaki, Spyros P. Panagos, Emmanouil Kasotakis, Anna Mitraki, Winnie E. Svendsen, and Jaime Castillo-León. Electrostatic force microscopy of self-assembled peptide structures. *Scanning*, 33:201–207, 2011.

[35] Sivan Yuran, Yair Razvag, and Meital Reches. Coassembly of aromatic dipeptides into biomolecular necklaces. *Amarican Chemical Society Nano*, 2012.

[36] Claire Tang, Andrew M. Smith, Richard F. Collins, Rein V. Ulijn, and Alberto Saiani. Fmoc-diphenylalanine self-assembly mechanism induces apparent pka shifts. *Langmuir*, 25:9447–9453, 2009.

[37] Wilda Helen, Piero de Leonardies, Rein V. Ulijn, Julie Gough, and Nicola Tirelli. Mechanosensitive peptide gelation: mode of agitation controls mechanical properties and nano-scale morphology. *Soft Matter*, 7:1732–1740, 2011.

[38] Assaf Mahler, Meital Reches, Meirav Rechter, Smadar Cohan, and Ehud Ghazit. Rigid, self-assembled hydrogel composed of a modified aromatic dipeptide. *Advanced Materials*, 18:1365–1370, 2006.

[39] jaclyn Raeburn, Guillaume Pont, Lin Chen, Yann Cesbron, Raphaë Lévy, and Dave J. Adams. Fmoc-diphenylalanine hydrogels: understanding the variability in reported mechanical properties. *Soft Matter*, 8:1168–1174, 2012.

[40] Vineetha Jayawarna, Murtza Ali, Thomas A. Jowitt, Aline F. Miller, Alberto Saiani, Julie E. Gough, and Rein V. Ulijn. Nanostructured hydrogels for three-dimensional cell culture through self-assembly of fluorenylmethoxycarbonyl–dipeptides. *Advanced Materials*, 18:611–614, 2006.

[41] Ron Orbach, Lihi Adler-Abramovich, Sivan Zigerson, Iris Mironi-Harpaz, Dror Seliktar, and Ehud Ghazit. Self-assembled fmoc-peptides as a platform for the formation of nanostructures and hydrogels. *Biomacromolecules*, 10:2646–2651, 2009.

[42] Andrew M. Smith, Richard J. Williams, Claire Tang, Paolo Coppo, Richard F. Collins, Michael L. Turner, Alberto Saiani, and Rein V. Ulijn. Fmoc-diphenylalanine self assembles to a hydrogel via a novel architecture based on p–p interlocked b-sheets. *Advanced Materials*, 20:37–41, 2007.

[43] Thomas Liebmann, Susanna Rydholm, Victor Akpe, and Hjalmar Brismar. Self-assembling fmoc dipeptide hydrogel for in situ 3d cell culturing. *BMC Biotechnology*, 7, 2007.

[44] Vineetha Jayawarna, Stephen M. Richardson, Andrew R. Hirst, Nigel W. Hodson, Alberto Saiani, Julie E. Gough, and Rein V. Ulijn. Introducing chemical functionality in fmoc-peptide gels for cell culture. *Acta Biomaterialia*, 5:934–943, 2009.

[45] Mi Zhou, Andrew M. Smith, Apurba K. Das, Nigel W. Hodson, Richard F. Collins, Rein V. Ulijn, and Julie E. Gough. Self-assembled peptide-based hydrogels as scaffolds for anchoragedependent cells. *Biomaterials*, 30:2523–2530, 2009.

[46] Jae Hong Kim, Seong Yoon Lim, Dong Heon Nam, Jungki Ryu, Sook Hee Ku, and Chan Beum Park. Self-assembled, photoluminescent peptide hydrogel as a versatile platform for enzyme-based optical biosensors. *Biosensors and Bioelectronics*, 26:1860–1865, 2011.

[47] Renliang Huang, Wei Qi, Libin Feng Rongxin Su, and Zhimin He. Self-assembling peptide–polysaccharide hybrid hydrogel as a potential carrier for drug delivery. *Soft Matter*, 7:6222–6230, 2011.

[48] Jungki Ryu, Sung-Wook Kim, Kisuk Kang, and Chan Beum Park. Mineralization of self-assembled peptide nanofibers for rechargeable lithium ion batteries. *Advanced Materials*, 22:5537–5541, 2010.

[49] Meital Reches and Ehud Gazit. Self-assembly of peptide nanotubes and amyloid-like structures by charged-termini-capped diphenylalanine peptide analogues. *Israel Journal of Chemistry*, 45:363–371, 2005.

[50] Yi Cui, Qingqiao Wei, Hongkun Park, and Charles M. Lieber. Nanowire nanosensors for highly sensitive and selective detection of biological and chemical species. *Science*, 293:1289–1292, 2001.

[51] Gengfeng Zheng, Fernando Patolsky, Yi Cui, Wayne U. Wang, and Charles M. Lieber. Multiplexed electrocal detection of cancer markers with nanowire sensor arrays. *Nature Biotechnology*, 23:1294–1301, 2005.

[52] Adam K. Wanekaya, Wilfred Chen, Nosang V. Myung, and Ashok Mulchandani. Nanowire-based electrochemical biosensors. *Electroanalysis*, 18:533–550, 2006.

[53] Kuan-I Chen, Bor-Ran Li, and Yit-Tsong Chen. Silicon nanowire field-effect transistor-based biosensors for biomedical diagnosis and cellular recording investigation. *Nano Today*, 6:131–154, 2011.

[54] J. K. W. Sandler, J. E. Kirk, I. A. Kinloch, M. S. P. Shaffer, and A. H. Windle. Ultra-low electrical percolation threshold in carbon-nanotube-epoxy composites. *Polymer*, 44:5893–5899, 2003.

[55] F. H. Gojny, M. H. G. Wichmann, U. Köpke, B. Fiedler, and K. Schulte. Carbon nanotube-reinforced epoxy-composites: enhanced stiffness and fracture toughness at low nanotube content. *Composites Science and Technology*, 64:2363–2371, 2004.

[56] Hye-Mi So, Keehoon Won, Yong Hwan Kim, Byoung-Kye Kim, Beyong Hwan Ryu, Pil Sun Na, Hyojin Kim, and Jeong-O Lee. Single-walled carbon nanotube biosensors using aptamers as molecular recognition elements. *Journal of American Chemical Society*, 127:11906–11907, 2005.

[57] Jonghwan Suhr, Nikhil Koratkar, Pawel Keblinski, and Pulickel Ajayan. Viscoelasticity in carbon nanotube composites. *Nature Materials*, 4:134–137, 2005.

[58] Brett Lee Allen, Padmakar D. Kichambare, and Alexander Star. Carbon nanotube field-effect-transistor-based biosensors. *Advanced Materials*, 19:1439–1451, 2007.

[59] Zonghua Wang, Jun Liu, Qionglin Liang, Yiming Wang, and Guoan Luo. Carbon nanotube-modified electrodes for the simultaneous determination of dopamine and ascorbic acid. *Analyst*, 127:653–658, 2002.

[60] Sofia Sotiropoulou and Nikolas A. Chaniotakis. Carbon nanotube array-based biosensor. *Analytical and Bioanalytical Chemistry*, 375:103–105, 2003.

[61] Abdollah Salimi, Richard G. Compton, and Rahman Hallaj. Glucose biosensor prepared by glucose oxidase encapsulated sol-gel and carbon-nanotube-modified basal plane pyrolytic graphite electrode. *Analytical Biochemistry*, 333:49–56, 2004.

[62] Xia Chu, Daxue Duan, Guoli Shen, and Ruqin Yu. Amperometric glucose biosensor based on electrodeposition of platinum nanoparticles onto covalently immobilized carbon nanotube electrode. *Talanta*, 71:2040–2047, 2007.

[63] Lihi Adler-Abramovich, Michal Badihi-Mossberg, Ehud Gazit, and Judith Rishpon. Characterization of peptide-nanostructure-modified electrodes and their application for ultrasensitive environmental monitoring. *Small*, 6:825–831, 2010.

[64] Miri Yemini, Meital Reches, Judith Rishpon, and Ehud Gazit. Novel electrochemical biosensing platform using self-assembled peptide nanotubes. *Nano Letters*, 5:183–186, 2005.

[65] Eun Chan Cho, Jeong-Woo Choi, Moonyong Lee, and Kee-Kahb Koo. Fabrication of an electrochemical immunosensor with self-assembled peptide nanotubes. *Colloids and Surfaces A*, 313-314:95–99, 2008.

[66] Byung-Wook Park, Rui Zheng, Kyoung-A Ko, Brent D. Cameron, Do-Young Yoon, and Dong-Shik Kim. A novel glucose biosensor using bi-enzyme incorporated with peptide nanotubes. *Biosensors and Bioelectronics*, 38:295–301, 2012.

[67] Byung-Wook Park, Kyoung-A. Ko, Do-Young Yoon, and Dong-Shik Kim. Enzyme activity assay for horseradish peroxidase encapsulated in peptide nanotubes. *Enzymatic and Microbial Technology*, 51:81–85, 2012.

[68] Jae Hong Kim, Minah Lee, Joon Seok Lee, and Chan Beum Park. Self-assembled light-harvesting peptide nanotubes for mimicking natural photosynthesis. *Angewandte Chemie International Edition*, 51:517–520, 2011.

[69] Jae Hong Kim, Jungki Ryu, and Chan Beum Park. Selective detection of neurotoxin by photoluminescent peptide nanotubes. *Small*, 7:718–722, 2011.

[70] N. B. Sopher, Z. R. Abrams, Meital Reches, Ehud Ghazit, and Y. Hanein. Integrating peptide nanotubes in micro-fabrication process. *Journal of Micromechanics and Microengineering*, 17:2360–2365, 2007.

[71] Ohad Carny, Deborah E. Shalev, and Ehud Gazit. Fabrication of Coaxial Metal Nanocables Using a Self-Assembled Peptide Nanotube Scaffold. *Nano Letters*, 6(8):1594–1597, 2006.

[72] Miri Yemini, Meital Reches, Ehud Gazit, and Judith Rishpon. Peptide nanotube-modified electrodes for enzyme-biosensor applications. *Analytical Chemistry*, 77:5155–5159, 2005.

[73] Iorquirene de Oliveira Matos and Wendel Andrade Alves. Electrochemical determination of dopamine based on self-assembled peptide nanostructure. *Applied Materials & Interfaces*, 3:4437–4443, 2011.

[74] Byung-Wook Park, Do-Young Yoon, and Dong-Shik Kim. Encapsulation of enzymes inside peptide nanotubes for hydrogen peroxide detection. *ECS Transactions*, 33:25–29, 2010.

[75] K. Goldshtein, D. Golodnitsky, E. Peled, Lihi Adler-Abramovich, Ehud Gazit, S. Khatun, P. Stallworth, and S. Greenbaum. Effect of peptide nanotube filler on structural and ion-transport properties of solid polymer electrolytes. *Solid State Ionics*, 220:39–46, 2012.

[76] Nitzan Even, Lihi Adler-Abramovich, Ludmila Buzhansky, Hanna Dodiuk, and Ehud Gazit. Improvement of the mechanical properties of epoxy by peptide nanotube fillers. *Small*, 7:1007–1011, 2011.

[77] Carl Henrik Görbitz. The structure of nanotubes formed by diphenylalanine, the core recognition motif of alzheimer's β-amyloid polypeptide. *Chemical Communications*, 22:2332–2334, 2006.

[78] Tae Hee Han, Jun Kyun Oh, Ji Sun Park, Se-Hun Kwon, Sung-Wook Kim, and Sang Ouk Kim. Highly entangled hollow tio2 nanoribbons templating diphenylalanine assembly. *Journal of Material Chemistry*, 19:3512–3516, 2009.

[79] J. Kim, T. H. Han, Y.-I. Kim, J. S. Park, J. Choi, D. G. Churchill, S. O. Kim, and H. Ihee. Role of water in directing diphenylalanine assembly into nanotubes and nanowires. *Advanced Materials*, 22:583–587, 2010.

[80] Nitzan Kol, Lihi Adler-Abramovich, David Barlam, Roni Z. Shneck, Ehud Gazit, and Itay Rousso. Self-Assembled Peptide Nanotubes Are Uniquely Rigid Bioinspired Supramolecular Structures. *Nano Letters*, 5(7):1343–1346, 2005.

[81] Lijiang Niu, Xinyong Chen, Stephanie Allen, and Saul J. B. Tendler. Using the Bending Beam Model to Estimate the Elasticity of Diphenylalanine Nanotubes. *Langmuir*, 23:7443–7446, 2007.

[82] Victoria L. Sedman, Lihi Adler-Abramovich, Stephanie Allen, Ehud Gazit, and Saul J. B. Tendler. Direct Observation of the Release of Phenylalanine from Diphenylalanine Nanotubes. *Journal of American Chemical Society*, 128:6903–6908, 2006.

[83] Lihi Adler-Abramovich, Meital Reches, Victoria L. Sedman, Stephanie Allen, Saul J. B. Tendler, and Ehud Gazit. Thermal and Chemical Stability of Diphenylalanine Peptide Nanotubes: Implications for Nanatechnological Applications. *Langmuir*, 22:1313–1320, 2006.

[84] Jaime Castillo-León, Simone Tanzi, Maria Dimaki, and Winnie E. Svendsen. Manipulation of self-assembly amyloid peptide nanotubes by dielectrophoresis. *Electrophoresis*, 29:5026–5032, 2009.

[85] Karsten B. Andersen, Jaime Castillo-León, and Winnie Edith Svendsen. Conductance investigation of self organizing biological nanotube structures. In *Biosensors*, 2010.

[86] Joon Seok Lee, Ilsun Yoon, Jangbae Kim, Hyotcherl Ihee, Bongsoo Kim, and Chan Beum Park. Self-assembly of semiconducting photoluminescent peptide nanowires in the vapor phase. *Angewandte Chemie International Edition*, 50:1164–1167, 2010.

[87] N. Santhanamoorthi, P. Kolandaivel, Lihi Adler-Abramovich Ehud Gazit, S. Filipek, Sowmya Viswanathan, Anthony Strzelzyk, and V. Renugopalakrishnan. Diphenylalanine peptide nanotube: charge transport, band gap and its relevance to potential biomedical applications. *Adavanced Material Letters*, 2:100–105, 2011.

[88] Nadav Amdursky, Peter Beker, Itai Koren, Becky Bank-Srour, Elena Mishina, Sergey Semin, Theo Rasing, Yuri Rosenberg, Zahava Barkay, Ehud Gazit, and Gil Rosenman. Structural transition in peptide nanotubes. *Biomacromolecules*, 12:1349–1354, 2011.

[89] Magdalena Jaworsky, Agata Jeziorna, Ewelina Drabik, and Marek J. Potrzebowski. Solid state nmr study of thermal process in nanoassemblies formed by dipeptides. *Journal of Physical Chemistry C*, 116:12330–12338, 2012.

[90] Dongmok Whang, Song Jin, and Charles M. Lieber. Nanolithography using hierarchically assembled nanowire masks. *Nano Lett.*, 3:951–954, 2003.

[91] Alan Colli, Andrea Fasoli, Simone Pisana, Yongqing Fu, Paul Beecher, William I. Milne, and Andrea C. Ferrari. Nanowire Lithography on Silicon. *Nano Letters, Nano Lett.*, 8:1358–1362, 2008.

[92] Dongmok Whang, Song Jin, Yue Wu, and Charles M. Lieber. Large-scale hierarchical organization of nanowire arrays for integrated nanosystems. *Nano Letters*, 3:1255–1259, 2003.

[93] Bo He, Thomas J. Morrow, and Christine D. Keating. Nanowire sensors for multiplexed detection of biomolecules. *Current Opinion in Chemical Biology*, 12:522–528, 2008.

[94] Nikolas Chronis and Luke P. Lee. Electrothermally activated su-8 microgripper for single cell manipulation in solution. *Journal of Microelectromechanical Systems*, 14:857–863, 2005.

[95] K. Carlson, K. N. Andersen, V. Eichhorn, D. H. Petersen, K. Mølhave, I. Y. Y. Bu, K. B. K. Teo, W. I. Milne, S. Fatikow, and P. Bøggild. A carbon nanofibre scanning probe assembled using an electrothermal microgripper. *Nanotechnology*, 18:345501, 2007.

[96] Felix Beyeler, Adrian Neild, Setfano Oberti, Dominik J. Bell, Yu Sun, Jürg Dual, and Bradley J. Nelson. Monolithically fabricated microgripper with integrated force sensor for manipulating microobjects and biological cells aligned in an ultrasonic field. *Journal of Microelectromechanical Systems*, 16:7–15, 2007.

[97] O Sardan, V. Eichhorn, D. H. Petersen, S. Fatikow, O. Sigmund, and P. Bøggild. Rapid prototyping of nanotube-based devices using topology-optimized microgrippers. *Nanotechnology*, 19:495503, 2008.

[98] Rachael Daunton, Andrew Gallant, David Wood, and Ritu Kataky. A thermally actuated microgripper as an electrochemical sensor with the ability to manipulate single cells. *Chemical Communications*, 47:6446–6448, 2011.

[99] Guangyong Li, Ning Xi, Heping Chen, Ali Saeed, and Mengmeng Yu. Assembly of nanostructure using afm based nanomanipulation system. *Proceedings IEEE International Conference on Robotics and Automation*, 1:428–433, 2004.

[100] K. Reynolds, J. Komulainen, J. Kivijakola, P. Lovera, D. Iacopino, M. Pudas, J. Vähäkangas, J. Röning, and G. Redmond. Probe based manipulation and assembly of nanowires into organized mesostructures. *Nanotechnology*, 19:485301, 2008.

[101] Suenne Kim, Farbod Shafiei, Daniel Ratchford, and Xiaoqin Li. Controlled afm manipulation of small nanoparticles and assembly of hybrid nanostructures. *Nanotechnology*, 22:115301–115306, 2011.

[102] Ritesh Agarwal, Kosta Ladavac, Yael Roichman, Guihua Yu, Charles Lieber, and David Grier. Manipulation and assembly of nanowires with holographic optical traps. *Optics Express*, 13:8906–8912, 2005.

[103] Peter J. Pauzauskie, Aleksandra Radenovic, Eliane Trepagnier, Hari Shroff, Peidong Yang, and Jan Liphardt. Optical trapping and integration of semiconductor nanowire assemblies in water. *Nature Materials*, 5:97–101, 2006.

[104] Arash Jamshidi, Peter J. Pauzauskie, P. James Schuck, Aaron T. Ohta, Pei-Yu Chiou, Jeffrey Chou, Peidong Yang, and Ming C. Wu. Dynamic manipulation and separation of individual semiconducting and metallic nanowires. *Nature Photonics*, 2:85–89, 2008.

[105] J. Cecil, D. Vasquez, and D. Powell. A review of gripping and manipulation techniques for micro-assembly applications. *International Journal of Production Research*, 43:819–828, 2005.

[106] Jaime Castillo-León, Maria Dimaki, and Winnie Edith Svendsen. Manipulation of biological samples using micro and nano techniques. *Integrative Biology*, 1:30–42, 2009.

[107] Jaime Castillo-León and Winnie Edith Svendsen. *Micro and Nano Techniques for the Handling of Biological Samples.* Taylor & Francis, 2011.

[108] Miaomiao Tan, Ziyi Zhang, Linhui Zhao, and Jiancheng Zhang. Review of fabrication methods of nanotube / nanowire devices. *Advanced Materials Research*, 411:427–431, 2012.

[109] M. Reches and E. Gazit. Controlled patterning of aligned self-assembled peptide nanotubes. *Nature*, 1:295–200, 2006.

[110] Maria Dimaki and Peter Bøggild. Waferscale assembly of field-aligned nanotube networks. *Physica status solidi (a)*, 203:1088–1093, 2006.

[111] Maria Dimaki and Peter Bøggild. Frequency dependence of the structure and electrical behaviour of carbon nanotube networks assembled by dielectrophoresis. *Nanotechnology*, 16:759–763, 2005.

[112] J. J. Boote, K. Critchley, and S. D. Evans. Surfactant mediated addembly og gold nanowires on surfaces. *Journal of Experimental Nanoscience*, 1:125–142, 2010.

[113] Guihua Yu, Anyuan Cao, and Charles M. Lieber. Large-area blown bubble films of aligned nanowires and carbon nanotubes. *Nature Nanotechnology*, 2:372–377, 2007.

[114] Guihua Yu, Xianglong Li, Charles M. Lieber, and Anyuan Cao. Nanomaterial-incorporated blown bubble films for large-area, aligned nanostructures. *Journal of Materials Chemistry*, 18:728–734, 2008.

[115] Michael C. P. Wang and Byron D. Gates. Directed assembly of nanowires. *Materialstoday*, 12:34–43, 2009.

[116] Yun-Ze Long, Miao Yu, Bin Sun, Chang-Zhi Gu, and Zhiyong Fan. Recent advances in large-scale assembly of semiconducting inorganic nanowires and nanofibers for electronics, sensors and photovoltaics. *Chemical Soiaty Review*, 41:4560–4580, 2012.

[117] C. Zhang, K. Khoshmanesh, A. Mitchell, and K. Kalantar-Zadesh. Dielectrophoresis for manipulation of micro/nano particles in microfluidic systems. *Analytical and Bioanalytical Chemistry*, 396:401–420, 2010.

[118] J. J. Boote and S. D. Evans. Dielectrophoretic manipulation and electrical characterization of gold nanowires. *Nanotechnology*, 16:1500–1505, 2005.

[119] A. W. Maijenburg, M. G. Maas, E. J. B. Rodijk, W. Ahmed, E. S. Kooij, E. T. Carlen, D. H. A. Blank, and J. E. ten Elshof. Dielectrophoretic alignment of metal and metal oxide nanowires and nanotubes: A universal set of parameters for bridging prepatterned microelectrodes. *Journal of Colloid and Interface Science*, 355:486–493, 2011.

[120] S. Evoy, N. DiLello, V. Deshpande, A. Narayanan, H. Liu, M. Riegelman, B. R. Martin, B. Hailer, J.-C. Bradley, W. Weiss, T. S. Mayer, Y. Gogotsi, H. H. Bau, T. E. Mallouk, and S. Raman. Dielectrophoretic assembly and integration of nanowire devices with functional cmos operating circuitry. *Microelectronic Engineering*, 75:31–42, 2004.

[121] S. H. Hong, M. G. Kang, H.-Y. Cha, M. H. Son, J. S. Hwang, H. J. Lee, S. H. Sull, S. W. Hwang, D. Whang, and D. Ahn. Fabrication of one-dimensional devices by a combination of ac dielectrophoresis and electrochemical deposition. *Nanotechnology*, 19:105305, 2008.

[122] Sourobh Raychaudhuri, Shadi A. Dayeh, Deli Wang, and Edward T. Yu. Precise semiconductor nanowire placement through dielectrophoresis. *Nano Letters*, 9:2260–2266, 2009.

[123] Erik M. Freer, Oleg Grachev, Xiangfeng Duan, Samuel Martin, and David P. Stumbo. High-yield self-limiting single-nanowire assembly with dielectrophoresis. *Nature Nanotechnology*, 5:525–530, 2010.

[124] H. Möhwald. Phospholipid and phospholipid-protein monolayers at the air/w ater interface. *Annual Reviews of Physical Chemistry*, 41:441–476, 1990.

[125] J. A. DeRose and R. M. LeBlanc. Scanning tunneling and atomic force microscopy studies of langmuir-blodgett films. *Surface Science Reports*, 22:73–126, 1995.

[126] Daniel K. Schwartz. Langmuir-blodgett film structure. *Surface Science Reports*, 27:241–334, 1997.

[127] Dongmok Whang, Song Jin, and Charles M. Lieber. Large-scale hierarchical organization of nanowires for functional nanosystems. *Japanese Journal of Applied Physics*, 43:4465–4470, 2004.

[128] Song Jin, Dongmok Whang, Michael C. McAlpine, Robin S. Friedman, Yue Wu, and Charles M. Lieber. Scalable interconnection and integration of nanowire devices without registration. *Nano Letters*, 4:915–919, 2004.

[129] Somobrata Acharya, Asit Baran Panda, Nataly Belman Shlomo Efrima, and Yuval Golan. A semiconductor-nanowire assembly of ultrahigh junction density by the langmuir–blodgett technique. *Advanced Materials*, 18:210–213, 2006.

[130] Andrea Tao, Franklin Kim, Christian Hess, Joshua Goldberger, Rongrui He, Yugang Sun, Younan Xia, and Peidong Yang. Langmuir-blodgett silver nanowire monolayers for molecular sensing using surface-enhanced raman spectroscopy. *Nano Letters*, 3:1229–1233, 2003.

[131] Yu Huang, Xiangfeng Duan, Qingqiao Wei, and Charles M. Lieber. Directed assembly of one-dimensional nanostructures into functional networks. *Science*, 291:630–633, 2001.

[132] Mei Liu, Ying Chen, Qiuquan Guo, Ruying Li, Xueliang Sun, and Jun Yang. Controllable positioning and alignment of silver nanowires by tunable hydrodynamic focusing. *Nanotechnology*, 22:125302, 2011.

[133] Sai Li, Ningyi Liu, Mary B. Chan-Park, Yehai Yan, and Qing Zhang. Aligned single-walled carbon nanotube patterns with nanoscale width, micron-scale length and controllable pitch. *Nanotechnology*, 18:455302, 2007.

[134] Mei Liu, Yan Peng, Quiquan Guo, Jun Luo, and Jun Yang. Large-scale patterning and assembly of carbon nanotubes by microfluidic hydrodynamic focusing. *Advanced Materials Research Vols.*, 194-196:503–506, 2011.

[135] Filipo G. Bosco, En-Te Hwu, Ching-Hsiu Chen, Stephan Keller, Michael Bache, Mogens H. Jakobsen, Ing-Shouh Hwang, and Anja Boisen. High throughput label-free platform for statistical bio-molecular sensing. *Lab on a Chip*, 11:2411–2416, 2011.

[136] Anna Line Brøgger, Dorota Kwasny, Filipo G. Bosco, Asli Silahtaroglu, Zeynep Tümer, Anja Boisen, and Winnie E. Svendsen. Centrifugally driven microfluidic disc for detection of chromosomal translocations. *Lab on a Chip*, 12:4628–4634, 2012.

[137] T. D. Yuzvinsky, A. M. Fennimore, A. Kis, and A. Zettl. Controlled placement of highly aligned carbon nanotubes for the manufacture of arrays of nanoscale torsional actuators. *Nanotechnology*, 17:434–438, 2006.

[138] Alan R. Hopkins, Natalie A. Kruk, and Russel A. Lipeles. Macroscopic alignment of single-walled carbon nanotubes (swnts). *Surface & Coatings Technology*, 202:1282–1286, 2007.

[139] Winnie Edith Svendsen, Michael Jørgensen, Lars Andresen, Karsten Brandt Andersen, Martin Benjamin Barbour Spanget Larsen, Søren Skov, and Maria Dimaki. Silicon nanowire as virus sensor in a total analysis system. *Procedia Engineering*, 25:288–291, 2011.

[140] Dorota Kwasny, Karsten Brandt Andersen, Kasper Bayer Frøhling, Asli Silahtaroglu, Zeynep Tümer, Jaime Castillo-León, and Winnie Edith Svendsen. Label free chromosome translocation detection with silicon nanowires. 2012.

[141] Innam Lee, Xiliang Luo, Xinyan Tracy Cui, and Minhee Yun. Highly sensitive single polyaniline nanowire biosensor for the detection of immunoglobulin g and myoglobin. *Biosensors and Bioelectronics*, 26:3297–3302, 2011.

[142] Innam Lee, Xiliang Luo, Jiyong Huang, Xinyan Tracy Cui, and Minhee Yun. Detection of cardiac biomarkers using single polyaniline nanowire-based conductometric biosensors. *Biosensors*, 2:205–220, 2012.

[143] Xiliang Luo, Innam Lee, Jiyong Huang, Minhee Yun, and Xinyan Tracy Cui. Ultrasensitive protein detection using an aptamer-functionalized single polyaniline nanowire. *Chemical Communications*, 47:6368–6370, 2011.

[144] A. Das, C. H. Lei, M. Elliott, J. E. Macdonald, and M. L. Turner. Non-lithographic fabrication of pedot nano-wires between fixed au electrodes. *Organic Electronics*, 7:181–187, 2006.

[145] Yun-Ze Long, Jean-Luc Duvail, Zhao-Jia Chen, Ai-Zi Jin, and Chang-Zhi Gu. Electrical conductivity and current-voltage characteristics of individual conducting polymer pedot nanowires. *Chinese Physics Letters*, 25:3474–3477, 2008.

[146] Y. Z. Long, J. L. Duvail, Z. J. Chen, A. Z. Jin, and C. Z. Gu. Electrical properties of isolated poly(3,4-ethylenedioxythiophene) nanowires prepared by template synthesis. *Polymers for Advanced Technologies*, 20:541–544, 2009.

[147] Yixuan Chen and Yi Luo. Precisely defined heterogeneous conducting polymer nanowire arrays – fabrication and chemical sensing applications. *Advanced Materials*, 21:2040–2044, 2009.

[148] Carlos M. Hangarter, Sndra C. Hernandez, Xueing He, Nicha Chartuprayyoon, Yong Ho Choa, and Nosang V. Myung. Tuning the gas sensing performance of single pedot nanowire devices. *Analyst*, 136:2350–2358, 2011.

[149] Jessica A. Arter, David K. Taggart, Theresa M. Mcintire, Reginald M. Penner, and Gregory A. Weiss. Virus-pedot nanowires for biosensing. *Nano Letters*, 10:4858–4862, 2010.

[150] Jessica A. Arter, Juan E. Diaz, Keith C. Donavan, Tom Yuan, Reginald M. Penner, and Gregory A. Weiss. Virus-polymer hybrid nanowires tailored to detect prostate specific membrane antigen. *Analytical Chemistry*, 84:2776–2783, 2012.

[151] Bhuvaneswari Kannan, David E. Williams, Cosmin Laslau, and Jadranka Travas-Sejdic. A highly sensitive, label-free gene sensor based on a single conducting polymer nanowire. *Biosensors and Bioelectronics*, 35:258–264, 2012.

[152] R. H. Farahi, A. Passian, L. Tetard, and T. Thundat. Critical issues in sensor science to aid food and water safety. *American Chemical Society Nano*, 6:4548–4556, 2012.

[153] Michael Jørgensen. Silicon nanowire biosensor system. Master's thesis, DTU Nanotech, 2011.

Peptide Based Fabrication Approach

In this Appendix a detailed description of the peptide based fabrication approach will be presented. First a few initial consideration regarding the fabrication process will be presented followed by presentation of the mask design. Finally a discussion of the different steps of the fabrication procedure will be given.

A.1   General Considerations

The design of the masks for the PNT based lithography approach is highly dependent on the actual manipulation approach utilized in the procedure. In chapter 5 the modified spin casting technique developed in this project was presented. In this manipulation technique a solution containing the PNT's was dropped on the spinning substrate. This procedure caused the PNT's to align in the axial direction. To increase the yield the electrodes should be placed perpendicular to the nanotube orientation and hence the orientation of the electrodes should change over the wafer.

It was decided to deposit the metal layer on the SOI wafers before the definition of the nanowires for two reason. The practical reason was that it would be easier to evaluate the result of the manipulation and whether it should be repeated or not if the electrodes were already present on the wafer. Furthermore a better electrical connection between the metal electrodes and the polysilicon layer can be established in this way, since there will be no step to cover by the metal.

A.2   Mask Design

As mentioned above the chip design varied over the wafer and therefore it was necessary to apply multiple electrode designs for the different areas of the wafer as discussed in the section below. The individual chips was designed so that the electrical connections and the fluidic interconnections was located at the same positions for the individual chips regardless of the chip design so that the same holder could be utilized for all chips. In figure A.1 the masks used in the fabrication is illustrated.
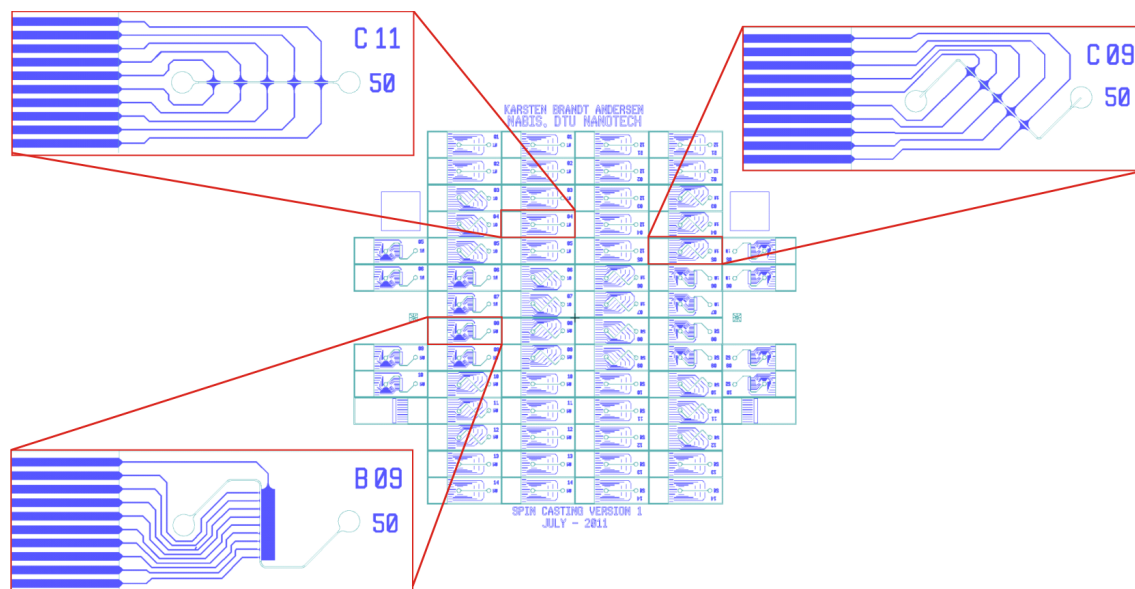
Figure A.1: *Illustration of the masks used in the fabrication of the silicon nanowire devices based on the PNT lithography. The blue parts correspond to the mask designed for the electrodes and the transparent part with green edges corresponds to the passivation layer. In order to ensure that the electrodes are oriented perpendicular to the direction of the spin casted PNT's different chip design is required for different parts of the wafer as indicated in the figure.*

A.2.1   Metal Electrodes and Contact Pads

The metal layer will form both the electrodes in contact with the nanowires and the contact pads for the connection to the macroscopic world. The devices are designed to fit into standard zif sockets to enable a fast and reliable electrical interconnection approach. The different electrode patterns are designed so that they will be perpendicular to the orientation of the spin casted PNT's. Note that the outer geometry of the different chips and the position of the contact pads is the same regardless of the chip design simplifying the final dicing procedure. To enable this identical outer geometry the chips must have different electrode geometries depending on position on the wafer to ensure prober electrode orientation. In figure A.1 the three different chip design implemented in this mask is shown.

In the spin casting procedure the PNT's will not only be positioned at the electrode location, they will be positioned all over the wafer while still being oriented in the axial direction. In this fabrication approach the length of the PNT's are utilized to ensure that they will only bridge the gab between the electrodes and not between the contact pads or leads between the two. A PNT connecting the later two would result in short circuits compromising the useability of the chip. This is realized by having a short distance (shorter than the average length of the PNT's) between the electrodes but a much larger distance (larger than the average length of the PNT's) between the any other metal parts in the chip. In this way the number of short circuits is limited since it would require more than one PNT in series to bridge the gap between metal parts outside the electrode gaps. Of course this fabrication approach will lead to the presence of silicon nanowires all over the wafer. However, only those bridging the gap between two contacts will influence the performance of the sensor.

A.2.2 Passivation Layer

The passivation layer mask is designed so that it can be used both as a mask for the patterning of SU8 microfluidic channels and for the ion beam deposition of a silicon dioxide passivation layer. Note that the microfluidic inlets (in case of the SU8 layer) are positioned at the same positions for all the devices regardless of the electrode design. Furthermore, all sharp corners have been avoided to prevent nucleation of air bobbles at these locations.

A.3 Fabrication Discussion

A.3.1 Metal Electrodes

The decision to deposit the metal prior to etching of course places limitations on which metal to use. Therefore in this fabrication procedure aluminum was used since this is the only metal that are allowed to cover more than 5 % of the wafer in the reactive ion etch procedure. In the fabrication of the PEDOT:TsO nanowires a new electrode mask was designed with a metal coverage of less than 5 % for the implementation of gold electrodes (This mask had fewer devices). This change was necessary because the aluminum oxide formed on the aluminum electrodes made it impossible to establish electrical contact with the PEDOT:TsO ontop.

A.3.2 Peptide Nanotubes Lithography

The central step in this fabrication procedure is the positioning of the PNT's followed by the pattern transfer in a reactive dry etching procedure of the peptide pattern to the poly silicon layer. In chapter 5 the spin casting procedure was presented and therefore in this appendix only a few practical remarks regarding the procedure will be given.

It is important to understand that the specific spin casting procedure must be changed and optimized for new materials in order to provide proper alignment. This is illustrated by the different spin casting procedures utilized for the fabrication of silicon nanowire and PEDOT:TsO nanowires.

If for some reason the alignment of the PNT's is not satisfactory one can simply flush the wafer with milli Q water and repeat the manipulation procedure until a satisfactory results has been achieved. It is my experience that there is a whole range of parameters greatly affecting the results of the manipulation which can be optimized for other materials than poly silicon. These are: The spin rate of the substrate, The height from where the peptides are dropped, The surface properties of the substrate, The age-, Concentration-, HFP content-, Temperature-, and treatment of the peptide solution and finally the presence of flushing steps (As the isopropanol drops for the polysilicon). All of which of course are not equally important but may serve a role in the optimal procedure.

After the spin casting procedure the pattern of the PNT's are transferred to the polysilicon layer beneath in a reactive ion etch procedure. Note that if to thick metal electrodes were deposited in the previous step there will be an underetching below the PNT's at the edge of the electrodes, since the PNT will be hanging above the substrate rather than being immobilized onto it (a side effect of the high stiffness of the PNT's). Therefore a thickness of less than 50 nm is preferred.

A.3.3 Passivation Layer

The goal of the PNT lithography based fabrication process is provide a rapid and low cost fabrication scheme for the fabrication of nanowire devices. Before the nanowire sensor can be utilized in any biosensor applications it is important that the metal electrodes is passivated, since otherwise

the current would simply be running through the medium in which the measurements are performed. Traditionally either polymer layers such as SU8 or PECVD deposited insulating materials such as silicon nitride has been used. However, both of these solutions are time consuming and for the case of the PECVD silicon nitride layer it is nor possible to pattern this without compromising either the thin polysilicon nanowires or the aluminum electrodes and contact pads. In this fabrication approach a ion beam deposited layer of silicon dioxide will be used as the passivation layer. This layer can be patterned in a traditional lift off procedure and therefore the entire passivation layer step of the fabrication sequence can be realized in less than 3 hours for with 4 wafers.

A.4 Fabrication Sequence

	Contact email	Contact person	Contact phone
DTU Nanotech Department of Micro- and Nanotechnology	karsten.andersen@nanotech.dtu.dk	Karsten B. Andersen	31164864
	Labmanager group	Batch name	Date of creation	Date of revision
	NaBIS	PepPolySi	19-Dec-12	10-Jan-13

Objective

Batch name: Peptide Poly Silicon Nanowires

The objective with this process flow is to fabricate poly silicon nanowire devices utilizing peptide nanotubes (PNTs) formed in water from the dipeptide diphenylalanine as a masking material

The PNTs is formed from a small dipeptide consisting of two phenylalanine amino acids. The formed peptide nanotubes are non toxic and dissolve rapidly in all liquids including water. However it has been proven able to mask dry etching procedures in the reactive ion etch machines.
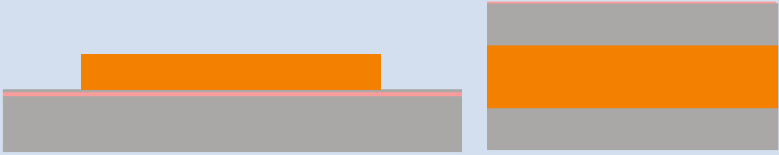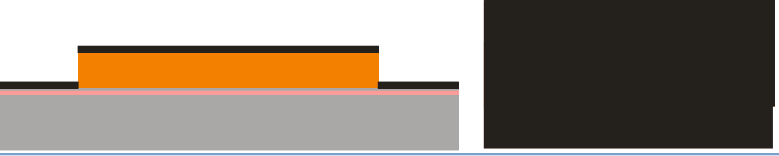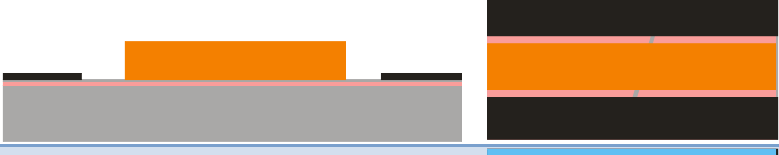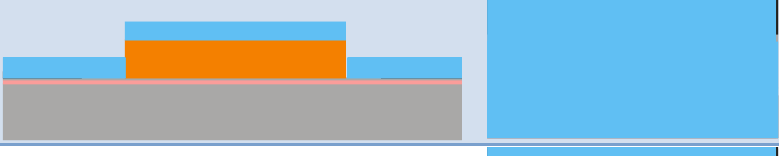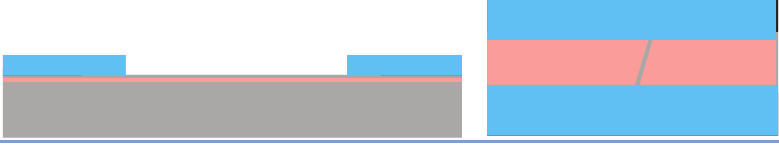
The current fabrication procedure can also be used for the fabrication of single crystalline silicon nanowires and the patterning of silicon nanowires on quartz wafer providing the user with transparent silicon nanowires. Such devices would make it easier to work with biological samples since these chips can be used in inverted microscopes with allowing time lapse experiments with cells.

Note: The diphenylalanine peptide nanotubes have been approved as an allowed material in the clean room. And it has been approved to be used in all the processes and machines that it is introduced to in this process flow by the safety comity and the machine responsible.

Substrates

Substrate	Orient.	Size	Doping/type	Polish	Thickness	Box	Purpose	#	Sample ID
Silicon	<100>	4"	n (Phos.)	DSP	350±25µm		Substrate	4	SI 1-4

Figures

Figure	Caption	Step	Figure (Side and top view)
1	After Poly Si Deposition	2.2	
2	After lithography	3.8	
3	After Aluminum deposition	4.1	
4	After lift off	4.2	
5	After Peptide positioning	5.1	
6	After Poly si etch and water dip	5.4	
7	After photolithography	6.7	
8	After TiO2 deposition	7.1	
9	After lift off	7.2	

Comments: Color Legend

- Silicon
- photoresist
- Aluminum
- Silicon dioxide
- Passivation layer

Step Heading	Equipment	Procedure	Comments
1 Preparation			SI 1-4
1.1 Wafer selection	Wafer box	Take the wafers from the storage and put them in a wafer box.	Note the wafer IDs in the batch traveler.
1.2 Oxide growth	Drive In furnace	Recipe: Wet1050 Time: 4 hours Temperature: 1050°C Gas flow: 2.5 SLM O_2 and 3 SLM H_2 Aneal: 20 min at 5 SLM H_2	To grow 500 nm SiO_2, remember to include test wafers
2 Poly Silicon deposition			SI 1-4
2.1 RCA cleaning	RCA Bench		Note that procedure must be performed right before polysilicon deposition. Remember to include test wafer with oxygen for polydeposition. If step 2.2 is performed immediately after 1.2 this cleaning step can be skipped.
2.2 Poly Silicon deposition	LPCVD Poly-Si (B4)	Place a test wafer in the center of the boat and place device wafers equally distributed on each side of the test wafer (wafer with oxide). Finally fill up with dummy wafers for p-type poly. Wafers in every other slot Recipe: Poly620PX, time: 5min Target thickness: 55±5nm Gas flow: 80 SCCM SiH_4 and 7 SCCM B_2H_6	Measure poly silicon thickness on the filmtech and note the result in the furnace log. Remember to leave the test wafer in the designated box after investigation
3 Lithography – 1.5µm standard			SI 1-4
3.1 Surface treatment	HMDS oven	Load wafers in oven for ~30 mins Recipe: program 4	Note time in logbook, can be replaced by 15 s. HF dip
3.2 Clean spinner	SSE spinner	Clean spinner nozzle and run the dummy wafers Recipe: 1.5 4inch	1-3 dummies
3.3 Coat wafers	SSE spinner	Coat the device wafers 1.5 µm AZ5214e Novolac resist Softbake on hotplate Recipe: 1.5 4inch (Temp: 90°C, time:60 sec)	Note in logbook
3.4 Exposure	Aligner-6inch	Align to flat. Hard contact Recipe: first print neg. process Exposure time: 1.7 sec Mask: Electrodes	Note time in logbook
3.5 Reverse bake	Manual Hot plate	Temp: 110 °C Time: 100 sec	Placed in the old yellow room
3.6 Flood exposure	Aligner-6inch	Recipe: Flood exposure Exposure time: 15 sec Mask: none	Note time in logbook

3.7	Transport of wafers	transport box	Load wafers into the Black or blue transport box	To avoid unwanted exposure from the white light
3.8	Develop	Developer bench	Develop in 351B for 60±10 sec	Note time in logbook
3.9	Rinse/dry	Wet bench/ Spin dryer	Rinse in DI water for 5 min (300±30 sec). Spin dry	
3.10	Inspection	Optical microscope	Check pattern and alignment marks	

4 Aluminum deposition

SI 1-4

4.1	Aluminum deposition	Alcatel	Metal: Al Thickness: 50 nm	Note in logbook
4.2	Lift-off	Remover 1165 lift off	Ultrasound on for 30 min	
4.3	Rinse/dry	Wet bench/ Spin dryer	Rinse in DI water for 5 min (300±30 sec). Spin dry	
4.4	Inspection	Optical microscope	Check for completeness	
4.5	Inspection	Dektak	Measure heights and widths	Note on measurement sheet

5 Nanowire Definition with Peptides

SI 1-4

5.1	Spin casting peptides	Portable spinner	4000 rpm for 15 s. Spin dry	Specific process described in Chapter 5 and Appendix A
5.2	Inspection	Optical microscope	Check for alignment and density	If not successful rinse in Di water and redo step 5.1
5.3	Poly Silicon Etching	RIE 2	Recipe: oh_polya Time: ~30s. Pressure: 80 mTorr Gas Flow: 32 SCCM SF_6 and 8 SCCM O_2 RF power: 30 W	Use endpoint detection to determine when the silicon layer has been removed
5.4	Removal of peptides	Dedicated petridish	Place in water in dedicated petridish for ~1h	
5.5	Verify peptide removal	Optical microscope	Check removal for peptides	Most easily seen at the border of the electrodes

6 Lithography – 1.5μm standard

SI 1-4

6.1	Surface treatment	HMDS oven	Load wafers in oven for ~30 mins Recipe: program 4	Note in logbook
6.2	Clean spinner	SSE spinner	Clean spinner nozzle and run the dummy wafers Recipe: 1.5 4inch	1-3 dummies
6.3	Coat wafers	SSE spinner	Coat the device wafers 1.5 μm AZ5214e Novolac resist Softbake on hotplate Recipe: 1.5 4inch (Temp: 90°C, time:60 sec)	Resist thickness not checked Note in logbook
6.4	Exposure	Aligner-6inch	Align to flat. Hard contact Recipe: 1.5 μm positive resist Exposure time: 3 sec Mask: Passivation	Note time in logbook
6.5	Transport of wafers	transport box	Load wafers into the Black or blue transport box	To avoid unwanted exposure from the white light
6.6	Develop	Developer bench	Develop in 351B for 60±10 sec	Note time in logbook

| 6.7	Rinse/dry	Wet bench/ Spin dryer	Rinse in DI water for 5 min (300±30 sec). Spin dry	
6.8	Inspection	Optical microscope	Check pattern and alignment marks	
7	**SiO2 Deposition**			SI 1-4
7.1	SiO2 deposition	Ion FAB	Recipe: SiO2 Acceptance Time: 30 min Thickness: 100 nm	Note in logbook
7.2	Lift-off	Dedicated petridish	In single wafer ultrasound bath for petridish Time: 15 min	Can be performed in parallel with SiO2 deposition on following wafer
7.3	Rinse/dry	Fumehood	Flush with DI water and Spin dry on single wafer dryer	
7.4	Inspection	Optical microscope	Check for Complete lift off	
7.5	Inspection	Dektak	Measure heights and widths	Note on measurement sheet

Contents

APPENDIX B

Experimental Setup

In this appendix the manual for the silicon nanowire experimental setup written by a master student (Michael Jørgensen) supervised by me is included. For a more detailed description of the setup, which is out of the scope of this thesis I refer the interested reader to the master thesis of Michael Jørgensen.[153]

Manual

Fully automated LabVIEW-system for performing
IV-measurements and controlling the syringe pump
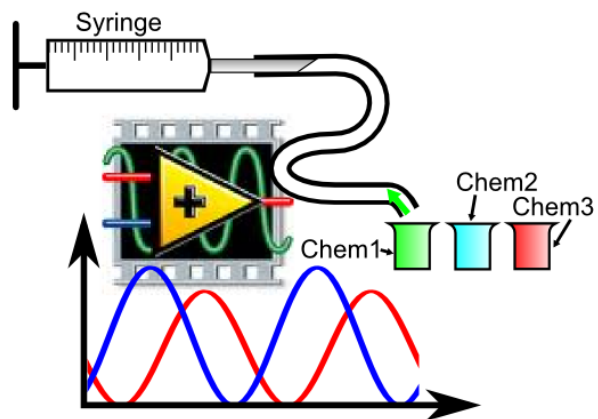
June 23 2010

By Michael Jørgensen, s052927

Course: 33523 Project in Nanosystems Engineering

Under supervision of
Winnie Edith Svendsen, Associate Professor
Karsten Brandt Andersen, Ph.d.-student

Contents

1 How the devices are connected

The purpose of this measurement system is to fully automate IV- and impedance measurements of silicon nanowires while controlling which solution the nanowires are exposed to.

This section describes which devices the measurement system consists of and how they are connected. Section 2 describes the basic principle behind the IV- and impedance measurements and explains how to use the LabVIEW program. Section 3 is build up in the same way, just for batch processing.

The system consists of a computer controlling 3 different devices and is seen in figure 1 (a)

The impedance measurements are done using the LabVIEW devices (NI PCIe-6251 and NI BNC-2111) and the current preamplifier (Stanford Research SR570), which are connected to the nanowire chip inside the Faraday Cage. The electric diagram is seen in figure 1 (b). The LabVIEW devices applies a variable voltage using analog output, `AO0`, across the unknown impedance of the nanowire, Z. The actual voltage is measured using analog input, `AI0`.

The current through the impedance, Z, is measured using the current preamplifier, which converts the current to an amplified voltage with an amplification the PC controls through the RS232 cable. This voltage is then measured by the LabVIEW device using analog input, `AI1`.

To control which chemical the nanowire is in contact with, the syringe pump, Chemyx Nexus 3000, is used to pump chemicals though the tube into the microfluidic channels containing the nanowires, see figure 1(c). The syringe pumps is controlled by the PC through the RS232 cable.
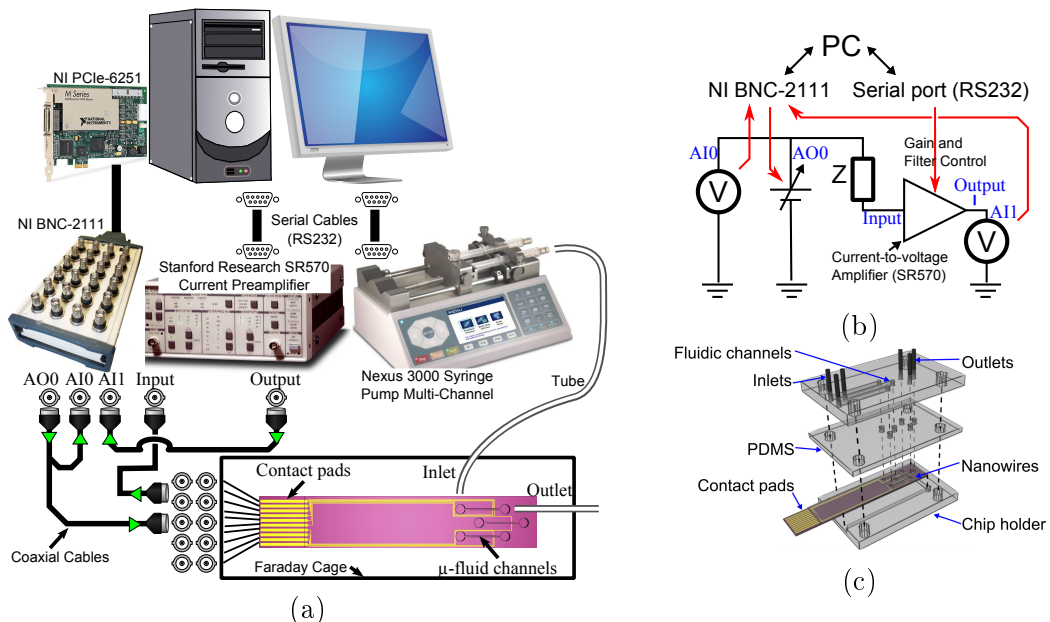

Figure 1: (a) the entire measurement system where the PC is connected to a LabVIEW device, a current preamplifier and a syinge pump. Using these three devices IV- and impedance measurements can be performed on the nanowires on the chip, while controlling which chemical the nanowires are in contact with. (b) the electrical diagram of the system, where the LabVIEW device and the current preamplifier are used to determine the unknown impedance Z. (c) the microfluidic system.

2 IV- and impedance measurements

In section 2.1 the principle behind determening the impedance from current and voltage measurements is described, and section 2.2 explains how to use the LabVIEW program. In section 2.3 the procedure for autocalibrating the preamplifier is described and the frequency responses of the digital filters are seen in section 2.4.

2.1 Determination of impedance

This section describes how the LabVIEW program processes its data, when determining the impedance.

When measuring the voltage and current, the signal will contain some noise shown in Step 1 of figure 2. The noise is filtered out using one or more of the digital filters described in section 2.4. At Step 2 one period is cut out. In Step 3 the phase difference between the current and the voltage is determined, which will be the same as the negative phase of the impedance. Knowing the phase diffence, the current and voltage are aligned. The aligned signals in Step 4 are then plotted as current vs. voltage in Step 5 and a linear fit is done, where its reciprocal slope will be the modulus of the impedance.
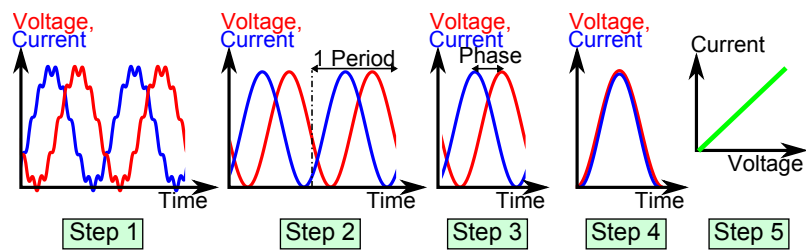

Figure 2: A sketch showing how the raw signals are being filtered, cut out to 1 period, aligned and plotted.

2.2 How to use the program for IV-measurements

Because a large forest of buttons and indicators on the user interface, the screenshots of the user interface has been split up into 5 smaller pictures in this section. The overview of the user interface is seen in figure 3(a), where the numbers indicate which order they are explained in.

Output settings, figure 3(b)

A **Output 1** *Offset*, *Amplitude* and *Frequency* of the applied sine voltage at output `AO0`

B **Frequency sweep** The same as in **A** where a series of measurements are performed with frequencies between *Start* and *Stop* with a given *Step*. The *# of measurements* performed for each frequency is configured in **G** .

C **Output 2** The same as **A** at output `AO1`. This output can be used to apply a gate voltage.

D **Save data** If *Save ON* is true, the measured data will be saved in the subdirectory entered in *Save to Path*. In this directory a folder is automatically created and is named after the current time. In this folder there is created 4 files:

    Current.dat and Voltage.dat: This is the data from the measured current and voltage, which is saved in the format: Native binary file format as a Single precision floating point. This reduces the filesize with a factor of 3 compared to default settings. These files can be read in Matlab using the command

```
current=fread(fopen('Current.dat','r+','native'),inf,'single');.
```

    In **Parameters.dat** the parameters of the measurement and the comment field is stored.

    In **Impedance.dat** the modulus in Ohm, phase in degrees and signal-to-noise ratio is saved as a comma-seperated-value file.
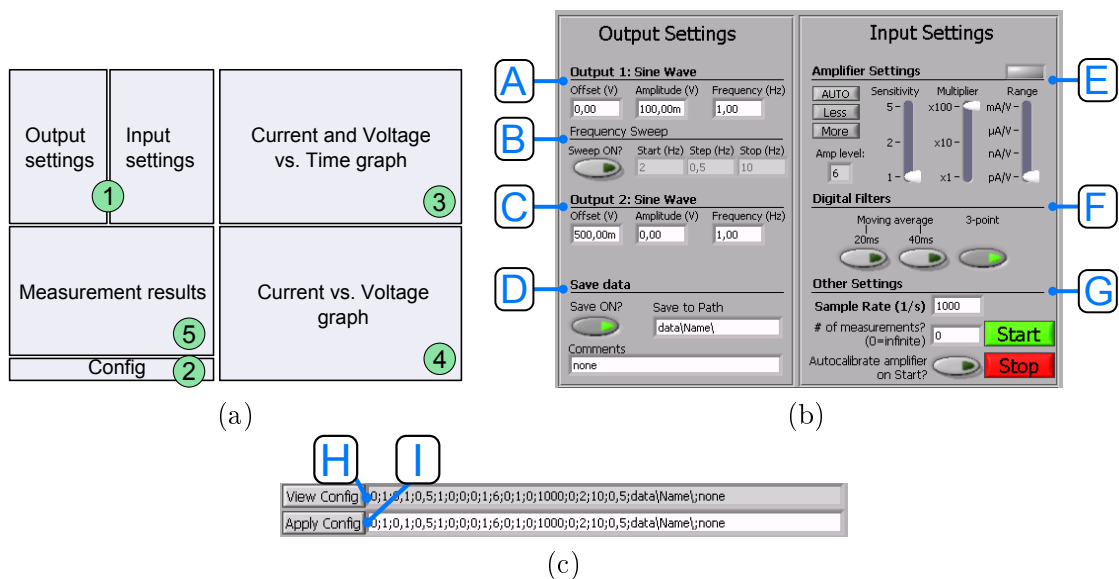

(a)   (b)

(c)

Figure 3: (a) overview of the LabVIEW program. Each box is a seperate figure in this manual and are explained in the order of the numbers. (b) is number 1 in (a) and defines the input and output parameters. (c) is used to save the measurement parameters.

Input settings, figure 3(b)

E **Amplifier settings** Here the amplification of the current preamplifier can be turned up, turned down or be autocalibrated. The autocalibration algoritm is described in section 2.3.

F **Digital Filters** Three digital filters can be applied and are all mainly designed to remove 50Hz noise, but also removes high frequencies. The filters are both applied to the current and the voltage data. The frequency response of these filters are described in section 2.4.

G **Other Settings** The *Sample Rate* of the current and voltage measurements can be setup. *# of measurements* is how many impedance measurements before the measurement are automatically stopped. If *Autocalibrate amplifier on Start* is activated the *AUTO* button on **E** is automatically pushed when starting the measurement. The *Start* and *Stop* button starts and stops the measurement.

Configurations string, figure 3(c)

H **View Configuration** The configuration of all parameters described above are converted into a single string which can be viewed by pushing *View Config*. This can be used to save the configuration of the measurement.

I **Apply Configuration** To load a configuration, insert the configuration string and push *Apply Config*. The configuration string can be used in the batch process, which is described in **S** in section 3.2.
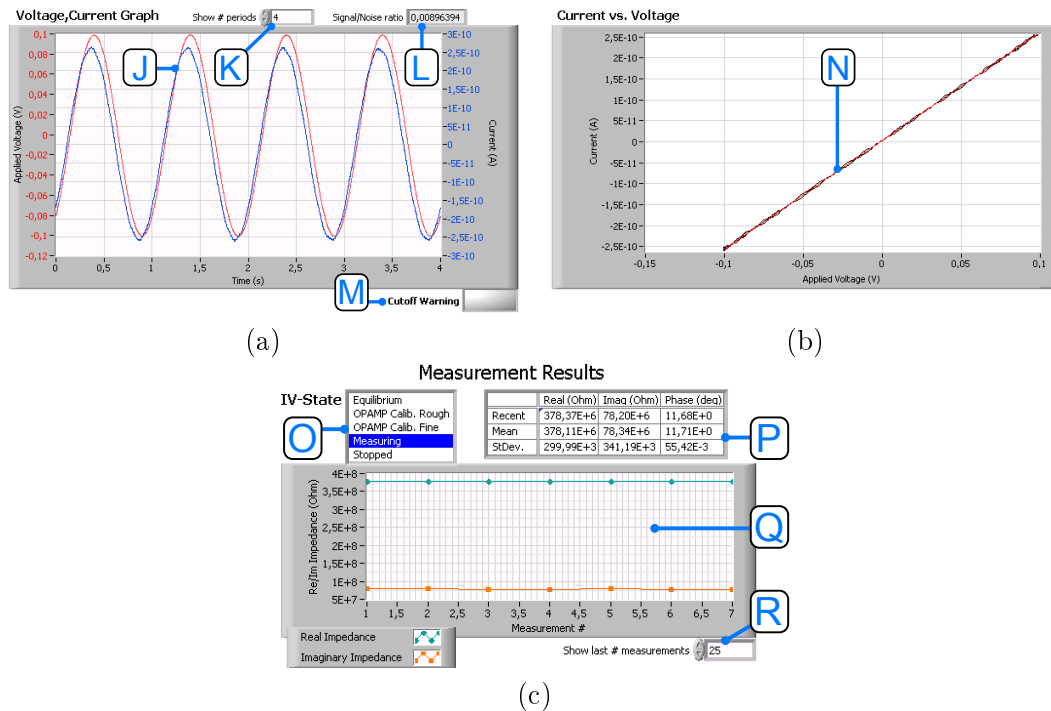

(a)

(b)

(c)

Figure 4: (a) voltage and current vs. time where the phase difference is the argument of the impedance. (b) current vs. voltage where the reciprocal slope is the modulus of the impedance. (c) the real and imaginary part of the impedance is shown in the graph and the table.

Voltage, Current Graph, figure 4(a)

J **Voltage,Current vs. time** Applied voltage from output `AO0` and measured current from input `AI0`.

K **Show # periods** on the graph.

L **Signal/Noise ratio** of the last period of the measured current.

M **Cutoff warning** flashes red if the raw current signal is to high and gets cutoff. **Notice:** when cutoff occurs the current change will be reduced leading to an overestimation of the impedance.

Current vs. voltage, figure 4(b)

N **Current vs. voltage** The red curve is the filtered data and the black curve is the linear fit. The reciprocal slope determines the modulus of the impedance.

Measurement results, figure 4(c)

O **IV-State** indicates which state the measurement procedure is in within the measurement procedure. More can be read in section 2.3.

P **Result table** shows the real part, imaginary part and the phase of the impedance. The rows show the most recent impedance, the mean impedance and the standard deriviation of the graph in Q .

Q **Impedance graph** shows the real and imaginary part of the impedance vs. measurement #.

R **Show last # measurements** in the graph.

2.3 Preamplifier calibration

To reduce the noise, the amplification of the preamplfier is important. Too low amplification gives noise and to much amplification gives cutoff, which in this case is at 5V of the preamplifiers output voltage and is shown in figure 5. To get a signal in equilibrium where the preamplifier is calibrated the measurement process goes through 5 states:

State 1, Equilibrium Let the electronics reach equilibrium by start appling the sine wave and do nothing else for two periods.

State 2, OPAMP Cali. Rough Tempoarily disable filters and if

$$\begin{cases} \max\left(|V_{\text{OPAMP-out}}|\right) < 1\text{V} & \Rightarrow \text{Turn up amplification} \\ \max\left(|V_{\text{OPAMP-out}}|\right) > 4\text{V} & \Rightarrow \text{Turn down amplification} \\ \text{elsewhere} & \Rightarrow \text{Goto State 3} \end{cases}$$

State 3, OPAMP Cali. Fine Reapply filters and determine the signal-to-noise ratio for the current amplification level and for the two neighbourg levels. Then use the amplification level with the lowest signal-to-noise ratio.

State 4, Measuring The measurements are performed and the current, voltage, impedance and measurement parameters are saved.
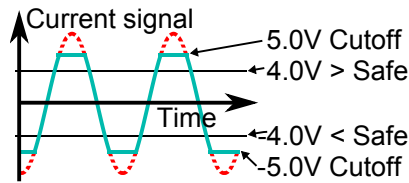
State 5, Stopped

Figure 5: The cutoff voltage and the safety margin for the output of the preamplifier.

2.4 Digital filters

There are 3 digital filters: Moving average 20ms, Moving average 40ms and 3 point. The filters are designed to mainly remove 50Hz noise and their frequency response can be seen in figure 6. As seen the fourier transform of the 50Hz noise has a certain width, which makes the 3 point filter the best of the three to remove 50Hz noise, but does not remove higher frequencies as effective as the other two.
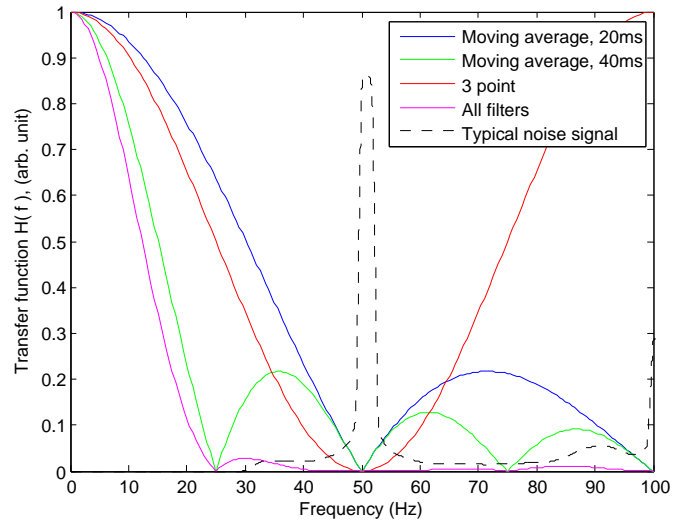

Figure 6: The transfer functions of 3 different digital filter and of all filter combined. The typical noise is also shown.

3   Batch process

In the following section the basic principle of batch processing is explained and in section 3.2 is described how the LabVIEW is used to create and execute batch processes.

3.1   Basic principle batch processing

When executing a batch process there are two modes, which are seen in figure 7:

1. In the **Refill mode** one solution at a time is loaded into the tube and can be seperated by air to prevent the solutions from mixing. **Notice:** the solution one wish to add first in Infuse mode should be loaded in last.

2. In **Infuse mode** the solutions can be pumped into the chip one at a time. Here measurements can be done simultaniously. It is also possible to pump a solution into the chip and wait a defined amount of time until the chemical has reacted and thereafter continue the batch process.
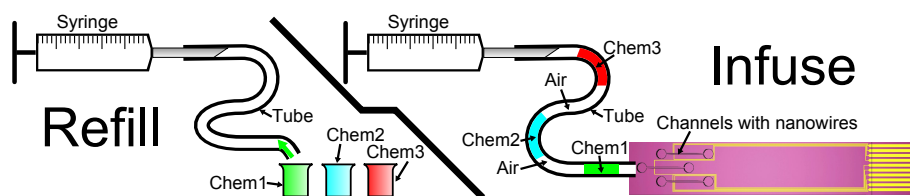

Figure 7: Sketch of the refill and infuse mode.

3.2 How to use the program for batch processing

The user interface of this part the program is seen in figure 8

$\boxed{\text{S}}$ The batch process is created in the table. To add a chemical the syringe pump is to infuse first, type in the chemical name in the first column and fill in two of the three parameters: Volume, Infusion Rate and Time. When this is done the unfilled parameter is automatically calculated and column 2, 3 and 4 are disabled.

In the first column commands for the batch can also be entered. There exist three different commands which can only be used in **Infuse mode**

'pause' (Column 2, 3 and 4 are disabled) stops the batch until the *Next step* button in $\boxed{\text{V}}$ is pressed.

'wait' (Column 2 and 3 are disabled) stops the batch for the amount of seconds typed in the time column.

'meas [config]' (Column 2, 3 and 4 are disabled) performs impedance measurements using the parameters typed in [config]. The syntax of [config] is each of the parameters in the first column of $\boxed{\text{T}}$ seperated with semicolon. The easiest way to type in [config] is to copy the string in the text field shown in $\boxed{\text{H}}$ in figure 3(c).

The measurement is performed while the next step of the batch process is activated, and is performed as long as the next step of the batch process is not finished or if *# of measurement* $\boxed{\text{G}}$ is reached. In this way impedance measurements can be performed using three diffenet stop conditions by typing 'meas [IV-config]' and in the following row typing

'pause'	$\Rightarrow$ IV-measurements until # of measurement is reached
'wait'	$\Rightarrow$ IV-measurements until the waiting time or # of measurement is reached
'Chemical'	$\Rightarrow$ IV-measurements until the chemical is infused or # of measurement is reached

By Right-Clicking the table a row can be deleted or an extra row can be added in the middle of the batch.

Example:
Row 0 and 1 in $\boxed{\text{S}}$ infuses a solution for 10 seconds and continues the batch when *Next step* is pushed.
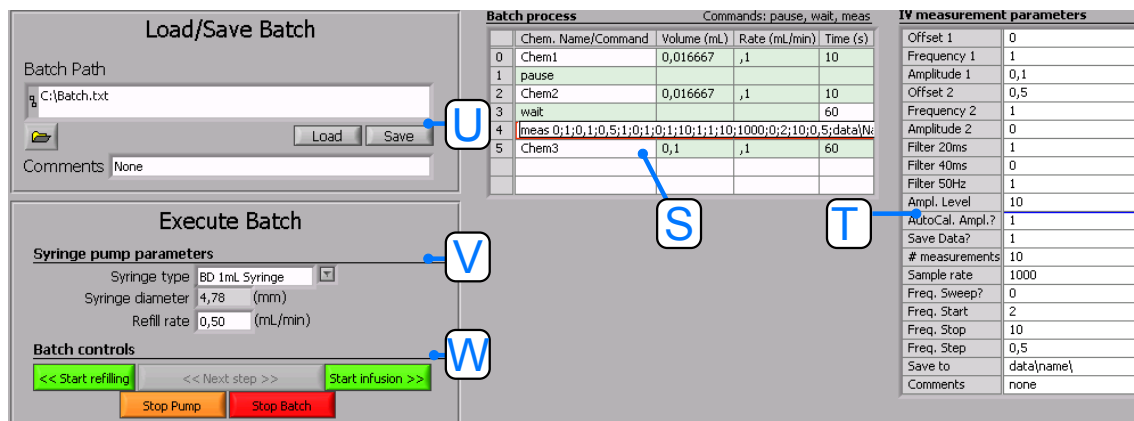

Figure 8: Screenshot batch processing part of the LabVIEW program

Row 2 and 3 infuses a solution for 10 seconds and then waits for 60 seconds before continuing the batch.
Row 4 and 5 does IV-measurements while infusing Chem3 and stops after 60 seconds or when *# of measurements* is reached.

`T` **IV measurement parameters** shows the parameters of a meas-command selected in `S`

`U` **Load/Save Batch** Load/Save the comment field and the table in `S` to a comma seperated value file.

`V` **Syringe pump parameters** In *Syringe Type* some syringes are predefined, which is used to define the syringe diameter. Refill rate defines the rate when the batch is in **Refill mode**.

`W` **Batch controls** Using the green buttons **Infuse mode** or **Refill mode** can be entered. The last three buttons skips a step in the batch, stops the syringe pump and stops the batch.

The Refill mode

In this mode the batch process starts from the bottom and goes up and ignores the 'pause', 'wait' and 'meas' command. In this mode the infusion rates (third column in `S`) are ignored and the refill rate in `V` is used. When a solution has finished to be loaded into the tube the batch is paused until *Next step* in `W` is pushed.

List of Publications

Journal Articles

- *In preparation for advanced materials* Christiansen, N. O.; **Andersen, K. B.**; Castillo-León, J.; Svendsen, W. E.; Rozlosnik, N. All polymer based nanowire biosensor based on peptide nanotube nanolithography.

- *In Preparation for Nano Letters* **Andersen, K. B.**; Kwasny, D.; Castillo-León, J.; Frøhling, K. B.; Svendsen, W. E. Live Chromosome Translocation Detection with Silicon Nanowires based on Exploded Peptide Nanotube Mask.

1. **Andersen, K. B.**; Christiansen, N. O.; Castillo-León, J.; Rozlosnik, N.; Svendsen, W. E. Fabrication and Characterization of PEDOT Nanowires Based on Self-Assembled Peptide Nanotube Lithography. *Organic Electronics*, Submitted.

2. Domigan, L.; **Andersen, K. B.**; Sasso, L.; Dimaki, M.; Svendsen, W. E.; Juliet, G. Castillo-León, J. Dielectrophoretic manipulation and solubility of protein nanofibrils formed from crude crystallins. *Electrophoresis*, **2013**, accepted for publication

3. **Andersen, K. B.**; Castillo-León, J.; Bakmand, T.; Svendsen, W. E. Alignment and Use of Self-Assembled Peptide Nanotubes as Dry-Etching Mask. *Japanese Journal of Applied Physics*, **2012**, 51, 06FF13 .

4. Svendsen, W. E.; Jørgensen, M.; Andresen, L.; **Andersen, K. B.**; Larsen, M. B. B. S.; Skov, S.; Dimaki, M. Silicon Nanowire as Virus Sensor in a Total Analysis System *Procedia Engineering*, **2011**, 25, 288-291.

5. Larsen, M. B. B. S.; **Andersen, K. B.**; Svendsen, W. E.; Castillo-León, J. Self-assembled peptide nanotubes as an etching material for the rapid fabrication of silicon wires. *Bio-NanoScience*, **2011**, 1, 31-37.

6. **Andersen, K. B.**; Castillo-León, J.; Hedström, M.; Svendsen, W. E. Stability of diphenylalanine peptide nanotubes in solution. *Nanoscale*, **2011**, 3, 994-998.

Book Chapter

7. Castillo-León, J.; **Andersen, K. B.**; Svendsen, W. E. Self-Assembled Peptide Nanostructures for Biomedical Applications: Advantages and Challenges, *Intech*, **2011**.

Proceedings

8. Svendsen, W. E.; Jørgensen, M.; Andresen, L.; **Andersen, K. B.**; Larsen, M. B. B. S.; Skov, S.; Dimaki, M. Silicon Nanowire as Virus Sensor in a Total Analysis System *Eurosensors XXV*, **2011**.

9. Castillo-León, J.; **Andersen, K. B.**; Christiansen, N. O.; Dimaki, M.; Svendsen, W. E. Peptide self-assembled nanostructures: advances and challenges for their use in nanobiotechnology applications. *3rd International Conference on Advanced Nano Materials*, **2010**.

10. Castillo-León, J.; Olsen, M. H.; Larsen, M. B. B. S.; Sasso, L.; Vedarethinam, I.; **Andersen, K. B.**; Dimaki, M.; Svendsen, W. E. Biological and non-biological nanostructures for biomedical applications. *BIT's 1st Annual World Congress of NanoMedicine*, **2010**.

Patents

- *In preparation* **Andersen, K. B.**; Bakmand, T.; Okkels, F.; Svendsen, W. E. *Confidential* New type of microfluidic inlet that allow the user to introduce liquid samples to microfluidic chips without the need of tubings and pumps.

11. Sasso, L.; **Andersen, K. B.**; Castillo-León, J.; Gramsberg, J. B.; Svendsen, W. E. Multifunctional sensing membrane-based platform for tissue culturing and monitoring, European patent number: 12175877.5 (2012)

Conference Contributions

- Hawaii **2012** - IEEE EMBS Micro- and Nanotechnology in Medicine
  Bakmand, T.; Sørensen, A. R.; **Andersen, K. B.**; Sasso, L.; Svendsen, W. E.
  Poster: Microfluidic System for Long Term Culturing of Organotypic Brain Tissue.

- Hawaii **2012**- IEEE EMBS Micro- and Nanotechnology in Medicine
  Kwasny, D.; **Andersen, K. B.**; Frøhling, K. B.; Silahtaroglu A.; Tumer, Z.; Castillo-León, J.; Svendsen, W. E.
  Poster: Label Free Chromosome Translocation Detection with Silicon nanowires.

- Ålborg **2012** - 1st International Conference on Self Assembly and Molecular Electronics
  Andersen, K. B.; Frøhling, K. B.; Kwasny, D.; Castillo-León, J.; Svendsen, W. E.
  Invited Talk: Self assembled peptide nanotubes as a low cost nanofabrication tool.

- Barcelona **2012** WAM nano 3rd International Workshop on Analytical Miniaturization and Nanotechnologies
  Frøhling, K. B.; Kwasny, D.; **Andersen, K. B.**; Svendsen, W. E.; Castillo-León, J.
  Poster: Rapid fabrication of silicon nanowire using self-assembled diphenylalanine peptide nanostructures.

- Barcelona **2012** WAM nano 3rd International Workshop on Analytical Miniaturization and Nanotechnologies
  Bakmand, T.; **Andersen, K. B.**; Castillo-León, J.; Svendsen, W. E.
  Poster: Spin casting of self-assembled peptide nanotubes for cheap and fast cleanroom fabrication.

- Hawaii **2011** - 2nd NanoToday Conference
  Andersen, K. B.; Larsen, M. B. B. S.; Castillo-León, J.; Svendsen, W. E.
  Presentation: Low Cost and Fast Clean Room Fabrication Techniques using Peptide Nanotubes.

- Kyoto **2011** - MNC 24th International Microprocesses and Nanotechnology Conference
  Andersen, K. B.; Castillo-León, J.; Bakmand, T.; Svendsen, W. E.
  Poster: Use of self-assembled peptide nanostructures for the fabrication of silicon nanowires.

- Agadir **2010** - 3rd International Conference on Advanced Nano Materials
  Castillo-León, J.; **Andersen, K. B.**; Christiansen, N. O.; Dimaki, M.; Svendsen, W. E.
  Presentation: Peptide self-assembled nanostructures: advantages and challenges for their use in Nanobiotechnology applications.

- Glasgow **2010** - 11th World Congress on Biosensors
  Andersen, K. B.; Castillo-León, J.; Svendsen, W. E.
  Poster: Conductance investigation of self organizing biological nanotube structures.

- Beijing **2010** - BIT's 1st Annual World Congress of NanoMedicine
  Castillo-León, J.; Olsen, M. H.; Larsen, M. B. B. S.; Sasso, L.; Vedarethinam, I.; **Andersen, K. B.**; Dimaki, M.; Svendsen, W. E.
  Presentation: Biological and non-biological nanostructures for biomedical applications.

- Singapore **2009** - 1st NanoToday Conference
  Andersen, K. B.; Clausen, C. H.; Castillo-León, J.; Svendsen, W. E.
  Poster: Easy and Inexpensive Fabrication of a Nanofluidic Channel with a Build in Valve Mechanism using a Biological Nanotube.